5-2020

Cloning, Protein Expression, and Characterization of Interleukin 1 Alpha

Musaab Habeeb Ali Al Ameer
University of Arkansas, Fayetteville

Cloning, Protein Expression, and Characterization of Interleukin 1 Alpha

A dissertation submitted in partial fulfillment
of the requirements for the degree of
Doctor of Philosophy in Cell and Molecular Biology

by

Musaab Habeeb Ali Al Ameer
University of Baghdad
Bachelor of Science degree in Veterinary Medicine and Surgery, 2001
University of Al-Nahrain
Master of Science in Physiology, 2005

May 2020
University of Arkansas

This dissertation is approved for recommendation to the Graduate Council.

_____
Suresh Kumar Thallapuranam, Ph.D.
Dissertation Director

_____
Navam Hettiarachchy, Ph.D.
Committee Member

_____
Joshua Sakon, Ph.D.
Committee Member

_____
Paul Adams, Ph.D.
Committee Member

Abstract

Recombinant DNA technology and the ability to produce recombinant proteins have significantly changed the world of pharmaceutical market. Recombinant DNA technology using *E. coli* cells has successfully produced many therapeutic proteins. In this study, the designed tag Ark-RUBY-tag facilitates rapid, and reproducible purification of recombinant proteins expressed as inclusion bodies in *E. coli* cells. Purification of Ark-RUBY-fused recombinant protein(s) can be obtained by using imidazole fractions. Target protein can be easily removed from the Ark-RUBY-tag by enzymatic cleavage. Ark-RUBY-fused recombinant proteins can be quantitatively detected using polyclonal antibodies. Ark-RUBY-tag can be used to purify small peptides. By using Ark-RUBY-tag, purified recombinant protein regains fully biologically active form. Therefore, bioactive protein has wide range of application in drug-delivery.

Copper is crucial in many cellular functions. It is known that copper is necessary in non-classical secretion by inducing multiprotein realize complex, but the involvement of copper in complex formation is not clear. In this study, the role of copper in non-classical protein secretion of IL-1α was investigated. This framework demonstrates the role of copper to induce IL-1α dimerization under in vitro conditions. The dimerization mechanism is mediated by the single cysteine at position 143 that gets oxidized resulting in the formation of an inter-disulfide bond. The ratio of copper to induce IL-1α dimerization is one to two that means one copper can induce two molecules of IL1-α. The binding affinity of IL-1α to copper study showed that IL-1α binds to copper with Kd value 1.9 μM, which suggests IL-1α is copper binding protein. Also, some binding affinity experiments were conducted to elucidate whether copper is the only metal that

induce dimerization. Some metals showed good binding affinity, but no one induced dimerization. Interestingly, corpus form showed high binding affinity, but it did not induce dimerization. Also, the monomer and the dimer forms of IL-1α have binding affinity to S100A13 with Kd values 1.30 μM and 1.34 μM respectively, which could be crucial in the non-classical secretion of signal-less IL-1α.

The study also shows that Amlexanox (AMX), the anti-allergic drug, can bind to IL-1α and chelates copper with kd 1.9 μM and 1.6 μM respectively. It also inhibits the copper induced dimer formation of IL-1α. The mechanism that underlies dimer formation inhibition of AMX is either because it binds close to cysteine 143 of IL-1α where copper can bind and inhibits the induction of homodimer formation of IL-1α by masking the thiol group of Cys134 or by chelating copper and preventing it from binding to IL-1α. The results of AMX role in inhibiting dimer formation of IL-1α may help in designing a drug that inhibits non-classical secretion of IL-1α.

Acknowledgements

I cannot express enough thanks to my supervisor Dr. Suresh Kumar for his endless support, kindness, and encouragement. I really offer my appreciation for the learning opportunities provided by him. He always has kept saying scientists are made not born.

I would like to show my appreciation to my committee members for allocating their time to conduct my Ph.D. defense. Also, thank you for bringing your valuable suggestions that would improve my thesis.

I am thankful for the support that I got from my lab mates during my journey perusing my Ph.D. degree. Our post docs: Dr. Srinivas Jayanthi, Dr. Ravi Kumar Gundampati, and Dr. Sanhita Maity and grad students: Ziena Al-Rawi, Shilpi Agrawal, Mercede Furr, Patience Okoto, I have not accomplished my work without the decent atmosphere that all of you have created in the lab making me feel like I was working with my family.

I would like to offer many thanks to Kz Shein and Zay Lynn who were presenting at any time I asked to fix any lab machine with kindness.

Finally, to my caring, loving, and supportive wife, Ethar, my deepest appreciation when the times got rough during my PH.D. journey is noticed, and much appreciated. Also, I would like to thank my lovely kids Safa and Maad who kept their tears inside their eyes just to make me feel comfortable at any times I leave Kansas.

Table of Contents

List of Abbreviations

IL1 α Interleukin 1 alpha

IL1 β Interleukin 1 beta

ER Endoplasmic Reticulum

RNA Ribonucleic acid

FGF1 Fibroblast Growth Factor 1

FGF2 Fibroblast Growth Factor 2

Ca^{++} Calcium

Cu^{++} Copper

PIP2 Phosphatidylinositol 4,5-bisphosphate

NK Natural Killer

IL-1R1 Interleukin 1 Receptor 1

IL-1R2 Interleukin receptor 2

NLS Nuclear Localization Signal

SK1 Sphingosin Kinase 1

TM Tetrathiomolybdate

AMX Amlexanox

SDS-PAGE Sodium Dodecyl Sulfate–Polyacrylamide Gel electrophoresis

EP Endogenous Pyrogen

MAP Mitogen Activated Protein

Kd Dissociation constant

ITC Isothermal titration calorimetry

NMR Nuclear magnetic resonance

Chapter One

Introduction

Classical and non-classical protein secretion

Signal peptide mediates protein secretion

Cellular growth, progress, and communication need large number of different proteins that are synthesized in the ribosomes and transported to endoplasmic reticulum (ER)-Golgi apparatus[1]. In order to response to exogenous stimuli, newly synthesized proteins are exported by secretory system to their final destinations[2]. The secretory pathway applies specialized processes to the newly made proteins such as post-translational modifications, protein sorting, and secretion. During protein synthesis, protein translocation into ER membrane is an initial and critical step in protein biosynthesis in eukaryotes[3-5]. ER contains chaperons that provide good environments for nascent proteins by facilitating proteins folding and correct proteins conformation. Also, ER works as proteins folding checkpoint that eliminates unfolded proteins before delivering to Golgi machine[6, 7]. Protein trafficking has been an area of discussion for a long time since Blobel and colleagues pioneered the basis of proteins translocation across intracellular membranes[8].Reaching the right targets, newly made proteins need to be carried to protein sorting in the ER-Golgi system. In biological system of eukaryotic cells, signal peptide mediates proteins translocation across the membrane like system of ER that composes the secretory machine of living cells. Passing the ER existing sites, proteins are packed into membranous vesicles. After vesicles carrying proteins are delivered to Golgi apparatus, post Golgi apparatus cargos undergo fusion with the plasma membrane that results in the release of conventional secretory proteins into extracellular chamber. Each delivered protein requires a valid cellular address tag to govern protein export from the synthesis site to functional sites[9]. However, many aspects of protein

transporting processes were not clear. Synthesized proteins contain specific amino acid sequences that is called signal segment guiding the protein to the final destination[9, 10]. Intracellular compartments are delivered right proteins based on the signal segment. Signal segments are either a linear sequence of amino acids or a given residues forming up for interaction in the correct three-dimensional conformation of the cargo protein[10]. Each organelle is received a specific protein based on the interaction between the different receptors on their surface with a specific signal sequence, thus the information that are encoded in the signal sequence directs the specificity of targeting (Figure 1). Once a protein/receptor interaction has occurred, some kinds of translocation channels are opened. In mammalian cells, specific channels are called translocons that translocate newly synthesized proteins into final destination[11, 12]. Sometimes, for some proteins, it needs to reach a sub compartment within the target organelle[4, 13]. Lastly, once the translocation across the membrane is complete, a specific protease removes the signal sequence from the mature protein[14, 15].

Signal-less proteins and Non-classical pathways

In classical protein secretion, proteins containing N-terminal signal peptide translocate into the lumen of ER, which is followed by ER/Golgi dependent transport to the cell surface for example, albumin, fibrinogen, and immunoglobulin[8]. However, signal peptide is not presented in many primary structure of different proteins and yet they exert their actions by binding to specific surface receptor[16, 17]. Moreover, signal-less peptide secreted proteins play a key role in many physiological processes such as inflammation, angiogenesis, and cell growth and differentiation[18]. Some secretory proteins are known for extracellular functions, but they do not have signal peptides and ER does not mediate

their membrane transportation into extracellular space[19].These proteins are found to be involved in diseases. Examples of these proteins are interleukin-1 α, interleukin-1β, galectin 1 and 3, β galactoside specific lectins, fibroblast growth factor 1 and 2, infection related cell surface markers of *Leishmania* parasites (HASP family), and viral proteins such as *Herpes simplex* tegument proteins vp22 and HIV-TAT proteins etc. Interestingly, these proteins have non-endoplasmic localization or Golgi apparatus localization, with no ER/Golgi post translation modification such as glycosylation and most importantly their release cannot be interfered by protein secretion inhibitors such as berfeldin A, which is the classical proteins secretion inhibitor[20]. These findings bring a new term in proteins secretory mechanism that assures fully cellular functions in absence of signal peptides. Therefore, proteins secretion that mediates out of ER/Golgi system is called non-classical/unconventional protein secretion process[21, 22]. Unconventional secretory pathway involves four mechanisms (Figure 1), two of which include intracellular vesicles of endocytic system such as secretory lysosomes and exosomes and the third export mediates plasma membrane-resident transport and the last one involves the plasma membrane shedding of micro-vesicles[23, 24]. FGF2 export is mediated through the cell membrane. Pores formation helps in moving leaderless proteins through without breaking the membrane. During stress, membrane pores construction needs fully folded leaderless proteins that accumulate near and interact with phosphatidylinositol 4,5-bisphosphate (P1P2) of cytoplasmic side of the membrane. The interactions induce conformational changes of P1P2 that triggers pores formation. Once the pores are made, leaderless proteins can easily translocate to the extracellular space. Even though pores formation explains how the membrane is kept intact, it does not elucidate how proteins that do not

interact with P1P2 can induce oligomerization to make pores. FGF1 and FGF2 are prototypic members of FGFs family and they share some structural properties, but FGF1 secretion requires another signal-less protein to form multiprotein complex that includes S10A13, sphingosine kinase, synaptotagmin, and annexin 2. Then, with the help of annexin 2, the membrane is flipped outside to release the protein complex. Some cytoplasmic proteins are secreted during inflammation by either cell lysis or changing in cell membrane permeabilization. Cell lysis occurs during the inflammation while some immune cells work to destroy irritant action. Best example for lysis protein secretion is IL-1 β. However, some researchers have shown that IL-1 β is secreted without destroying the cells. It is secreted when cells permeability changes after gasdermin-N, a result of caspase 1 catalyzed gasdermin cleavage, is inserted in the cell membrane. However, IL-1 α secretion needs to interact with S100A13 to be exported outside the cells.

Non-classical protein secretion of IL-1α

The most common form of IL-1α found in cells is the precursor protein[25, 26]. Precursor IL-1α (proIL-1α) can generate the IL-1R1 signaling once it is released. ProIL-1α is processed by the Ca^{2+} dependent protease calpain to form mature form of IL-1α [27, 25,26]. IL-1α export requires Cu^{2+} and its binding protein S100A13. IL-1α-S100A13 complex is in a Cu^{2+} dependent manner and the complex formation is released from the cells when the cells are exposed to heat stress[16, 28]. Interestingly, precursor IL-1α is active by its own and the necessity of cleavage is not clear. The latest study suggested that cleavage process might increase its potency[29]. Several proteases play role in precursor IL-1α cleavage include, neutrophil elastase, NK-granzyme-B, mast cell chymase, and calpain proteolysis[30].

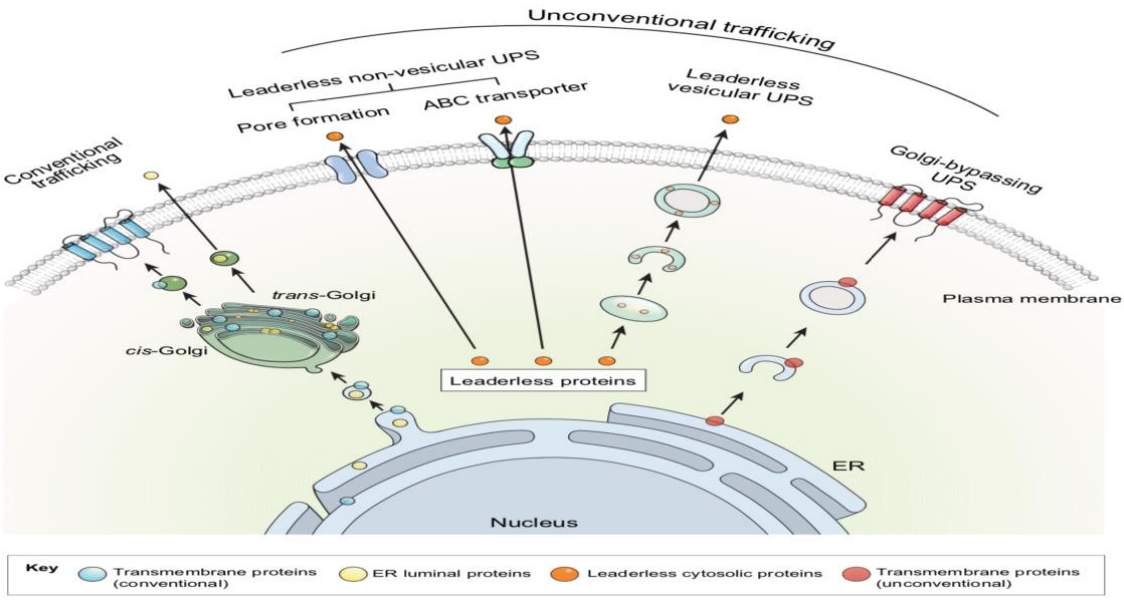

Figure 1: Demonstrates different mechanisms of proteins transport (export) systems.

It is well known that products of cleavage of enzymatic proteolysis are more potent than the precursor protein in activating cells. During NK-mediated killing of target cells, granzyme-B cleavage of proIL-1α occurs. ProIL-1α can be cleaved to enhanced inflammatory response of inflammatory cells. Cleavage of the precursor takes away the carboxyl-terminal mature part of the molecule where the NLS which is the nuclear translocation and DNA binding part of the protein[31]. Therefore, the mature form of IL-1α produces from cleavage process, cannot be retained in the nucleus leading to its release from the cell with great affinity to the receptor. Caspase-1 was recognized to have a role in processing and secretion of IL-1β. It is secreted in combination with IL-1β from specialized secretory lysosomes. In regard to IL-1α, Caspase-1 might assist the secretion of IL-1α[32]. Several studies on Caspase-1 knockout mice shown a reduction in the secretion of both IL-1 α and IL-1β[33-80]. At intracellular level, a binding protein, called interleukin-1 receptor 2 (IL-1R2), protects IL-1α precursor. Certainly, IL-1R2 binding to precursor IL-1α inhibits its cleavage and release from necrotic cells. It is suggested that

caspase-1 helps removing IL-1R2 from precursor IL-1α that ultimately leads to cleavage and secretion of IL-1α. Several players are affecting the inflammatory potential including, the levels of IL-1 α, calpain, the extent of necrosis and the expression of intracellular IL-1R2, and its cleavage by caspase-1 and intracellular levels of Ca^{2+}[26, 34, 35].

Copper and Unconventional protein secretion mechanism

In non-classical protein secretion of FGF1, copper is required in order to form multi proteins complex of FGF1, P40, S100A13 and Syt1. Kumar group has demonstrated that copper stimulates FGF1 dimers as well as S100A13 dimers in the stressed release of FGF1[36]. Many proteins have been linked to FGF1 secretion during stress. Sphingosine kinase 1 (SK1), a copper-binding protein, mediates sphingosine-1-phosphate formation, lacks the signal peptide sequence, and is also secreted by non-classical protein secretion. In presence of copper, FGF1 is found to make high molecular weight complex with SK1[37]. Prudovsky group has showed that SK1 has high affinity to copper that makes the protein to be copper donor in stress release of FGF1. Treating the cells with copper chelating agent called tetrathiomolybdate (TM) blocks the effects of copper induce dimerization leading to decrease cancer growth. However, large expression of SK1 seemed to rescue FGF1 release in present of TM. Many studies have shown that proteins binding to different metals have various effects[38]. For example, S100A13 binds to calcium as well as copper, but each ion has diverse binding matters. It is very interesting that the bindings sites of those two ions are located close to each other on the S100A13. Moreover, thermodynamic stability of S100A13 dimers totally depends on these ions in a way that this protein structure usually destabilized significantly when it binds to copper whereas binding to calcium structure is more stabilized. Copper not only

stimulates protein conformational changes but also it helps in cellular communications. Even though IL-1α, IL-1β, FGF1, and FGF2 have low amino acids homology, they share unique biological aspects. They all have no signal peptide, secreted by unconventional protein secretion, and they all compose twelve β-sheets. More interesting, some of them share the secretion pathway. For example, IL-1α and FGF1 export is similar in responding to cellular stress[39]. In addition, some complex structure formation upon stress exposure follows similar traits in both proteins. This is noted in the release complex formation that includes S100A13 and Cu^{2+}-dependence, which is stress-dependent[40]. As SK1 is a copper provider for stress secretion of FGF1, it may work for IL-1α (Figure 2).

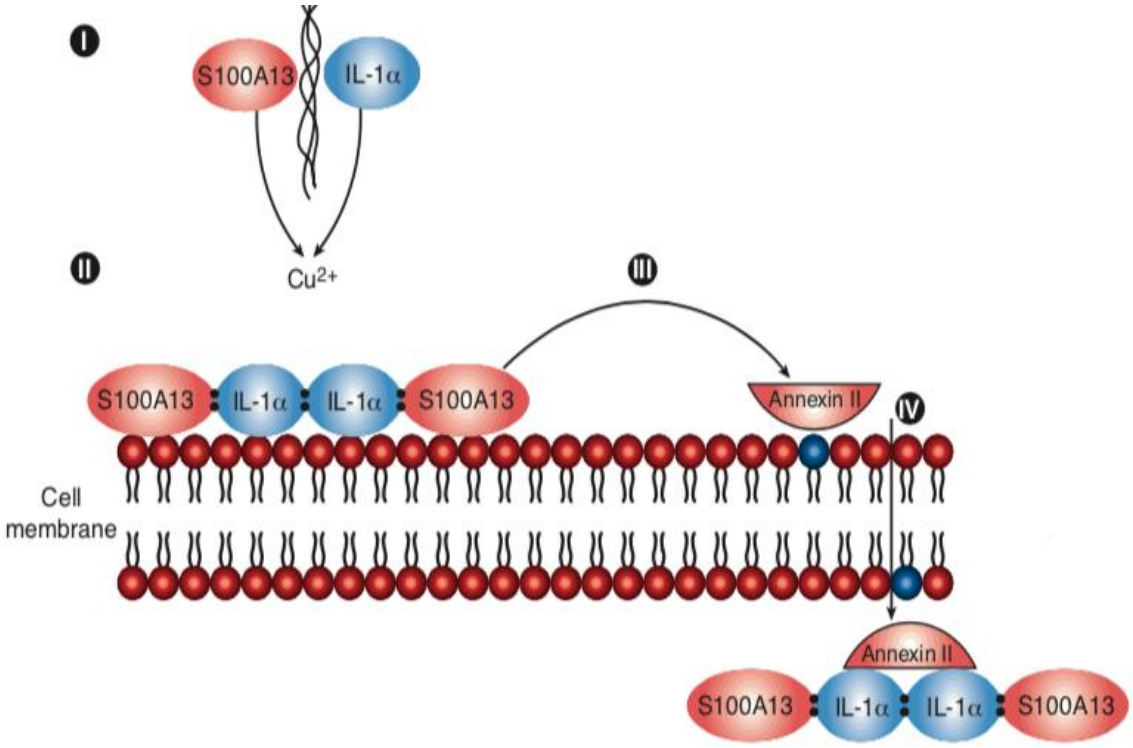

Figure 2: Elucidates the proposed mechanism of copper induces IL-1 α secretion by non-classical secretin[16].

However, IL1α export does not require p40 Syt1 compared to FGF1export. Kumar group has proposed that, it might indicate another unknown cytosolic protein is

playing this role instead of p40 Syt1 in the IL1α release complex. The p40 Syt1 protein is involved in other proteins stress-induced export like syntaxin 2 (epimorphin) in addition to annexin II. The export of IL1β and FGF2 might require S100A13, p40 Syt1, SK1, annexin II, and Cu2+ but this assumption need to be further clarified. Cu^{2+} might be involved in the association of the members of multiprotein aggregates involving FGF1, IL-1α, S100A13 and p40 Syt1 that are all Cu^{2+}-binding proteins. Cu2+ induces FGF1 homodimer but not FGF2 even though two of the three cysteine residues present in FGF1 are conserved in FGF2[16]. In addition, Cu^{2+} might participate in the non-classical release of angiogenic and pro-inflammatory polypeptides as many studies have demonstrated angiogenic and pro-inflammatory effects of Cu^{2+}. It has been noted that attenuation of the stress-induced release of IL-1α and FGF1, as well as of S100A13 when co-expressed with IL-1α or FGF1 is achievable via the depletion of intracellular free Cu^{2+} through continuous application of a specific chelate, tetrathiomolybdate (TM). Therefore, the stress-induced Cu^{2+}-dependent assembly of IL-1α and FGF1 multiprotein release complexes is indeed a requirement for the non-classical export of these proteins in vitro as demonstrated by different studies[41, 42].

Cell Signaling and Growth Factors

In multicellular organisms, cellular communication between millions of cells is critical function for allowing different cells work together. Cellular responds to environmental changes are essential for regulating biological pathways. Cellular commination can be taken place by sending different molecules including proteins, lipid, gas, and polypeptide[43]. The process of cell signaling is either by passing molecules between two adjacent cells through the gap junctions or by releasing growth factors[44, 45].

Cellular response occurs when a cell recognizes a signal that comes from either the environment or produced by another cell, via a receptor; then receptor-ligand complex generates signal transductions[46]. In multicellular organisms, the growth factors are important cell signaling molecules because growth factors provide different cell-to-cell communication mechanisms including endocrine signaling (long distance interaction), paracrine signaling (nearby interaction), and autocrine signaling (self-interaction). Growth factors carry information to trigger gene expression, cellular differentiation, and mitogenesis[47]. They help promoting cellular growth and cellular productions in response to many environmental changes. Growth factors are usually small proteins known as cytokines[48]. Cytokines are secreted proteins that have specific roles on cellular interactions and communications.

Based on the type of secreting cells, there are many kinds of cytokines including lymphokines (secreted by lymphocytes), monokines (secreted by monocytes), and interleukins (secreted by leukocytes and interact with leukocytes). Interleukins are a set of proteins that thought to be particularly secreted by the leukocytes. Interleukins play important functions in cellular communication, cellular growth, and immune responses. They are categorized into various families based on the homology of their amino acids sequences, targeting specific receptors, and performing similar functions[49]. Interleukin-1 family (IL-1) was the first group of interleukins that was identified[50]. IL-1 family is a pro-inflammatory cytokine with several effects on cellular proliferation, differentiation and immune reactions. Nine members are under the name of IL-1 family[51]. Among many other cytokines, IL-1 family of cytokines is primarily mediated with inflammatory response against several harm irritations[52].

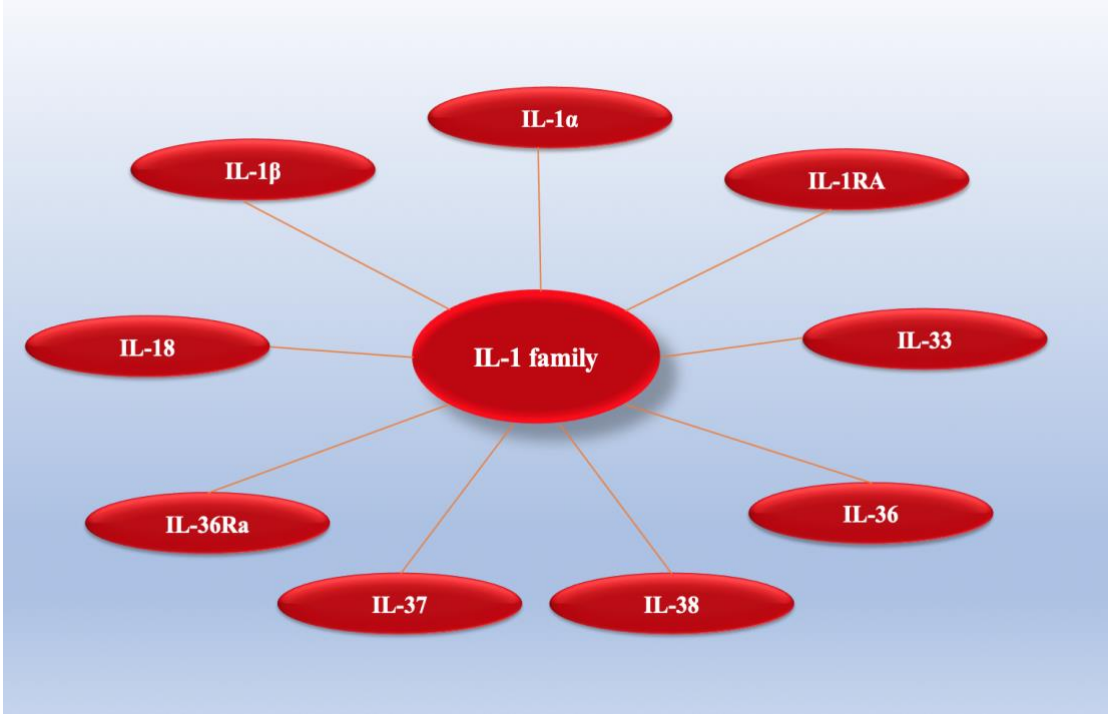

Figure 3: Interleukin 1 family members tree.

Even though members of IL-1 family of cytokines are associated with innate immunity response, many inflammatory disease such as degenerative diseases are linked to uncontrolled secretion of some interleukin-1 family members[53].

Interleukin 1 alpha (IL-1α)

In 1974, two different isoelectric forms of IL-1 with two different molecular weights were reported by Dinarello[54]. An acidic human form with molecular weight of 31,000 Da corresponding to IL-1α and another neutral human form corresponded to human IL-1β with a molecular weight of 17,000 Da. Interleukin-1α (IL-1α), is one of the molecules that have been recognized long time ago; still a lot of data about its role in various diseases are vague. The term of interleukin has roots started in the early 1940s, when sterile pus was injected into rabbits causing a fever[55]. Many years later, a group of researchers conducted an in vivo study on white blood cells investigating the causative

agent(s) that induced the fever[56]. At that time, they found a molecule acted as a thymocyte mitogen, so the term endogenous pyrogen was used (EP)[57]. Later, in the second international lymphokine workshop that held in Interlaken, Switzerland, the term interleukin came up in honor of the city where the meeting was conducted[58]. IL-1α is one of the leaderless proteins that lack a signal peptide. This means its secretion is aimed without endoplasmic/Golgi system[59]. IL-1α is an exceptional type of cytokine as it always presents inside all resting non-hematopoietic cells as well as hematopoietic cells in both healthy and unhealthy situations[60]. In addition, it is usually up regulated during hypoxic situations. Moreover, it has a vital role in necrosis that mediates early inflammatory reactions triggered by its release from damaged tissues[61]. It acts through recruitment of neutrophils to the damage site, besides its induction by different released cytokines and chemokine from inflammatory cells in the surrounding tissue. It has a unique role in multiple inflammatory diseases. Moreover, IL-1α plays key roles in many cellular processes such as cellular proliferation, angiogenesis, and tumor growth. IL-1α is known to act as transcription factor inside the nucleus to induce cells to make many mRNA expressions of other cytokines such as IL-6 and IL-8 and itself as positive feedback control (Figure 2). Also, it acts as secreted protein outside the cells binding to specific receptors[62]. Furthermore, some studies showed that IL-1α is expressed as membrane bounded protein works as cancer cells surveillance[62]. IL-1α can increase immunogenicity against tumor cells and serve as anti-tumor immune. Upon membrane bound form, IL-1α can be glycosylated and placed on the cell membrane of activated cells like monocytes or macrophages, and other cells, by a lectin-like association to induce inflammation[63, 64]. This membrane-associated IL-1α activates IL-1R1 on target

cells, such as endothelial cells and T-cells, and in fibroblasts. Membrane-associated IL-1α has been recognized as main cytokine that potentiates stimulation of other cytokines in the senescence-associated secretory phenotype (SASP) response. This response involves secretion of pro-inflammatory cytokines, such as IL-6 and IL-8[65]. On the other side, when a tumor cell reaches senescent, the resulting inflammatory response can promote invasiveness[66-67]. Also, when cancer cell dies, precursor IL-1α is released acting as inflammatory inducer that may lead to tumor invasiveness and angiogenesis[62, 68].

Interleukin-1 α expression

Interleukin-1α is expressed in many different cells at steady state in both healthy and non-healthy condition, but its secretion level is increased in response to stressed conditions. In contrast to other interleukins, IL-1α can be generated by endothelial cells as well as epithelia cells[57, 69, 70].

Interestingly, IL-1α gene contains a binding site for Sp1 transcription factor that is known to regulate housekeeping genes instead of canonical TATA and CAAT regulatory regions[71]. IL-1α expression varies based on the type of the cells. For example in monocytes, the regulation involves the long noncoding RNA-AS IL-1α transcription factor that is partially complementary to IL-1α mRNA[72]. However, in human CD4+ T cells, the hypo/hyper methylation of CpG nucleotides in the transcription initiation site regulates IL-1α gene expression[73]. The IL-1α gene is located on the long arm of chromosome 2 end to end to the IL-1β gene[74]. The first IL-1 cDNA was cloned in 1984 from two different species, human blood monocyte and a mouse cell line[75, 76]. The IL-1 gene product in those sources was different as the human product was neutral and the other was acidic[54]. The IL-1 α gene primary product is a 271 amino acid precursor then it

is processed to produce a shorter mature protein, which is the carboxyl terminal end of the precursor[27].

Interleukin 1 alpha structure

After removing the pro-piece mature form of interleukin 1 alpha is 162 amino acids protein with 18.5 KDa. It is entirely made of twelve antiparallel β-sheets. In the center, six-stranded β-barrels are arranged to be closed to another six β-strands forming a bowl like structure. At the N-terminus, a short β-strand that composes 6-18 then another short β-strands of amino acids 97-99. Amino acids 101-105 make two turns. Three-fold structural symmetry in the protein core.

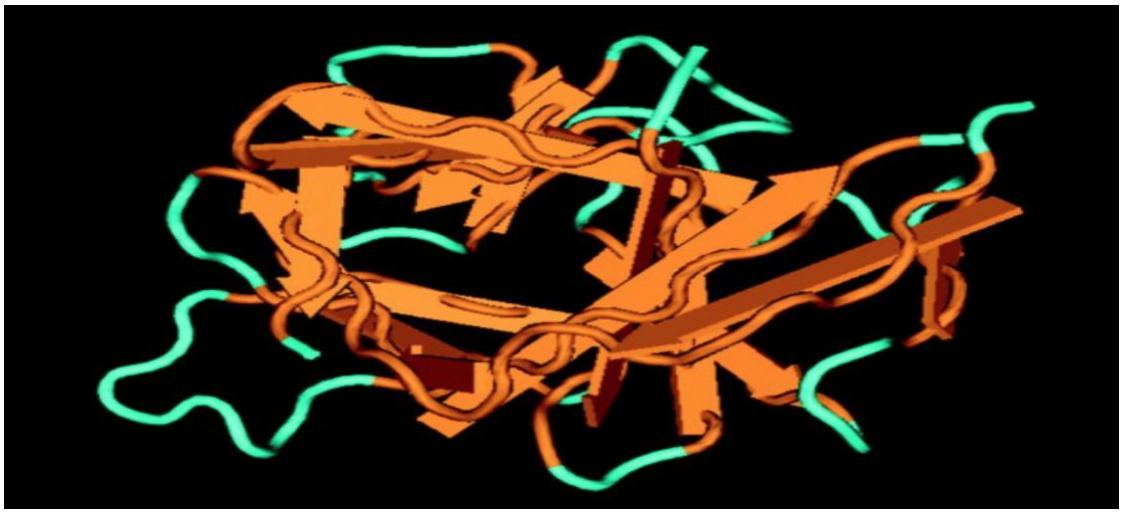

Figure 4: shows the three-dimensional structure of interleukin 1 alpha. Twelve anti parallel beta strands that make the bowl shape at the center of protein core[16].

IL-1α receptors

IL-1α, IL-1β and IL-1Ra exhibit the biological functions by specific binding to IL-1R1[77, 78]. Various human cells such as T-cells and fibroblasts express the 80 KDa IL-1R1. The extracellular domain of IL-1R1 composes of 319 amino acids assembled in

three Ig-like domains[79]. Also, the cytoplasmic domain that has strong homology to toll like receptor comprises of 215 amino acids[80]. IL-1α can bind to IL-1R2 with no effects. Interestingly, IL-1R2 is 60 KD and it is shorter than IL-1R1[81]. This observation explains that IL-1R1 and IL-1R2 are produced from different genes. It is believed that IL-1R2 works as decoy to control and regulate the biological functions of IL-1α and IL-1β[82]. The extracellular domain of IL-1R2 also consists of three immunoglobulin domains. IL-1R2 contains a short intracellular cytoplasmic tail that is 29 amino acids long. This indicates that two IL-1 receptors interact with different signal transduction pathways[83]. IL-1R2 is expressed by a number of cells including B and T-lymphocytes. Upon exerting the biological roles, IL-1α binds with high affinity to the IL-1RAcP making tetramer protein complex with IL-1R1[81]. The binding reaction requires firstly IL-1α causes conformational changes to IL-1R1 upon binding then secondly the conformational changes in the IL-1R1 allow IL1-RAcP to bind to the IL-1/IL-1R1 complex leading to signal transduction. IL1-RAcP provides high stability signals that increase IL-1 binding affinity[84].

IL-1 α signaling

IL-1 α signaling is activated in response to infection, tissue injury or stress[85]. Mitogen-activated protein (MAP) kinase p38, extracellular signal-regulated kinase 1/2 (ERK1/2), c-Jun N-terminal kinase and nuclear transcription factor κB (NFκB) are the main pathways that are activated by IL-1 α[86, 87]. The hetero-tetramer complex of IL1-RAcP and IL-1R1 /IL-1α complex is required for increasing binding affinity and to introduce the signal transduction. The cytoplasmic domains of IL1-RI and IL1-RAcP belong to the Toll like receptor (TLR) family reported as Toll/interleukin-IL-1 (TIR). The

creation of the IL-1/IL-1RI /IL1-RAcP complex enables recruitment of the adapter molecule MyD88, which also contains TIR domain, to the TIR domains of IL1-RI and IL1-RAcP[81]. Binding of IL-1 with the IL1-RII decoy receptor leads to loss of the TIR domain, which is required for signal transduction. Subsequently, the serine/threonine of IL-1 Receptor Associated Kinase IRAK-1, IRAK-2 and the IRAK-4 are recruited and activated by MyD88. In a resting state, IRAK-1 is associated with a Toll-interacting protein (Tollip)[87]. The phosphorylation of Tollip is required for IRAK-1 activation. These multiple kinases cause the recruitment and activation of tumor necrosis receptor-associated factor-6 (TRAF6)[88]. The IRAK-1/TRAF6 complex interacts with transforming growth factor β-activated kinase-1 (TAK-1) within the cytoplasm, which then phosphorylates the IκB kinase (IKK) complex. The degradation of the phosphorylated IKK is leading to translocate NFκB to the nucleus and activate gene expression[89]. Alternatively, the interaction between TRAF6 and the TRAF associated protein named evolutionarily conserved signaling intermediate in Toll pathways (ECSI), causes activation of c-Jun through the Map kinase/JNK signaling cascade[90].

Role of IL-1 α in pathogenesis of various diseases

Role of IL-1α in inflammation and autoimmune diseases

IL-1α is associated with various scopes of many diseases and causes a sterile inflammatory response. Also, there are increased levels of IL-1α in synovial fluid of rheumatoid arthritis patients[91, 92]. In psoriasis, IL-1α amplified level is found to correlate positively with disease severity and keratinocytes express IL-1α constitutively[93]. The presence of IL-1α in resting cells constantly can explain why IL-1α has emerged as a key cytokine in eliciting sterile inflammation. Toll like receptor helps to distinguish between

self and non-self-molecules by binding to pathogen associated molecular pattern (PAMPs)[94]. On the other hand, tissue injury requires identifying alarm signals to approve a sterile environment. In this case, alarm signal is precursor IL-1α that activates inflammatory responses against dead cells[95, 96]. On the contrary, in cells directed to the apoptotic pathway, IL-1α stays inside the nucleus, and fails to initiate an inflammatory response[97, 98]. This retention of IL-1α ensures by binding chromatin to nuclear IL-1 α[89, 97]. This linkage is tight, that reduce the mobility of IL-1α preventing its release[97, 99]. Additional significant study showed that IL-1 α released from dead cells lead to activation of IL-1R1[100]. In experimental models to study peritonitis in mice, an inflammatory response and neutrophil infiltration occurred in an IL-1 α dependent manner by the injection of cell lysate in the peritoneal cavity[101]. It is believed that IL-1α was mainly released from necrotic cells and the surrounding mesothelial cells secrete C-X-C motif chemokine ligand 1 (CXCL1) through an IL-1R1-Myd88 signaling dependent manner[102].

Correlation of IL-1α with neurodegenerative diseases

Furutani *et al*. in 1986 had paved the way to new discovery in the field of inflammatory diseases when the sequence and the organization of the IL1α gene was published[103]. For instance, in systemic sclerosis (SSc), which is a known inflammatory disease, IL-1α is up regulated in fibroblast cells. This up regulation triggers an inflammatory process involving IL-6 and procollagen leads to worsening the auto-inflammation and fibrosis associated[104, 105]. Fibroblast cells obtained from SSc biopsies showed an increased level of transcription of IL-1α[106]. This activated IL-1α increases inflammation[107]. Alzheimer's disease (AD) is one of the neurodegenerative diseases, in

which an inflammatory process causes loss of neurons. Biopsies on postmortem human brain tissue sections from AD patients exhibited an elevated levels of IL-1α in the temporal lobe[108]. A characteristic finding in all AD biopsies is the presence of Beta-amyloid plaques that correlates with IL-1 α expression in microglia cells[109, 110, 111, 112, 113]. IL-1α genetic variation was found to play a role in the occurrence of periodontal disease, an inflammatory disease, which is associated with bacterial plaque due to poor oral hygiene, but is also common among smokers and diabetic patients[114, 115]. In non-smokers, the disease noticed to be associated with elevated IL-1α protein levels and the T allele at the −889 position[116, 117].

IL-1α role in tumor

There are a lot of pro-inflammatory cytokines that contribute to the process of carcinogenesis[118, 119]. The role of IL-1 in tumor progression and invasiveness has been extensively a focus of many researchers. Mutually IL-1 agonistic molecules (IL-1α and IL-1β) can promote tumor invasiveness, metastasis and chemical-induced carcinogenesis through inflammatory responses they induce if they are present in their secreted form. A lot of data clarified the fundamental role that IL-1 molecules play in the development of tumor-induced angiogenesis[120, 121]. Such as, IL-1α and recombinant IL-1β are well-known angiogenic promoting factor. Though, the effects of micro-environmental IL-1α on melanoma development in mice were significantly less than the effects of micro-environmental IL-1β.

Chronic inflammation has been linked with malignant transformations[122, 123]. Many studies have observed that secretory form of IL-1α is a well-recognized pro inflammatory cytokine in tumor microenvironment that fasten tumor growth and

invasiveness, whereas membranous form of IL-1α when present in tumor cells lead to trigger destruction of this cell by immune-mediated mechanisms[124, 125]. Early infiltration by macrophages and $CD8^+$ T cells lead to regression in tumors expressing IL-1 α in vitro. On the contrary, in vivo absence of $CD8^+$ T cells but not $CD4^+$ T cell abolishes regression of IL-1α- positive fibrosarcoma tumors. Long-term specific immune memory protects mice against a challenge with wild type cells (IL-1α-negative). The mechanism by which IL-1α expressing tumor cells cleared by the immune system has been a focus of a lot of researchers. Recently, it has been hypothesized that membrane-associated IL-1 α, may possibly serve as a second co-stimulatory signal or focused adjuvant for their direct activation when ligates to IL-1R1 on effector cells, such as CTLs. Additional, antigen presentation by the tumor cells themselves can be triggered by tumor cell-associated IL-1α through IFNα- induced MHC class II expression, or via cross-presentation by professional APCs. The eradication of IL-1α-positive fibrosarcomas might be through non-adaptive effector cells, such as NK cells and activated macrophages. Membrane-associated IL-1α immunotherapeutic effects were tested as anti-tumor in tumor-bearing mice. Therefore, Mitomycin-C-treated IL-1α expressing cells that introduced at the critical "therapeutic window" caused regression of wild type fibrosarcoma cells[124]. Similarly, regression of invasiveness of malignant lymphoma was shown if cell-associated IL-1α was expressed. Also, invasive T lymphoma cells, which metastasize to the spine showed regression if transient cell-associated IL-1α was expressed[126]. This shows that a difference present between cell-associated IL-1α and secreted IL-1α. In case of pancreatic adenocarcinoma, tumor-associated IL-1α was found to be the triggering factor of tumor growth. The binding of IL-1α to its receptor on cancer-associated

fibroblasts stimulates the production of inflammatory factors. For example, neutralization of IL-1α signaling was used to reduce these inflammatory effects. Extracellular IL-1α that was released from dying cells caused these effects[127]. IL-1α seems to be expressed in different varieties of tumors. It acts with IL-1β and MyD88 to increase reactive oxygen and nitrogen species, COX-2, phosphorylated NF-kB inhibitor (IkB) and stress-activated protein kinase/c-jun-NH(2)-kinase, inducing promotion of tumor progression[128]. Undoubtedly, IL-1 α behaves in different ways in tumor cells depending on whether it is secreted or being intracellular. Secreted form IL-1α might induce inflammation and favor tumor progression, as does IL-1β. Intracellular form, IL-1α is displayed on the membrane and induces anti-tumor cell immunity that might limit growth and regression. Certainly, IL-1α deficient mice displayed a delay in tumor growth and an impaired angiogenic response. Additionally, the role of IL-1α in pancreatic cancer progression might be through promoting angiogenesis and in prostate cancer it might be due to up-regulation of immunosuppression of cytokines in mesenchymal stem cells[129, 130].

References

1. Farhan, H.; Rabouille, C., Signalling to and from the secretory pathway. J Cell Sci 2011, 124 (2), 171-180.

2. Aridor, M.; Balch, W. E., Kinase signaling initiates coat complex II (COPII) recruitment and export from the mammalian endoplasmic reticulum. Journal of Biological Chemistry 2000, 275 (46), 35673-35676.

3. Rapoport, T. A.; Matlack, K. E.; Plath, K.; Misselwitz, B.; Staeck, O., Posttranslational protein translocation across the membrane of the endoplasmic reticulum. Biological chemistry 1999, 380 (10), 1143-1150.

4. Rapoport, T. A., Protein transport across the endoplasmic reticulum membrane: facts, models, mysteries. The FASEB journal 1991, 5 (13), 2792-2798.

5. Lee, M. C.; Miller, E. A.; Goldberg, J.; Orci, L.; Schekman, R., Bi-directional protein transport between the ER and Golgi. Annu. Rev. Cell Dev. Biol. 2004, 20, 87-123.

6. Grieve, A. G.; Rabouille, C., Golgi bypass: skirting around the heart of classical secretion. Cold Spring Harbor perspectives in biology 2011, 3 (4), a005298.

7. Rothman, J. E., Mechanisms of intracellular protein transport. Nature 1994, 372 (6501), 55.

8. Blobel, G., Protein targeting. Bioscience reports 2000, 20 (5), 303-344.

9. Görlich, D.; Prehn, S.; Hartmann, E.; Kalies, K.-U.; Rapoport, T. A., A mammalian homolog of SEC61p and SECYp is associated with ribosomes and nascent polypeptides during translocation. Cell 1992, 71 (3), 489-503.

10. Chevet, E.; Cameron, P. H.; Pelletier, M. F.; Thomas, D. Y.; Bergeron, J. J., The endoplasmic reticulum: integration of protein folding, quality control, signaling and degradation. Current opinion in structural biology 2001, 11 (1), 120-124.

11. Plath, K.; Mothes, W.; Wilkinson, B. M.; Stirling, C. J.; Rapoport, T. A., Signal sequence recognition in posttranslational protein transport across the yeast ER membrane. Cell 1998, 94 (6), 795-807.

12. Mothes, W.; Jungnickel, B.; Brunner, J.; Rapoport, T. A., Signal sequence recognition in cotranslational translocation by protein components of the endoplasmic reticulum membrane. The Journal of cell biology 1998, 142 (2), 355-364.

13. Park, E.; Rapoport, T. A., Mechanisms of Sec61/SecY-mediated protein translocation across membranes. Annual review of biophysics 2012, 41, 21-40.

14. Tsai, B.; Ye, Y.; Rapoport, T. A., Retro-translocation of proteins from the endoplasmic reticulum into the cytosol. Nature reviews Molecular cell biology 2002, 3 (4), 246-255.

15. Panzner, S.; Dreier, L.; Hartmann, E.; Kostka, S.; Rapoport, T. In Posttranslational protein transport into the endoplasmic reticulum, Cold Spring Harbor symposia on quantitative biology, Cold Spring Harbor Laboratory Press: 1995; pp 31-40.

16. Prudovsky, I.; Mandinova, A.; Soldi, R.; Bagala, C.; Graziani, I.; Landriscina, M.; Tarantini, F.; Duarte, M.; Bellum, S.; Doherty, H., The non-classical export routes: FGF1 and IL-1α point the way. Journal of Cell Science 2003, 116 (24), 4871-4881.

17. Nickel, W., Unconventional secretory routes: direct protein export across the plasma membrane of mammalian cells. Traffic 2005, 6 (8), 607-614.

18. Friesel, R.; Maciag, T., Fibroblast growth factor prototype release and fibroblast growth factor receptor signaling. Thrombosis and haemostasis 1999, 82 (2), 748-754.

19. Backhaus, R.; Zehe, C.; Wegehingel, S.; Kehlenbach, A.; Schwappach, B.; Nickel, W., Unconventional protein secretion: membrane translocation of FGF-2 does not require protein unfolding. Journal of cell science 2004, 117 (9), 1727-1736.

20. Nickel, W., The mystery of nonclassical protein secretion. European Journal of Biochemistry 2003, 270 (10), 2109-2119.

21. Osborne, A. R.; Rapoport, T. A.; van den Berg, B., Protein translocation by the Sec61/SecY channel. Annu. Rev. Cell Dev. Biol. 2005, 21, 529-550.

22. Malhotra, V., Unconventional protein secretion: an evolving mechanism. The EMBO journal 2013, 32 (12), 1660-1664.

23. Nickel, W., Pathways of unconventional protein secretion. Current opinion in biotechnology 2010, 21 (5), 621-626.

24. Rabouille, C., Pathways of Unconventional Protein Secretion. Trends in Cell Biology 2016.

25. Dinarello, C. A., Interleukin-1 in the pathogenesis and treatment of inflammatory diseases. Blood 2011, 117 (14), 3720-3732.

26. Kavita, U.; Mizel, S. B., Differential sensitivity of interleukin-1α and-β precursor proteins to cleavage by calpain, a calcium-dependent protease. Journal of Biological Chemistry 1995, 270 (46), 27758-27765.

27. Kobayashi, Y.; Yamamoto, K.; Saido, T.; Kawasaki, H.; Oppenheim, J. J.; Matsushima, K., Identification of calcium-activated neutral protease as a processing

enzyme of human interleukin 1 alpha. Proceedings of the National Academy of Sciences 1990, 87 (14), 5548-5552.

28. Mohan, S. K.; Yu, C., The IL1α-S100A13 Heterotetrameric Complex Structure A COMPONENT IN THE NON-CLASSICAL PATHWAY FOR INTERLEUKIN 1α SECRETION. Journal of Biological Chemistry 2011, 286 (16), 14608-14617.

29. Tapia, V. S.; Daniels, M. J.; Palazón-Riquelme, P.; Dewhurst, M.; Luheshi, N. M.; Rivers-Auty, J.; Green, J.; Redondo-Castro, E.; Kaldis, P.; Lopez-Castejon, G., The three cytokines IL-1β, IL-18, and IL-1α share related but distinct secretory routes. Journal of Biological Chemistry 2019, 294 (21), 8325-8335.

30. Afonina, I. S.; Tynan, G. A.; Logue, S. E.; Cullen, S. P.; Bots, M.; Lüthi, A. U.; Reeves, E. P.; McElvaney, N. G.; Medema, J. P.; Lavelle, E. C., Granzyme B-dependent proteolysis acts as a switch to enhance the proinflammatory activity of IL-1α. Molecular cell 2011, 44 (2), 265-278.

31. Wessendorf, J.; Garfinkel, S.; Zhan, X.; Brown, S.; Maciag, T., Identification of a nuclear localization sequence within the structure of the human interleukin-1 alpha precursor. Journal of Biological Chemistry 1993, 268 (29), 22100-22104.

32. Andrei, C.; Margiocco, P.; Poggi, A.; Lotti, L. V.; Torrisi, M. R.; Rubartelli, A., Phospholipases C and A2 control lysosome-mediated IL-1β secretion: implications for inflammatory processes. Proceedings of the National Academy of Sciences of the United States of America 2004, 101 (26), 9745-9750.

33. Kuida, K.; Lippke, J. A.; Ku, G.; Harding, M. W., Altered cytokine export and apoptosis in mice deficient in interleukin-1beta converting enzyme. Science 1995, 267 (5206), 2000.

34. Brough, D.; Le Feuvre, R. A.; Wheeler, R. D.; Solovyova, N.; Hilfiker, S.; Rothwell, N. J.; Verkhratsky, A., Ca2+ stores and Ca2+ entry differentially contribute to the release of IL-1β and IL-1α from murine macrophages. The Journal of Immunology 2003, 170 (6), 3029-3036.

35. Groß, O.; Yazdi, A. S.; Thomas, C. J.; Masin, M.; Heinz, L. X.; Guarda, G.; Quadroni, M.; Drexler, S. K.; Tschopp, J., Inflammasome activators induce interleukin-1α secretion via distinct pathways with differential requirement for the protease function of caspase-1. Immunity 2012, 36 (3), 388-400.

36. Sivaraja, V.; Kumar, T. K. S.; Rajalingam, D.; Graziani, I.; Prudovsky, I.; Yu, C., Copper binding affinity of S100A13, a key component of the FGF-1 nonclassical copper-dependent release complex. Biophysical journal 2006, 91 (5), 1832-1843.

37. Soldi, R.; Mandinova, A.; Venkataraman, K.; Hla, T.; Vadas, M.; Pitson, S.; Duarte, M.; Graziani, I.; Kolev, V.; Kacer, D., Sphingosine kinase 1 is a critical

component of the copper-dependent FGF1 export pathway. Experimental cell research 2007, 313 (15), 3308-3318.

38. Gilston, B. A.; Skaar, E. P.; Chazin, W. J., Binding of transition metals to S100 proteins. Science China Life Sciences 2016, 59 (8), 792-801.

39. Su, Y.; Xu, C.; Sun, Z.; Liang, Y.; Li, G.; Tong, T.; Chen, J., S100A13 promotes senescence-associated secretory phenotype and cellular senescence via modulation of non-classical secretion of IL-1α. Aging (Albany NY) 2019, 11 (2), 549.

40. Mandinova, A.; Soldi, R.; Graziani, I.; Bagalá, C.; Bellum, S.; Landriscina, M.; Tarantini, F.; Prudovsky, I.; Maciag, T., S100A13 mediates the copper-dependent stress-induced release of IL-1α from both human U937 and murine NIH 3T3 cells. Journal of cell science 2003, 116 (13), 2687-2696.

41. Prudovsky, I.; Tarantini, F.; Landriscina, M.; Neivandt, D.; Soldi, R.; Kirov, A.; Small, D.; Kathir, K. M.; Rajalingam, D.; Kumar, T. K. S., Secretion without golgi. Journal of cellular biochemistry 2008, 103 (5), 1327-1343.

42. Viotti, C., ER to golgi-dependent protein secretion: the conventional pathway. In Unconventional Protein Secretion, Springer: 2016; pp 3-29.

43. Sompayrac, L. M., How the immune system works. Wiley-Blackwell: 2019.

44. Radeva, M.; Waschke, J., Mind the gap: mechanisms regulating the endothelial barrier. Acta Physiologica 2018, 222 (1), e12860.

45. Delvaeye, T.; Vandenabeele, P.; Bultynck, G.; Leybaert, L.; Krysko, D. V., Therapeutic targeting of connexin channels: new views and challenges. Trends in molecular medicine 2018.

46. Uings, I. J.; Farrow, S. N., Cell receptors and cell signalling. Mol Pathol 2000, 53 (6), 295-9.

47. Nawaz, M.; Fatima, F.; Vallabhaneni, K. C.; Penfornis, P.; Valadi, H.; Ekström, K.; Kholia, S.; Whitt, J. D.; Fernandes, J. D.; Pochampally, R., Extracellular vesicles: evolving factors in stem cell biology. Stem cells international 2016, 2016.

48. Growth Factors and Cytokines- An Introduction. (accessed March 19).

49. Akdis, M.; Aab, A.; Altunbulakli, C.; Azkur, K.; Costa, R. A.; Crameri, R.; Duan, S.; Eiwegger, T.; Eljaszewicz, A.; Ferstl, R., Interleukins (from IL-1 to IL-38), interferons, transforming growth factor β, and TNF-α: Receptors, functions, and roles in diseases. Journal of Allergy and Clinical Immunology 2016, 138 (4), 984-1010.

50. Dinarello, C. A.; Renfer, L.; Wolff, S. M., Human leukocytic pyrogen: purification and development of a radioimmunoassay. Proceedings of the National Academy of Sciences 1977, 74 (10), 4624-4627.

51. Dinarello, C. A., Interleukin-1 Mediated Autoinflammation from Heart Disease to Cancer. In Textbook of Autoinflammation, Springer: 2019; pp 711-725.

52. Garlanda, C.; Riva, F.; Bonavita, E.; Mantovani, A. In Negative regulatory receptors of the IL-1 family, Seminars in immunology, Elsevier: 2013; pp 408-415.

53. Borsini, A.; Sawyer, K. M.; Zunszain, P. A.; Pariante, C. M., Neurogenesis, Inflammation, and Mental Health. In Inflammation and Immunity in Depression, Elsevier: 2018; pp 103-113.

54. Dinarello, C. A.; Goldin, N. P.; Wolff, S. M., Demonstration and characterization of two distinct human leukocytic pyrogens. The Journal of experimental medicine 1974, 139 (6), 1369-1381.

55. Dinarello, C. A., Immunological and inflammatory functions of the interleukin-1 family. Annual review of immunology 2009, 27, 519-550.

56. Goldbach-Mansky, R.; Kastner, D. L., Autoinflammation: the prominent role of IL-1 in monogenic autoinflammatory diseases and implications for common illnesses. Journal of Allergy and Clinical Immunology 2009, 124 (6), 1141-1149.

57. Garlanda, C.; Dinarello, C. A.; Mantovani, A., The interleukin-1 family: back to the future. Immunity 2013, 39 (6), 1003-1018.

58. Oppenheim, J. J., Cytokines: past, present, and future. International journal of hematology 2001, 74 (1), 3.

59. Truman-Rosentsvit, M.; Berenbaum, D.; Spektor, L.; Cohen, L. A.; Belizowsky-Moshe, S.; Lifshitz, L.; Ma, J.; Li, W.; Kesselman, E.; Abutbul-Ionita, I., Ferritin is secreted via 2 distinct nonclassical vesicular pathways. Blood 2018, 131 (3), 342-352.

60. Dinarello, C. A., Introduction to the interleukin-1 family of cytokines and receptors: Drivers of innate inflammation and acquired immunity. Immunological reviews 2018, 281 (1), 5-7.

61. Mantovani, A.; Barajon, I.; Garlanda, C., IL-1 and IL-1 regulatory pathways in cancer progression and therapy. Immunological reviews 2018, 281 (1), 57-61.

62. Di Paolo, N. C.; Shayakhmetov, D. M., Interleukin 1α and the inflammatory process. Nature immunology 2016, 17 (8), 906.

63. Kaplanski, G.; Farnarier, C.; Kaplanski, S.; Porat, R.; Shapiro, L.; Bongrand, P.; Dinarello, C., Interleukin-1 induces interleukin-8 secretion from endothelial cells by a juxtacrine mechanism. Blood 1994, 84 (12), 4242-4248.

64. Brody, D.; Durum, S. K., Membrane IL-1: IL-1 alpha precursor binds to the plasma membrane via a lectin-like interaction. The Journal of Immunology 1989, 143 (4), 1183-1187.

65. Orjalo, A. V.; Bhaumik, D.; Gengler, B. K.; Scott, G. K.; Campisi, J., Cell surface-bound IL-1α is an upstream regulator of the senescence-associated IL-6/IL-8 cytokine network. Proceedings of the National Academy of Sciences 2009, 106 (40), 17031-17036.

66. Rodier, F.; Coppé, J.-P.; Patil, C. K.; Hoeijmakers, W. A.; Muñoz, D. P.; Raza, S. R.; Freund, A.; Campeau, E.; Davalos, A. R.; Campisi, J., Persistent DNA damage signalling triggers senescence-associated inflammatory cytokine secretion. Nature cell biology 2009, 11 (8), 973-979.

67. Pu, Y.; Lin, P.; Vaughan, F.; Bernstein, I., Appearance of interleukin lα relates dna interstrand cross-links and cytotoxicity in cultured human keratinocytes exposed to bis-(2-chloroethyl) sulfide. Journal of Applied Toxicology 1995, 15 (6), 477-482.

68. Fahey, E.; Doyle, S. L., IL-1 family cytokine regulation of vascular permeability and angiogenesis. Frontiers in Immunology 2019, 10.

69. Bersudsky, M.; Luski, L.; Fishman, D.; White, R. M.; Ziv-Sokolovskaya, N.; Dotan, S.; Rider, P.; Kaplanov, I.; Aychek, T.; Dinarello, C. A., Non-redundant properties of IL-1α and IL-1β during acute colon inflammation in mice. Gut 2013, gutjnl-2012-303329.

70. Rider, P.; Kaplanov, I.; Romzova, M.; Bernardis, L.; Braiman, A.; Voronov, E.; Apte, R. N., The transcription of the alarmin cytokine interleukin-1 alpha is controlled by hypoxia inducible factors 1 and 2 alpha in hypoxic cells. Frontiers in immunology 2012, 3, 290.

71. McDowell, T. L.; Symons, J. A.; Duff, G. W., Human interleukin-1α gene expression is regulated by Sp1 and a transcriptional repressor. Cytokine 2005, 30 (4), 141-153.

72. Chan, J.; Atianand, M.; Jiang, Z.; Carpenter, S.; Aiello, D.; Elling, R.; Fitzgerald, K. A.; Caffrey, D. R., Cutting edge: a natural antisense transcript, AS-IL1α, controls inducible transcription of the proinflammatory cytokine IL-1α. The Journal of Immunology 2015, 195 (4), 1359-1363.

73. van Rietschoten, J. G.; Verzijlbergen, K. F.; Gringhuis, S. I.; van der Pouw Kraan, T. C.; Bayley, J.-P.; Wierenga, E. A.; Jones, P. A.; Kooter, J. M.; Verweij, C. L., Differentially methylated alleles in a distinct region of the human interleukin-1α

promoter are associated with allele-specific expression of IL-1α in CD4+ T cells. Blood 2006, 108 (7), 2143-2149.

74. Modi, W. S.; Masuda, A.; Yamada, M.; Oppenheim, J. J.; Matsushima, K.; O'Brien, S. J., Chromosomal localization of the human interleukin 1α (IL-1α) gene. Genomics 1988, 2 (4), 310-314.

75. Lomedico, P. T.; Gubler, U.; Hellmann, C. P.; Dukovich, M.; Giri, J. G.; Pan, Y.-C. E.; Collier, K.; Semionow, R.; Chua, A. O.; Mizel, S. B., Cloning and expression of murine interleukin-1 cDNA in Escherichia coli. Nature 1984, 312 (5993), 458-462.

76. Auron, P. E.; Webb, A. C.; Rosenwasser, L. J.; Mucci, S. F.; Rich, A.; Wolff, S. M.; Dinarello, C. A., Nucleotide sequence of human monocyte interleukin 1 precursor cDNA. Proceedings of the National Academy of Sciences 1984, 81 (24), 7907-7911.

77. Graves, B. J.; Hatada, M. H.; Hendrickson, W. A.; Miller, J. K.; Madison, V. S.; Satow, Y., Structure of interleukin 1. alpha. at 2.7-. ANG. resolution. Biochemistry 1990, 29 (11), 2679-2684.

78. Priestle, J. P.; Schär, H.-P.; Grütter, M., Crystal structure of the cytokine interleukin-1 beta. The EMBO journal 1988, 7 (2), 339.

79. Cook, A. D.; Christensen, A. D.; Tewari, D.; McMahon, S. B.; Hamilton, J. A., Immune cytokines and their receptors in inflammatory pain. Trends in immunology 2018, 39 (3), 240-255.

80. Dower, S. K.; Kronheim, S. R.; Hopp, T. P.; Cantrell, M.; Deeley, M.; Gillis, S.; Henney, C. S.; Urdal, D. L., The cell surface receptors for interleukin-1α and interleukin-1β are identical. 1986.

81. Dinarello, C. A., Introduction to the interleukin-1 family of cytokines and receptors: Drivers of innate inflammation and acquired immunity. Immunological reviews 2018, 281 (1), 5-7.

82. Palomo, J.; Dietrich, D.; Martin, P.; Palmer, G.; Gabay, C., The interleukin (IL)-1 cytokine family–Balance between agonists and antagonists in inflammatory diseases. Cytokine 2015, 76 (1), 25-37.

83. Shimizu, K.; Nakajima, A.; Sudo, K.; Liu, Y.; Mizoroki, A.; Ikarashi, T.; Horai, R.; Kakuta, S.; Watanabe, T.; Iwakura, Y., IL-1 receptor type 2 suppresses collagen-induced arthritis by inhibiting IL-1 signal on macrophages. The Journal of Immunology 2015, 194 (7), 3156-3168.

84. Afonina, I. S.; Müller, C.; Martin, S. J.; Beyaert, R., Proteolytic processing of interleukin-1 family cytokines: variations on a common theme. Immunity 2015, 42 (6), 991-1004.

85. Rupp, E.; Cameron, P.; Ranawat, C.; Schmidt, J.; Bayne, E., Specific bioactivities of monocyte-derived interleukin 1 alpha and interleukin 1 beta are similar to each other on cultured murine thymocytes and on cultured human connective tissue cells. Journal of Clinical Investigation 1986, 78 (3), 836.

86. Weber, A.; Wasiliew, P.; Kracht, M., Interleukin-1 (IL-1) pathway. Sci. Signal. 2010, 3 (105), cm1-cm1.

87. Ozbabacan, S. E. A.; Gursoy, A.; Nussinov, R.; Keskin, O., The structural pathway of interleukin 1 (IL-1) initiated signaling reveals mechanisms of oncogenic mutations and SNPs in inflammation and cancer. PLoS computational biology 2014, 10 (2), e1003470.

88. Thomas-Jardin, S. E.; Dahl, H.; Bautista, M.; Ha, F.; Jacob, J.; Nawas, A. F.; Kanshwala, M.; Xing, C.; Delk, N., NF-κB (p65) mediates interleukin-1 (IL-1) repression of androgen receptor (AR) in AR+ prostate cancer (PCa) cell lines. AACR: 2019.

89. Lamacchia, C.; Rodriguez, E.; Palmer, G.; Gabay, C., Endogenous IL-1α is a chromatin-associated protein in mouse macrophages. Cytokine 2013, 63 (2), 135-144.

90. Moussion, C.; Ortega, N.; Girard, J.-P., The IL-1-like cytokine IL-33 is constitutively expressed in the nucleus of endothelial cells and epithelial cells in vivo: a novel 'alarmin'? PloS one 2008, 3 (10), e3331.

91. Eastgate, J.; Symonns, J.; Wood, N.; Capper, S.; Duff, G., Plasma levels of interleukin-1-alpha in rheumatoid arthritis. Rheumatology 1991, 30 (4), 295-297.

92. Graudal, N. A.; Svenson, M.; Tarp, U.; Garred, P.; Jurik, A. G.; Bendtzen, K., Autoantibodies against interleukin 1α in rheumatoid arthritis: association with long term radiographic outcome. Annals of the rheumatic diseases 2002, 61 (7), 598-602.

93. Kristensen, M.; Deleuran, B.; Eedy, D.; LDMANN, M.; Breathnach, S.; Brennan, F., Distribution of interleukin 1 receptor antagonist protein (IRAP), interleukin 1 receptor, and interleukin 1α in normal and psoriatic skin. Decreased expression of IRAP in psoriatic lesional epidermis. British Journal of Dermatology 1992, 127 (4), 305-311.

94. Medzhitov, R., Origin and physiological roles of inflammation. Nature 2008, 454 (7203), 428-435.

95. Summers, C.; Rankin, S. M.; Condliffe, A. M.; Singh, N.; Peters, A. M.; Chilvers, E. R., Neutrophil kinetics in health and disease. Trends in immunology 2010, 31 (8), 318-324.

96. Mantovani, A.; Sozzani, S.; Locati, M.; Allavena, P.; Sica, A., Macrophage polarization: tumor-associated macrophages as a paradigm for polarized M2 mononuclear phagocytes. Trends in immunology 2002, 23 (11), 549-555.

97. Cohen, I.; Rider, P.; Carmi, Y.; Braiman, A.; Dotan, S.; White, M. R.; Voronov, E.; Martin, M. U.; Dinarello, C. A.; Apte, R. N., Differential release of chromatin-bound IL-1α discriminates between necrotic and apoptotic cell death by the ability to induce sterile inflammation. Proceedings of the National Academy of Sciences 2010, 107 (6), 2574-2579.

98. Luheshi, N. M.; McColl, B. W.; Brough, D., Nuclear retention of IL-1α by necrotic cells: A mechanism to dampen sterile inflammation. European journal of immunology 2009, 39 (11), 2973-2980.

99. Scaffidi, P.; Misteli, T.; Bianchi, M. E., Release of chromatin protein HMGB1 by necrotic cells triggers inflammation. Nature 2010, 467 (7315), 622-622.

100. Chen, C.-J.; Kono, H.; Golenbock, D.; Reed, G.; Akira, S.; Rock, K. L., Identification of a key pathway required for the sterile inflammatory response triggered by dying cells. Nature medicine 2007, 13 (7), 851-856.

101. Eigenbrod, T.; Park, J.-H.; Harder, J.; Iwakura, Y.; Núñez, G., Cutting edge: critical role for mesothelial cells in necrosis-induced inflammation through the recognition of IL-1α released from dying cells. The Journal of Immunology 2008, 181 (12), 8194-8198.

102. Kono, H.; Karmarkar, D.; Iwakura, Y.; Rock, K. L., Identification of the cellular sensor that stimulates the inflammatory response to sterile cell death. The Journal of Immunology 2010, 184 (8), 4470-4478.

103. Furutani, Y.; Notake, M.; Fukui, T.; Ohue, M.; Nomura, H.; Yamada, M.; Nakamura, S., Complete nucleotide sequence of the gene for human interleukin 1 alpha. Nucleic acids research 1986, 14 (8), 3167-3179.

104. Kawaguchi, Y.; Hara, M.; Wright, T. M., Endogenous IL-1α from systemic sclerosis fibroblasts induces IL-6 and PDGF-A. The Journal of clinical investigation 1999, 103 (9), 1253-1260.

105. Aden, N.; Nuttall, A.; Shiwen, X.; de Winter, P.; Leask, A.; Black, C. M.; Denton, C. P.; Abraham, D. J.; Stratton, R. J., Epithelial cells promote fibroblast activation via IL-1α in systemic sclerosis. Journal of Investigative Dermatology 2010, 130 (9), 2191-2200.

106. Kawaguchi, Y.; Hara, M.; Kamatani, N.; Wright, T. M., Identification of an IL1A gene segment that determines aberrant constitutive expression of interleukin-1α in systemic sclerosis. Arthritis & Rheumatism 2003, 48 (1), 193-202.

107. Kawaguchi, Y.; McCarthy, S. A.; Watkins, S. C.; Wright, T. M., Autocrine activation by interleukin 1alpha induces the fibrogenic phenotype of systemic sclerosis fibroblasts. The Journal of rheumatology 2004, 31 (10), 1946-1954.

108. Griffin, W.; Stanley, L.; Ling, C.; White, L.; MacLeod, V.; Perrot, L.; White, C.; Araoz, C., Brain interleukin 1 and S-100 immunoreactivity are elevated in Down syndrome and Alzheimer disease. Proceedings of the National Academy of Sciences 1989, 86 (19), 7611-7615.

109. Griffin, W. S. T.; Sheng, J. G.; Roberts, G. W.; Mrak, R. E., Interleukin-1 expression in different plaque types in Alzheimer's disease: significance in plaque evolution. Journal of Neuropathology & Experimental Neurology 1995, 54 (2), 276-281.

110. Grimaldi, L. M.; Casadei, V. M.; Ferri, C.; Veglia, F.; Licastro, F.; Annoni, G.; Biunno, I.; Bellis, G. D.; Sorbi, S.; Mariani, C., Association of Early-Onset Alzheimer's Disease with an Interieukin-1 x Gene Polymorphism. Annals of neurology 2000, 47 (3), 361-364.

111. Nicoll, J. A.; Mrak, R. E.; Graham, D. I.; Stewart, J.; Wilcock, G.; MacGowan, S.; Esiri, M. M.; Murray, L. S.; Dewar, D.; Love, S., Association of interleukin-1 gene polymorphisms with Alzheimer's disease. Annals of neurology 2000, 47 (3), 365.

112. Combarros, O.; Sánchez-Guerra, M.; Infante, J.; Llorca, J.; Berciano, J., Gene dose-dependent association of interleukin-1A [-889] allele 2 polymorphism with Alzheimer's disease. Journal of neurology 2002, 249 (9), 1242-1245.

113. Qin, X.; Peng, Q.; Zeng, Z.; Chen, Z.; Lin, L.; Deng, Y.; Huang, X.; Xu, J.; Wu, H.; Huang, S., Interleukin-1A− 889C/T polymorphism and risk of Alzheimer's disease: a meta-analysis based on 32 case–control studies. Journal of neurology 2012, 259 (8), 1519-1529.

114. Grossi, S. G.; Zambon, J. J.; Ho, A. W.; Koch, G.; Dunford, R. G.; Machtei, E. E.; Norderyd, O. M.; Genco, R. J., Assessment of risk for periodontal disease. I. Risk indicators for attachment loss. Journal of periodontology 1994, 65 (3), 260-267.

115. Kornman, K. S.; Crane, A.; Wang, H. Y.; Giovlne, F. S. d.; Newman, M. G.; Pirk, F. W.; Wilson, T. G.; Higginbottom, F. L.; Duff, G. W., The interleukin-1 genotype as a severity factor in adult periodontal disease. Journal of clinical periodontology 1997, 24 (1), 72-77.

116. López, N. J.; Valenzuela, C. Y.; Jara, L., Interleukin-1 gene cluster polymorphisms associated with periodontal disease in type 2 diabetes. Journal of periodontology 2009, 80 (10), 1590-1598.

117. Shirodaria, S.; Smith, J.; McKay, I.; Kennett, C.; Hughes, F., Polymorphisms in the IL-1A gene are correlated with levels of interleukin-1α protein in gingival crevicular fluid of teeth with severe periodontal disease. Journal of Dental Research 2000, 79 (11), 1864-1869.

118. Balkwill, F., Tumor necrosis factor or tumor promoting factor? Cytokine and Growth Factor Reviews 2002, 13 (2), 135-141.

119. Szlosarek, P. W.; Balkwill, F. R., Tumour necrosis factor α: a potential target for the therapy of solid tumours. The lancet oncology 2003, 4 (9), 565-573.

120. Voronov, E.; Shouval, D. S.; Krelin, Y.; Cagnano, E.; Benharroch, D.; Iwakura, Y.; Dinarello, C. A.; Apte, R. N., IL-1 is required for tumor invasiveness and angiogenesis. Proceedings of the National Academy of Sciences 2003, 100 (5), 2645-2650.

121. Carmi, Y.; Voronov, E.; Dotan, S.; Lahat, N.; Rahat, M. A.; Fogel, M.; Huszar, M.; White, M. R.; Dinarello, C. A.; Apte, R. N., The role of macrophage-derived IL-1 in induction and maintenance of angiogenesis. The Journal of Immunology 2009, 183 (7), 4705-4714.

122. Nathan, C., Points of control in inflammation. Nature 2002, 420 (6917), 846-852.

123. Vakkila, J.; Lotze, M. T., Inflammation and necrosis promote tumour growth. Nature Reviews Immunology 2004, 4 (8), 641-648.

124. Dvorkin, T.; Song, X.; Argov, S.; White, R. M.; Zoller, M.; Segal, S.; Dinarello, C. A.; Voronov, E.; Apte, R. N., Immune phenomena involved in the in vivo regression of fibrosarcoma cells expressing cell-associated IL-1α. Journal of leukocyte biology 2006, 80 (1), 96-106.

125. Song, X.; Voronov, E.; Dvorkin, T.; Fima, E.; Cagnano, E.; Benharroch, D.; Shendler, Y.; Bjorkdahl, O.; Segal, S.; Dinarello, C. A., Differential effects of IL-1α and IL-1β on tumorigenicity patterns and invasiveness. The Journal of Immunology 2003, 171 (12), 6448-6456.

126. Voronov, E.; Weinstein, Y.; Benharroch, D.; Cagnano, E.; Ofir, R.; Dobkin, M.; White, R. M.; Zoller, M.; Barak, V.; Segal, S., Antitumor and immunotherapeutic effects of activated invasive T lymphoma cells that display short-term interleukin 1α expression. Cancer research 1999, 59 (5), 1029-1035.

127. Tjomsland, V.; Spångeus, A.; Välilä, J.; Sandström, P.; Borch, K.; Druid, H.; Falkmer, S.; Falkmer, U.; Messmer, D.; Larsson, M., Interleukin 1α sustains the expression of inflammatory factors in human pancreatic cancer microenvironment by targeting cancer-associated fibroblasts. Neoplasia 2011, 13 (8), 664-IN3.

128. Qin, Y.; Ekmekcioglu, S.; Liu, P.; Duncan, L. M.; Lizée, G.; Poindexter, N.; Grimm, E. A., Constitutive aberrant endogenous interleukin-1 facilitates inflammation and growth in human melanoma. Molecular Cancer Research 2011, 9 (11), 1537-1550.

129. Matsuo, Y.; Sawai, H.; Ochi, N.; Yasuda, A.; Takahashi, H.; Funahashi, H.; Takeyama, H.; Guha, S., Interleukin-1α secreted by pancreatic cancer cells promotes angiogenesis and its therapeutic implications. Journal of Surgical Research 2009, 153 (2), 274-281.

130. Cheng, J.; Li, L.; Liu, Y.; Wang, Z.; Zhu, X.; Bai, X., Interleukin-1α induces immunosuppression by mesenchymal stem cells promoting the growth of prostate cancer cells. Molecular medicine reports 2012, 6 (5), 955-960.

Chapter Two

Molecular Cloning of Human Interleukin-1α Using Novel Thermostable Soluble Tag

Abstract

The efficiency of protein purification is vital to the development of pharmaceuticals and to the evolution of biomedical research. The cost of the most common techniques used for purification of recombinant proteins constitutes a significant portion of the multi-billion-dollar pharmaceutical industry, particularly due to the conversion of some proteins into inclusion bodies when using a heterologous host.

The investigations into more cost-effective and less labor-intensive methods for the purification of recombinant proteins are important to receive higher yields at a lowered monetary investment. Rubredoxin (Rd) is a 53 amino acid long protein, which is an ideal tag due to its low molecular weight (7kDa), red color for easy identification, and extreme thermostability. The Rd protein is the tag used in the purification of IL-1α, D2 (FGF1 receptor domain), and the anti-fungal peptide. This novel tag has been named ARK-RUBY-tag which stands for Arkansas Rubredoxin purification tag and ruby refers to the red color of the protein. The tag was able to keep all recombinant proteins in soluble form. The protein expression was monitored by the presence of the red color. Since the main subject of this project is IL-1α, the tag and the fusion protein were examined thoroughly, which shed light on the main properties and characterization of the tag. Utilizing the tag, IL-1α was purified in high yields and displayed good bioactivity. The Ark-RUBY- recombinant proteins showed significant thermal stability.

Introduction

Recombinant DNA technology and the production of recombinant proteins have evolved in the pharmaceutical and biotechnological industry through the introduction of drug-based protein production for use in healthcare[1]. Due to unsatisfactory yields of bioactive proteins isolated from their natural sources, the large-scale production of recombinant proteins in suitable heterologous host systems have been of significant interest[2, 3]. In particular, *Escherichia coli* (*E. coli*) has been extensively used as a suitable heterologous host to facilitate recombinant protein expression because it is compatible with various cloning vectors, its amenability to genetic modification(s), high transformation efficiency, and its adaptability for rapid high-density cultivation under variety conditions[4-6]. However, high yield of recombinant protein expression in *E. coli* causes protein aggregation and inclusion bodies (IBs) formation, which is a common major problem in the large-scale production of recombinant proteins in heterologous host systems[7, 8]. IBs are dense intracellular bodies mostly consisting of aggregated recombinant proteins that are misfolded and hence are functionally inactive[9]. Recovering of target recombinant proteins which form inclusion bodies involves multiple steps such as, isolation of pure inclusion bodies, solubilization of inclusion bodies, refolding of solubilized recombinant protein(s) and purification of refolded proteins using different various chromatographic techniques[10-12]. Inclusion bodies are highly specific aggregates and mostly consist of the recombinant protein of interest[13, 14]. Owing to the multiple steps involved, the yields of the pure and bioactive target recombinant proteins from IBs is often very low[15, 16]. Biotechnology and pharmaceutical companies incur huge losses amounting to millions of dollars in *lieu* of the multiple, cumbersome, time-consuming,

and labour-intensive steps involved in recovery of recombinant proteins that are biomedically significant or serve as potential therapeutics against a wide array of diseases[5, 17]. In this context, there is immense commercial interest in designing methods to thwart the overexpression of recombinant proteins, of biomedical importance, as inclusion bodies. The target fusion protein is overexpressed and the specific binding characteristics of the affinity tag are exploited to selectively purify target fusion proteins by employing a relevant affinity chromatographic technique[18, 19]. The affinity tag is subsequently separated from the target protein by selective cleavage of the target fusion protein using restriction proteases[20]. A number of fusion protein tags including, glutathione S-transferase (GST)[21], thioredoxin A (TrxA)[22], maltose-binding protein (MBP)[23], poly histidine (His)[24], green fluorescent protein (GFP)[25], streptavidin, ketosteroid isomerase (KSI)[26], and heparin binding (HB)[27] peptide have been successfully used for the overexpression and purification of recombinant proteins in different expression hosts including *E. coli*. However, use of these purification tags has one or more significant limitations such as, i) higher molecular weight of affinity tags which reduces column capacity[28], ii) poor solubility of affinity tag(s)[24], iii) high costs of affinity resins[29], iv) low expression yields[30], v) interference with the folding and functional properties of target recombinant proteins, vi) involvement of expensive mobile phase buffers[28], and vii) poor temperature stability and susceptibility to proteases secreted by expression hosts[31]. In this context, there is significant interest toward the development of a protein affinity tag that renders recombinant protein overexpression and purification simple, efficient, versatile, and cost-effective[32, 33].

Rubredoxin (Rd) is a small molecular weight monomeric non-heme iron-sulfur protein (7 kDa), composed of 53-58 amino acids[34, 35]. Rd has been isolated from several thermophilic and mesophilic organisms[36]. Rd was first identified from *Pyrococcus furiosus (PfRd),* a hyperthermophilic anaerobic archaeon able to thrive in oceanic hot springs at temperatures approaching 100°C[37, 38]. Rd protein has an exceptionally high thermal stability (T_m > 90°C)[36]. Rd from *Pyrococcus furiosus* is the most stable protein which has currently been identified[39]. Rd belongs to the α and β class of proteins consisting of 2 α-helices and 2 or 3 antiparallel β-strands[40]. The active site of Rubredoxin contains an iron-sulfur cluster [Fe_2S_2] wherein an iron ion is coordinated by the sulfurs of four cysteine residues of the protein[40]. The expression of recombinant proteins in *E. coli* was monitored using the absorption of Rd from *Thermotoga maritima* at 380 nm[41]. Overexpression and purification of recombinant proteins were achieved using rubredoxin from a mesophilic anaerobic bacteria, *Desulfovibrio vulgaris*[42]. However, using this technique was limited by the difficulty to prevent the formation of inclusion bodies due to the lower thermal stability and slower folding rates of this bacterial strain. Moreover, there was loss of the iron sulfur center, responsible for the red color formation, due to the lower stability of the rubredoxin from *Desulfovibrio vulgaris* during large-scale production of recombinant proteins[41]. Interestingly, Rubredoxin from *Pyrococcus furiosus* shares about 63 % amino acid sequence identity with its mesophilic counterpart[43, 44]. In this context, in the present study, a novel polyhistidine Rd purification tag was designed, which I would prefer to *hitherto* name as Ark-RUBY (Arkansas Rubredoxin purification tag), for the soluble overexpression of recombinant protein/peptides in heterologous hosts. Linking the polyhistidine tag to Rd is also

expected to aid in the purification of Ark-RUBY fused target protein/peptide(s) using nickel/cobalt affinity chromatography[45-47]. Also, the amino acid sequence of Rd does not contain methionine. This aspect will facilitate the cleavage of the Rd-fused methionine-less recombinant protein/peptide(s) in a cost-effective manner using cyanogen bromide (CNBr), a reagent that specifically cleaves polypeptide chains at the C-terminal end of methionine[48-50].

Experimental methods

pUARC-RUBY expression vector and construction and expression of the Ark-RUBY-IL-1α, Ark-RUBY-D2 and Ark-RUBY-AF gene

The designed expression vector with novel peptide fusion partner to Rd (Rubredoxin, little iron-Sulfur protein: originated in *P. furiosus*) for *E. coli* heterologous expression is outlined (Figure 1).

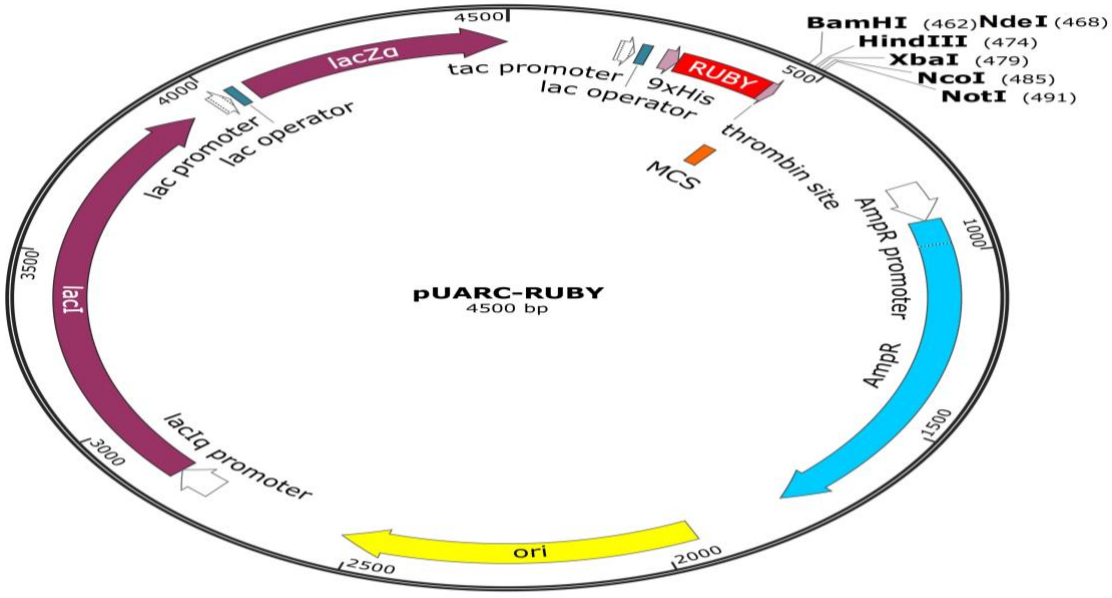

Figure 1: Map of pUARC-RUBY plasmid: The rubredoxin gene with 9-histidine tag cloned under *tac* promoter. The carboxyl terminus of RD gene sequence encodes specific thrombin site with overlapping BamHI and other MCS in pGEX series vector. The segment map of promoter, rbs, RD and MCS are highlighted below. The total sequence of pUARC-RUBY is 4500bp.

As depicted in illustration, the higher copy number origin, *Ori* is with tac promoter, as highly successfully used for GST tagged pGEX series vectors. The Rd gene sequence (5'-ATGGCGAAATGGGTGTGCAAAATTTGCGGCTATATTTATGATGAAGATGCGGGCGATCCGGATAACGGCATTAGCCCGGGCACCAAATTTGAAGAACTGCCGGATGATTGGGTGTGCCCGATTTGCGGCGCGCCGAAAAGCGAATTTGAAAAACTGGAAGAT-3') was used with unique 9-histidine tag encoded by (5'CATCATCACCATCACCATCACCATCAC3') the fusion partner at the amino terminus. The specific thrombin cleavage site of LVPRGS encoded by (5'CTGGTGCCGCGTGGATCC-3') was used as part of multi-cloning site, MCS (besides BamHI, underlined endonuclease sequence, other selective endonuclease sites at MCS are: NdeI, HindIII, XbaI, XhoI and NotI) for single step cloning of any host protein. The vector design originated by inserting the synthetic gene sequence (Genscript Inc.) with the GST replacement, which was inserted using BtgI and NotI restriction enzymes. The DNA sequence was verified by sequencing. The model host protein, interleukin-1α (IL-1alpha, commonly known as hematopoietin 1 is a cytokine of the interleukin 1 family which, in humans, is encoded by the *IL1A* gene) was cloned into pUARC-RUBY by utilizing the MCS, namely the NdeI and XhoI cloning sites in the expression vector. The final sequence of this construct was verified by DNA sequencing. Polymerase chain reaction (PCR) was used to amplify gene specific primers, which code for the Ark-RUBY-IL-1α. The vector that contains the 9×His-Ark-RUBY-IL-1α was then transformed into *E. coli* cells. After obtaining confirmation of the nucleotide sequences, protein was overexpressed in BL21(pLysS) *E. coli* cells cultured in 1 L of terrific broth (TB) medium containing 500 µg/mL ampicillin and 500 µg/mL chloramphenicol. The

induction of protein was accomplished by the addition of IPTG (final concentration 0.5 mM) when the OD at Abs 600 of the growing culture had reached 0.6. After 4 hours incubation of the culture at 37 °C with agitation at 250 rpm, the cells were harvested and lysed by ultra-sonication. The cell lysate was separated from the cell debris using ultra centrifugation at 19,000 rpm. The same methods were followed for the expression of Ark-RUBY-D2 and Ark-RUBY-AF by using Ark-RUBY-D2 and Ark-RUBY-AF genes, respectively (Figure 1 & 2 panel A, B, & C & Figure 3).

Negative staining Transmission electron microscope

Bacterial pellets of 6×His-IL-1α, Ark-RUBY-IL-1α, 6×His-D2 and Ark-RUBY-D2 were overexpressed in *E. coli* cells. The treated *E. coli* cells were resuspended with 10 mM PBS at pH-7.2. Each resuspended solution was spotted onto a Formvar and carbon-coated copper grid (Electron Microscopy Sciences, USA). A 2% solution of Uranyl acetate dissolved in distilled water (pH 4.2 to 4.5) was used to negatively stain the samples. Uranyl acetate solution was filtered through a 0.22 µm filter before use. After 2 minutes, the remaining solution was removed with filter paper and the samples were dried with filter paper. TEM images were taken at different magnifications by using high resolution transmission electron microscopy (Jeol-HRTEM-2011, USA) with an accelerating voltage of 80-100 kV.

Purification of recombinant Ark-RUBY-IL1α and IL-1α

Nickel (Ni^{2+})-Sepharose column (Amersham Biosciences, USA) was used for purification of Ark-RUBY-IL-1α. The clear bacterial cell lysate was centrifuged for 25 minutes at 19,000 rpm 4°C. Then the supernatant was loaded on to a nickel (Ni^{2+})-Sepharose column, and then the column was washed with 10mM PBS (phosphate

buffered saline) at pH 7.2. A stepwise gradient of imidazole was used to elute all proteins bound to the Ni^{2+}-Sepharose column. The elution of proteins was monitored by absorbance measured at 280 nm. Fractions collected at a concentration of 250 mM Imidazole contain the Ark-RUBY-IL-1α protein. At that point, pure Ark-RUBY-IL-1α was incubated with 100 NIH units of thrombin for 12 h (at 37°C) to cleave the affinity tag. After that, thrombin cleavage products were reloaded onto a Ni^{2+}-Sepharose column. In order to elute IL-1α, the column was washed thoroughly with 10 mM PBS at pH 7.2 and a stepwise imidazole gradient was used. IL-1α was eluted in the 250 mM imidazole fraction. The 250 mM Imidazole fraction was subjected to desalting by ultrafiltration using a 10 kDa cut-off membrane. Then, the bound Ark-RUBY tag was eluted in 250 mM and 500 mM imidazole fractions. At each step, SDS-PAGE was performed to check the purity. At the final point, IL-1α concentration was estimated by Abs 280 nm, using the extinction coefficient value ($\Sigma 280 = 21430\ M^{-1}\ cm^{-1}$) that is calculated from the amino acid sequence of the protein.

Western-blot detection method

Purified Ark-RUBY-fusion proteins were resolved on 15% SDS-PAGE under reduced conditions. The gel containing the fusion proteins was subjected to blot transfer for western blot. Blotted/spotted nitrocellulose membrane was blocked using 5% skim milk in 1x TBS-T (10mM tris, 100mM NaCl, 0.05% Tween-20; pH 7.4) at room temperature for 1hr. Subsequently, the membrane was washed with 0.2% BSA in 1XTBS-T and the primary antibodies raised in goat against the His tag was added at 1:2500 dilution and incubated overnight at 4°C. Secondary antibody conjugated with alkaline phosphatase that detects the IgG goat antibody was added to the membrane at

1:2500 dilution and incubated for 2 hours at 4◦C. The band on the membrane was detected using the NBT/BCIP (Nitro-blue tetrazolium/5-Bromo-4-chloro-3-indolyl phosphate) substrate within 60 seconds of exposure.

Purification of Ark-RUBY-AF by Heat treatment

The *E. coli* bacterial lysate was subjected to heat treatment at increasing temperatures in a water bath from 25 °C to 90 °C (at 5°C intervals) for 10 minutes. All samples were centrifuged at 13,000 rpm for 5 minutes to separate the aggregates from the cell lysates. The results were revealed by SDS-PAGE gel for both samples (pellets and lysates).

Far UV-Circular Dichroism study

All far UV-circular dichroism (CD) measurements were performed on a Jasco-1500 spectrophotometer at 25 °C using a quartz cell with 1 mm path length with a scan-speed of 100 nm/sec. Each spectrum was an average of 3 scans. The concentration of Ark-RUBY, Ark-RUBY-IL-1α and purified IL-1α were maintained as 20 μM. The final spectrum was obtained after the subtraction of the corresponding buffer spectrum.

Equilibrium unfolding

The equilibrium unfolding experiments were performed on a Jasco-1500 spectrophotometer at 5°C intervals by using a concentration of Ark-RUBY- IL-1α, purified IL-1α, and Ark-RUBY of 20 μM in 10 mM PBS at pH7.2. The unfolding process of the proteins was monitored through changes of protein structure in the far-UV region (190-250nm). Required background corrections were made for all spectra.

Biological activity assay

Splenocytes were isolated from 6-12 weeks old C57BL/6J mice. The mice were housed under pathogen free conditions and maintained in the microisolator cages. The Institutional Animal Care and the Committee of the University of Arkansas approved for raising of the mice. Animal care complied with the recommendations of the Guide for care and use of Laboratory Animals (National Research Council). Dulbecco's Modified Eagle's Medium (DMEM), RPMI 1640, Dulbecco's Phosphate Buffered Saline (PBS), and Fetal Bovine Serum (FBS) were obtained from HyClone Laboratories.

A

Ark-RUBY-IL1α:
Nucleotide sequence:
AUGCAUCAUCAUCAUCAUCAUAUGGCGAAAUGGGUGUGCAAAAUUUGCGGCUAUAUUUAUGAUGAAGAUGCGGGCGAU
CCGGAUAAUGGCAUUUCCCCGGGCACCAAAUUUGAAGAACUGCCGGAUGAUUGGGUGUGCCCGAUUUGCGGCGCGCC
GAAAUCCGAAUUUGAAAAACUGGAAGAUCUGGUGCCGCGUGGCUCCAUGCGUUCCGCGCCGUUUUCCUUUCUGUCCAA
UGUGAAAUAUAAUUUUAUGCGUAUUAUUAAAUAUGAAUUUAUUCUGAAUGAUGCGCUGAAUCAGUCCAUUAUUCGUGCG
AAUGAUCAGUAUCUGACCGCGGCGGCGCUGCAUAAUCUGGAUGAAGCGGUGAAAUUUGAUAUGGGCGCGUAUAAAUCC
UCCAAAGAUGAUGCGAAAAUUACCGUGAUUCUGCGUAUUUCCAAAACCCAGCUGUAUGUGACCGCGCAGGAUGAAGAU
CAGCCGGUGCUGCUGAAAGAAAUGCCGGAAAUUCCGAAAACCAUUACCGGCUCCGAAACCAAUCUGCUGUUUUUUUGG
GAAACCCAUGGCACCAAAAAUUAUUUUACCUCCGUGGCGCAUCCGAAUCUGUUUAUUGCGACCAAACAGGAUUAUUGG
GUGUGCCUGGCGGGCGGCCCGCCGUCCAUUACCGAUUUUCAGAUUCUGGAAAAUCAGCUGGAACAUCAUCAUCAUCAU
CAU
Amino acid Sequence:
MHHHHHHMAKWVCKICGYIYDEDAGDPDNGISPGTKFEELPDDWVCPICGAPKSEFEKLEDLVPRGSMRSAPFSFLSNVKYNF
MRIIKYEFILNDALNQSIIRANDQYLTAAALHNLDEAVKFDMGAYKSSKDDAKITVILRISKTQLYVTAQDEDQPVLLKEMPEIPKTITG
SETNLLFFWETHGTKNYFTSVAHPNLFIATKQDYWVCLAGGPPSITDFQILENQLEHHHHHH

B

Ark-RUBY-D2:
Nucleotide sequence:
AUGCAUCAUCAUCAUCAUCAUAUGGCGAAAUGGGUGUGCAAAAUUUGCGGCUAUAUUUAUGAUGAAGAUGCGGGCGAUCC
GGAUAAUGGCAUUUCCCCGGGCACCAAAUUUGAAGAACUGCCGGAUGAUUGGGUGUGCCCGAUUUGCGGCGCGCCGAAA
UCCGAAUUUGAAAAAGAAAAUCUGUAUUUUCAGCAGAAUAAUAAACGUGCGCCGUAUUGGACCAAUACCGAAAAAAUGGAA
AAACGUCUGCAUGCGGUGCCGGCGGCGAAUACCGUGAAAUUUCGUUGCCCGGCGGGCGGCAAUCCGAUGCCGACCAUG
CGUUGGCUGAAAAAUGGCAAAGAAUUUAAACAGGAACAUCGUAUUGGCGGCUAUAAAGUGCGUAAUCAGCAUUGGUCCCU
GAUUAUGGAAUCCGUGGUGCCGUCCGAUAAAGGCAAUUAUACCUGCGUGGUGGAAAAUGAAGCGGGCUCCAUUAAUCAU
ACCUAUCAUCUGGAUGUGGUGCUGGAAUCCACCCCGGAACUGGAAUUUGGCACCAAACUGGAUAUUCUGGAA
Amino acid Sequence:
MHHHHHHMAKWVCKICGYIYDEDAGDPDNGISPGTKFEELPDDWVCPICGAPKSEFEKENLYFQGNNKRAPYWTNTEKMEKRLH
AVPAANTVKFRCPAGGNPMPTMRWLKNGKEFKQEHRIGGYKVRNQHWSLIMESVVPSDKGNYTCVVENEAGSINHTYHLDVVLEE
LEFGTKLDILE

C

Ark-RUBY-AF:
Nucleotide sequence:
AUGCAUCAUCAUCAUCAUAUGGCGAAAUGGGUGUGCAAAAUUUGCGGCUAUAUUUAUGAUGAAGAUGCGGG
CGAUCCGGAUAAUGGCAUUUCCCCGGGCACCAAAUUUGAAGAACUGCCGGAUGAUUGGGUGUGCCCGAUUUGC
GGCGCGCCGAAAUCCGAAUUUGAAAAAGAAAAUCUGUAUUUUCAGCAGUCCUAUAAACGUAAAUUUUUUAAACGU
AAAUAU
Amino acid Sequence:
MHHHHHHMAKWVCKICGYIYDEDAGDPDNGISPGTKFEELPDDWVCPICGAPKSEFEKENLYFQGSYKRKFFKRKY

Figure 2: Panels- A, B, and C represent *Escherichia coli* codon optimized nucleotide sequence and single letter coded amino acid sequence of Ark-RUBY-IL-1α, Ark-RUBY-D2, and Ark-RUBY-AF [nucleotide sequence and corresponding amino acid sequence of Ark-RUBY tag shown in red, thrombin and TEV cleavage site shown in blue, target recombinant IL-1α, D2, and AF shown in black].

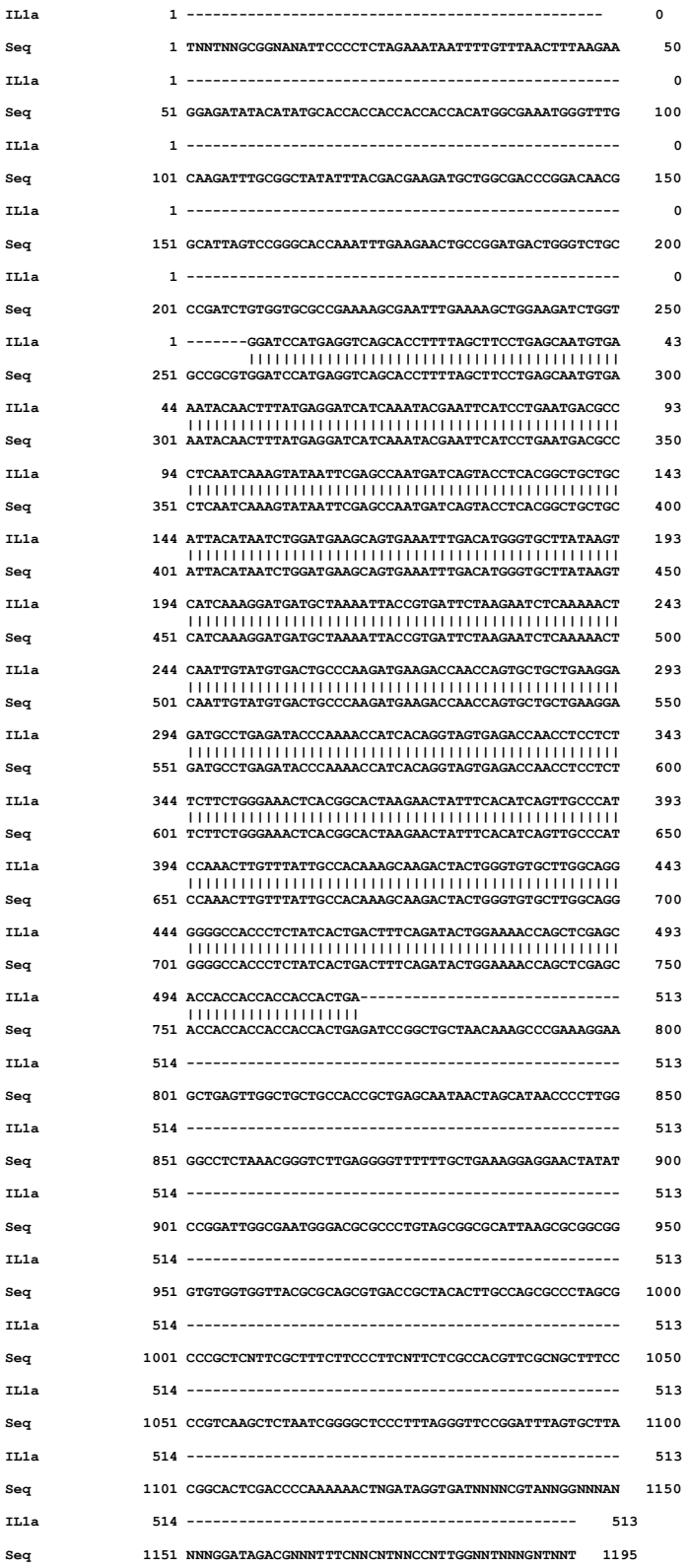

Figure 3: Represents experimental confirmation of the DNA sequence of human IL-1α.

Results & Discussion

Ark-RUBY prevents the formation of Inclusion bodies Ark-RUBY-IL-1α and Ark-RUBY-D2-FGFR1 are each overexpressed in *E. coli* as soluble proteins. In contrast, 6×His-IL-1α and 9×His-D2-FGFR1 were completely expressed as insoluble inclusion bodies. Transmission Electron Micrographs (TEM) of *E. coli* cells, induced by Isopropyl β-D thiogalactoside show that 6-His-IL-1α and 9xHis-D2-FGFR1 are overexpressed as dense and opaque inclusion bodies (Figure 4, Panel A and C). However, TEM data of the *E. coli* cells overexpressing Ark-RUBY-IL-1α and Ark-RUBY-D2-FGFR1 are mostly clear and do not show formation of inclusion bodies (Figure 3, Panel B and D).

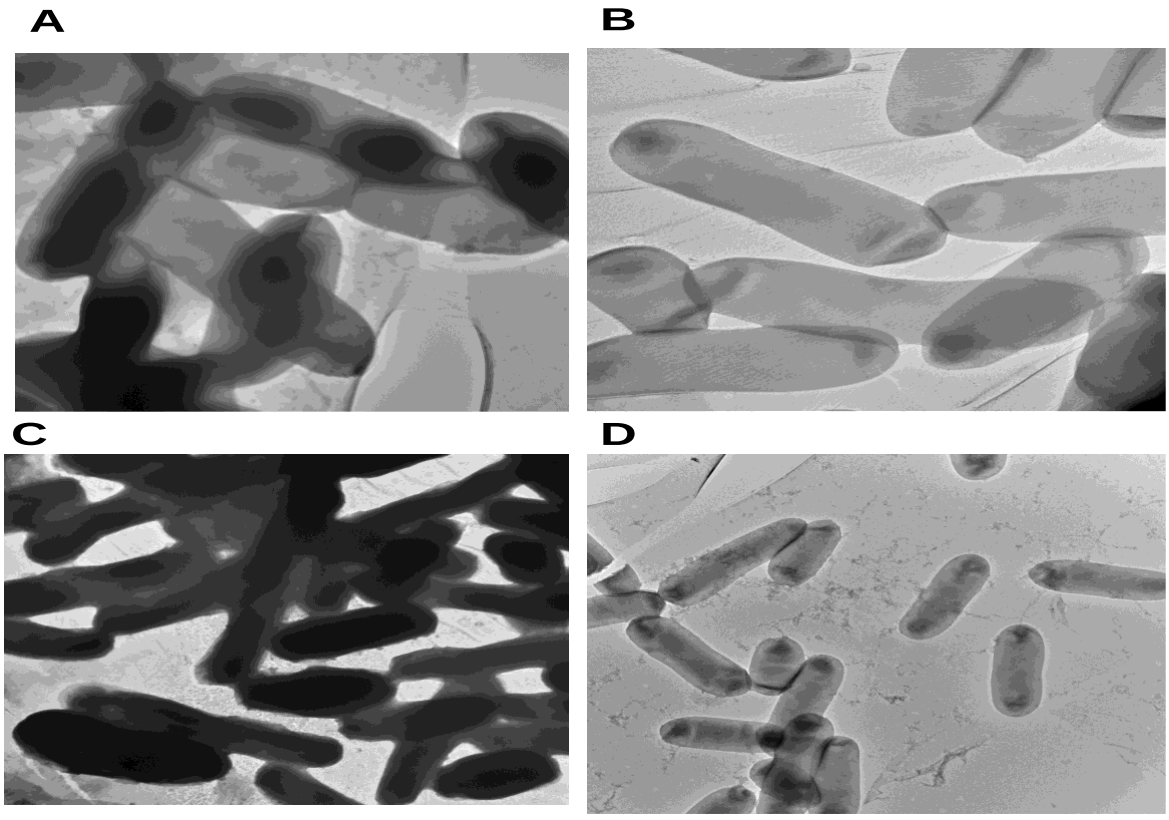

Figure 4: Panels-A, B, C and D represent selected negatively stained TEM images of 6×His-IL1-α, Ark-RUBY-IL-1α, 6XHis-D2, and Ark-RUBY-D2-FGFR1, overexpressed in *E. coli* cells. Scale bar is 500nm.

Color of the bacterial lysate containing overexpressed Ark-RUBY-target protein/peptide The bacterial lysate of Ark-Ruby tagged target proteins is pale to bright Ruby red (Figure 5). The RUBY red color of the bacterial lysate can be used as a reliable indicator of the overexpression of the Ark-RUBY tagged recombinant proteins/peptides and can be followed during. Data on the purification and characterization of recombinant IL1-α is elaborated subsequently in this study.

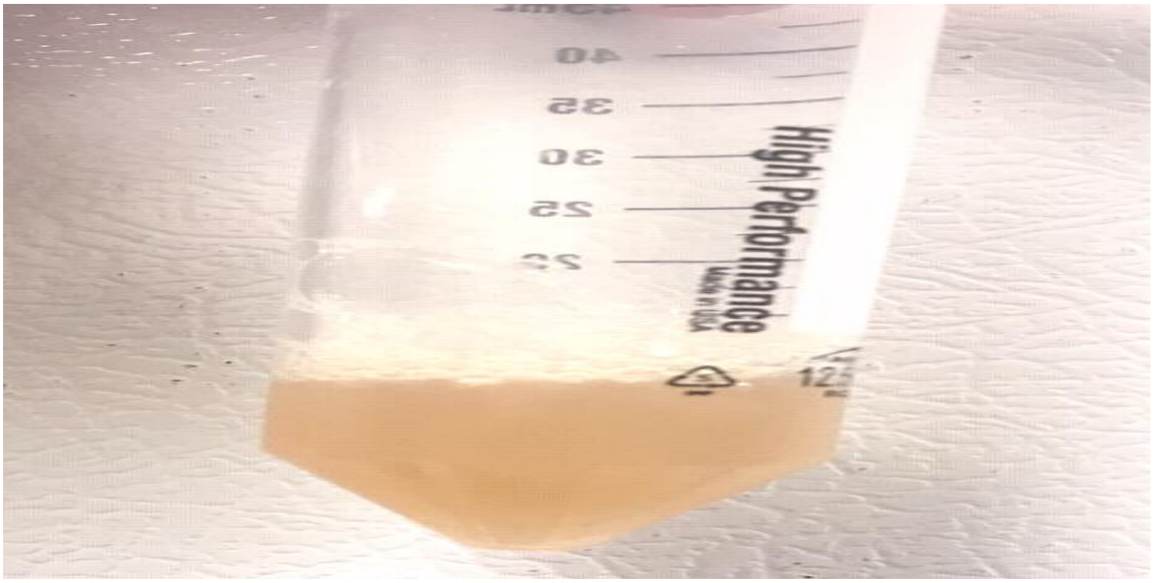

Figure 5: showing the Ruby red color of bacterial lysate of Ark-Ruby tagged target protein.

Ark-RUBY-IL-1α can be purified using Nickel-Affinity chromatography Both Ark-RUBY-Pro and Ark-RUBY-Pep clones contain an N-terminal 6xpolyhistidine tag and so are amenable to nickel (Ni)-affinity chromatography using an imidazole gradient. A ruby-red band formed when the bacterial lysate, containing overexpressed Ark-RUBY-IL-1α was loaded on the Ni-sepharose column. The movement of the ruby-red band corresponding to Ark-RUBY-IL-1α can be followed during the purification process

(Figure 6, Panel A). The elution profile of Ark-RUBY-IL-1α in different imidazole fractions is shown in Figure 7, Panel B.

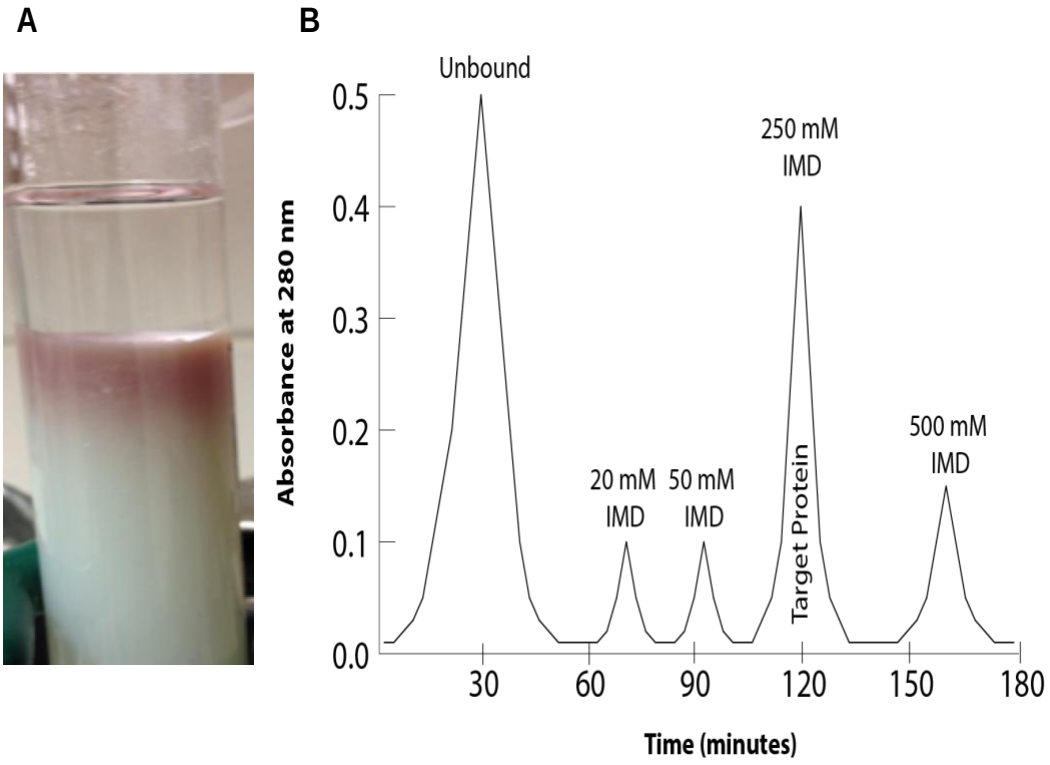

Figure 6: Panel-A showing the red color of Ark-RUBY tag fused to IL-1α, on Nickel (Ni^{2+})-Sepharose column. Panel-B represents elution profile of proteins contained in the supernatant, obtained by using stepwise imidazole (IMD) gradient. The profile depicts that the protein fractions eluted at different concentrations (20mM, 50mM, 100mM, 250mM and 500mM) of imidazole (IMD). Ark-RUBY-IL-1α is eluted at 250mM concentration of imidazole.

Ark-RUBY-IL-1α eluted completely in 250 mM imidazole fraction. SDS-PAGE of the eluted fractions revealed an intense band in the 250 mM fraction with a molecular mass (25kDa), which matches with that of Ark-RUBY-IL-1α (Figure 6, Panel A).

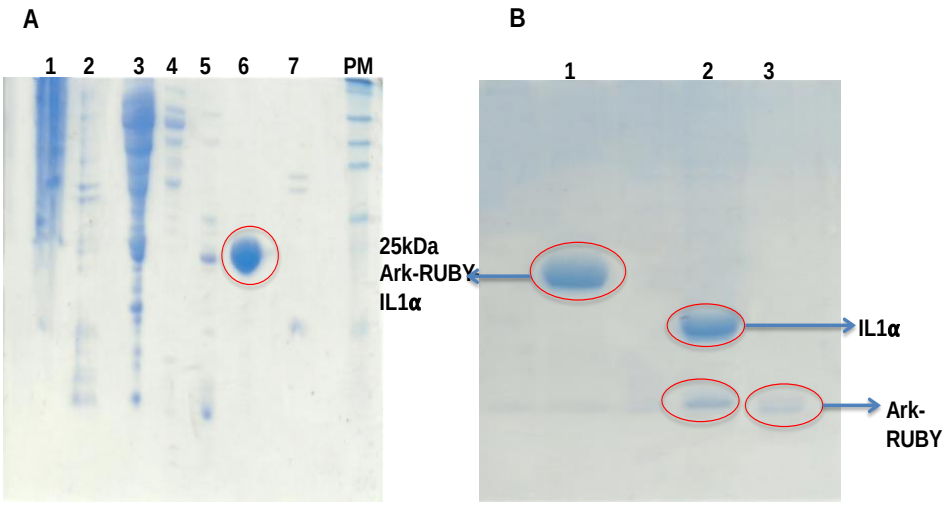

Figure 7: Purification of Ark-RUBY-IL-1α on Nickel (Ni^{2+})-Sepharose column. Elution of proteins in the supernatant was obtained by using a stepwise imidazole gradient. Panel- A shows SDS-PAGE gel of protein fractions eluted at different concentrations of imidazole as detected by Coomassie blue. Lane 1, Pellet (P); Lane 2, Supernatant; Lane 3, 20mM imidazole; Lane 4, 50mM imidazole; Lane 5, 100mM imidazole, Lane 6, 250mM imidazole; Lane 7, 500mM imidazole; PM, Protein molecular weight marker. Purified Ark-RUBY-IL-1α is eluted at 250mM imidazole concentration with corresponding molecular weight 25kDa. Panel-B represents Coomassie blue stained SDS-PAGE of Ark-RUBY-IL-1α reloaded on Ni-sepharose affinity chromatography after thrombin treatment. Lane 1, Ark-RUBY-IL-1α (before thrombin treatment); Lane 2, thrombin-cleaved Ark-RUBY-IL-1α eluted at 250mM imidazole Concentration (upper band corresponds to IL-1α and lower band corresponds to Ark-RUBY tag); After desalting 250mM imidazole fraction, the lower band is completely removed. Lane 3, Ark-RUBY tag is eluted at 500 mM imidazole concentration.

Coomassie blue and Silver staining data revealed that Ark-RUBY-IL-1α is > 98% pure (Figure 8, Panel A and Panel B). It should be mentioned the 6X polyHistidine-IL-1α is invariably expressed in inclusion bodies. Subsequent attempts to recover 6x polyHis-IL1α from the urea-denatured inclusion bodies was futile and did not yield any detectable amounts of the recombinant fusion protein. These results suggest that the Ark-RUBY tag not only thwarts the overexpression of the target protein(s) as inclusion bodies but also is amenable as an efficient purification method using Ni-affinity chromatography.

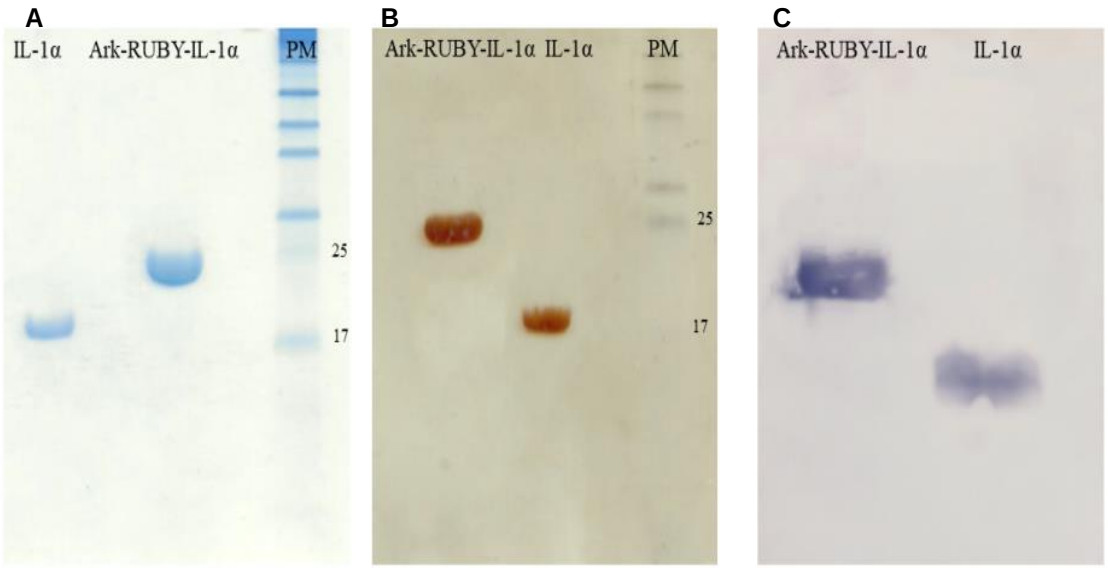

Figure 8: Panels- A and B represent Coomassie blue and silver stained SDS-PAGE of Ark-RUBY-IL-1α and thrombin-cleaved Ark-RUBY- IL-1α. Panel-C represents western blot of Ark-RUBY-IL-1α and thrombin-cleaved Ark-RUBY- IL-1α. Lane PM is the protein molecular weight marker. Coomassie blue staining, silver staining and western blot show a band (Mw ~17kDa) corresponds to pure IL-1α after thrombin cleavage.

Ark-RUBY tag can be successfully separated from the target recombinant protein/peptide Ark-RUBY-IL-1α has a -LVPRGS-thrombin cleavage site. Therefore, purified, Ark-RUBY-IL-1α was treated with thrombin at 37 °C. An additional chromatographic step of the thrombin cleaved products on Ni-sepharose showed that recombinant IL-1α elutes as expected in the 250 mM imidazole fraction with a small amount of Ark-RUBY tag but this band is completely eliminated during desalting and concentration of the 250 mM fraction by ultrafiltration using a 10 kDa cut-off membrane. The Ark-RUBY tag, due to the presence of the 6X poly-Histidine tag, is bound to the Ni-sepharose column and is subsequently eluted at 500 mM (Figure 7, Panel A). Coomassie blue staining, silver staining and Western blot of the 250 mM imidazole fraction shows a pure band corresponding to recombinant IL-1α (Figure 8, Panel B and Panel C). The final yield of pure recombinant IL-1α is 12 mg per liter of the bacterial culture. These results

clearly show that the linker between Ark-RUBY and the recombinant target protein (IL1-α) can be successfully cleaved and IL1-α can be subsequently purified by Ni-sepharose chromatography.

Ark-RUBY tag can be successfully used for the elimination of significant contaminants remaining after employing Nickel-Affinity chromatography for purification of heat stable proteins Ark-RUBY tag is a thermostable tag (Tm > 90°C). Owing to the excellent thermostability property of the Ark-RUBY tag, it is selectively used for the purification of heat stable recombinant proteins. Interestingly, if some strong contaminants were to be observed after employing Ni-affinity chromatography, they can be completely eliminated by thermal treatment. For example, the Ark-RUBY-D2 clone contains a N-terminal 6X poly-histidine tag and when subjected to purification using nickel (Ni)-affinity chromatography using a stepwise imidazole gradient showed an intense band in the 250 mM fraction (whose molecular mass (21 kDa) matched with that of Ark-RUBY-D2) along with some strong lower and higher molecular weight contaminant bands (Figure 9, Panel A). Those bands were completely eliminated by thermal treatment of the 250 mM fraction to 65°C. Coomassie blue staining revealed that Ark-RUBY-D2 showed that the fusion protein is > 98% pure (Figure 9. Panel B). These results suggest that Ark-RUBY tag can also be successfully used for the cost-effective production of heat stable recombinant proteins.

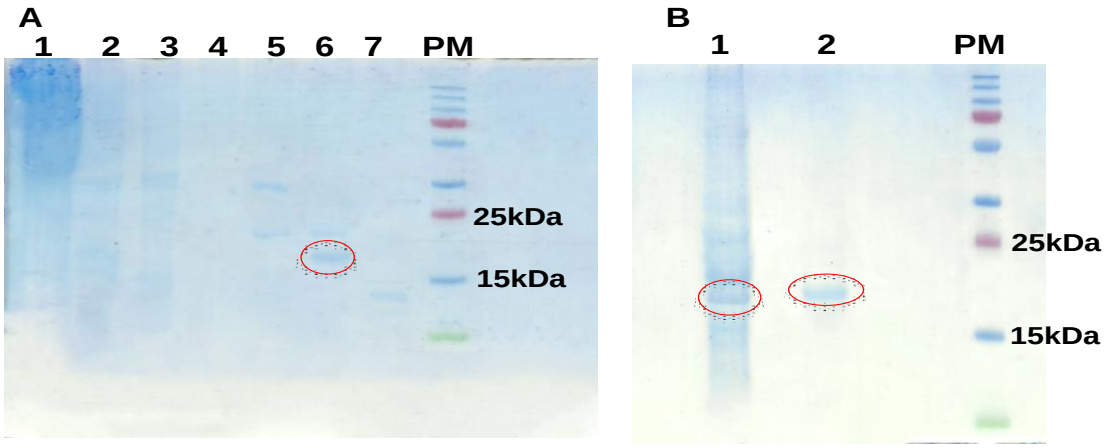

Figure 9: Purification of Ark-RUBY-D2 on Nickel-Sepharose column. Panel- A represents Coomassie blue stained SDS-PAGE gel of the protein fractions, eluted at different concentrations of imidazole. Lane 1, Pellet; Lane 2, Cell culture supernatant; Lane 3, 20mM imidazole; Lane 4, 50mM imidazole; Lane 5, 100mM imidazole; Lane 6, 250mM imidazole; Lane 7, 500 mM imidazole; PM, protein molecular weight marker. SDS-PAGE showed that 250mM imidazole fraction contains band for Ark-RUBY- D2 with contaminant bands and molecular weight of Ark-RUBY- D2 matches with ~21kDa. Panel-B represents Coomassie blue stained SDS-PAGE of 250mM imidazole fraction after heat treatment at 65 °C for 20 min. Lane 1, 250 mM imidazole fraction before heat treatment, Lane 2, pure Ark-RUBY-D2 (Mw ~21kDa) after heat treatment of 250mM imidazole fraction at 65 °C for 20 min; PM, protein molecular weight marker.

Ark-RUBY tag can be used for the purification of peptides in a single step without the use of sophisticated column chromatography techniques Ark-RUBY-FGF peptide and Ark-RUBY-Antifungal peptide (Ark-RUBY-AF) can be purified without the use of multiple purification steps. Purification of the Ark-RUBY-Antifungal peptide is elaborately described in this section. The *E. coli* bacterial lysate, obtained from 1 Liter of culture, was systematically heated in a water bath from 25 °C to 90 °C (at 5 °C intervals) and the precipitate obtained at each temperature was removed by centrifugation. Analysis of the supernatant by SDS-PAGE revealed that only Ark-RUBY-Antifungal peptide remained in solution (in the supernatant) as a pure single band at and beyond 75°C (Figure 10, Panel A). The presence of Ark-RUBY-Antifungal peptide is determined from

the ruby-red color of the supernatant. Coomassie blue staining of the supernatant fraction, obtained from 75°C-90°C, showed that the peptide is pure. These results suggest that Ark-RUBY-heat stable target peptides can be purified in single-step without the use of expensive chromatography techniques. This simple heat-induced purification is very applicable to recombinant peptides because peptides, which are mostly either unstructured or have simple higher order structure(s), are known to undergo reversible thermal unfolding.

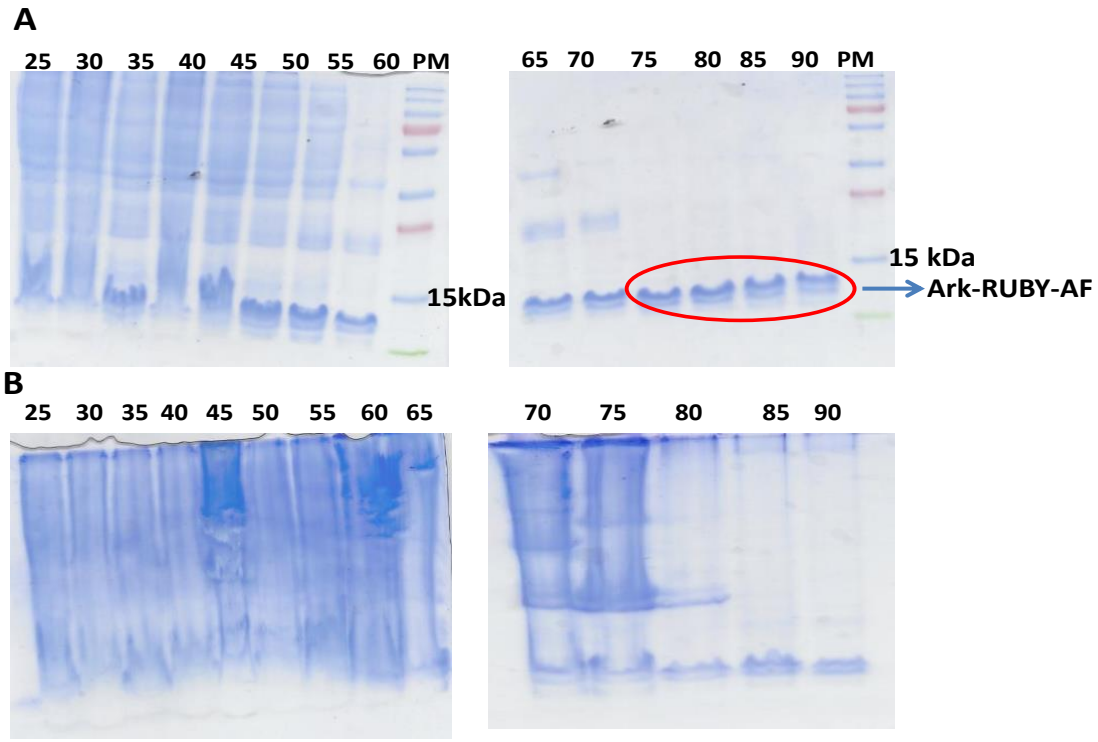

Figure 10: Purification of Ark-RUBY-AF by heat treatment without the use of column chromatography techniques. Panel-A represents Coomassie blue stained SDS-PAGE of *E. coli* bacterial lysate (supernatant) after heating from 25 °C to 90 °C. Coomassie blue staining showed that Ark-RUBY-AF remained in the supernatant as pure single band (Mw~12kDa) at and beyond 75 °C. PM is the protein molecular weight marker. Panel-B represents precipitated component (pellet) after heat treatment of *E. coli* lysate from 25 °C to 90 °C.

Recombinant IL-1α is in the native conformation Far UV-circular dichroism is a popular biophysical technique that is commonly used for the determination of the secondary structure of proteins. Far UV-CD spectrum of pure Ark-RUBY-IL-1α is characteristic of a helical conformation with a double minimum at 208 nm and 222 nm (Figure 10, Panel A). Upon separation of Ark-RUBY, pure recombinant IL1α shows a negative peak at 208 nm and a prominent positive peak in the range of 225 nm-230 nm, which is reminiscent of the native beta-barrel fold of IL-1α (Figure 11, Panel B).

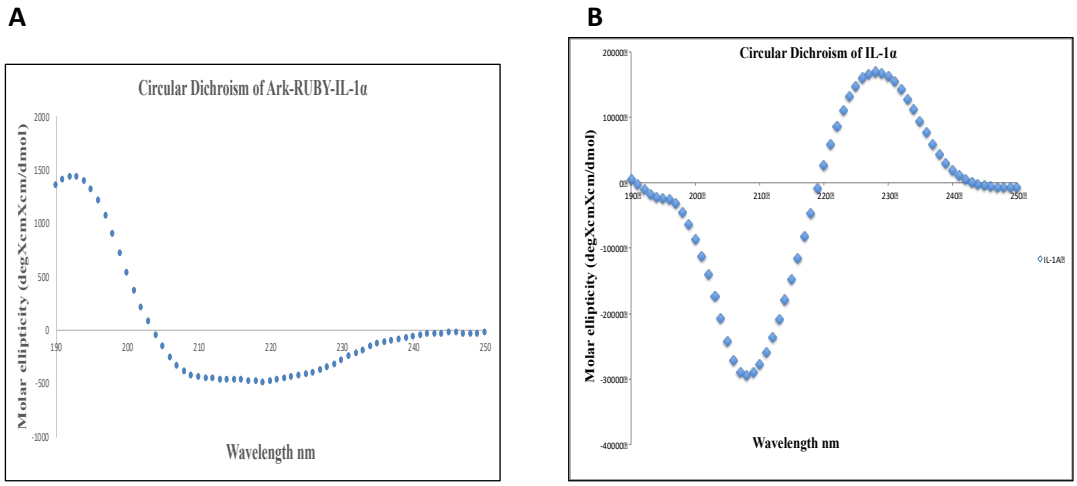

Figure 11: Panels- A and B represent far-UV CD spectrum of Ark-RUBY-IL-1α and IL-1α in 10mM PBS at pH-7.2 respectively.

Ark-RUBY-Tag is Thermostable tag Thermal denaturation of pure recombinant Ark-RUBY, Ark-RUBY-IL-1α, and IL-1α was monitored by Far UV-circular dichroism based on ellipticity changes at 228 nm. Ark-RUBY-tag showed high thermal stability since the secondary structure of the tag did not change at both temperatures at 25°C and 90°C. Even though at both temperatures the Ark-RUBY- IL-1α showed similar secondary structure, the intensity at 90°C compared to the intensity at 25°C was low (Figure 12). Interleukin 1 alpha was completely unfolded at 90°C. These results suggest that the

purified recombinant IL-1α is a well-folded and stable protein when it is attached to the thermal stable tag.

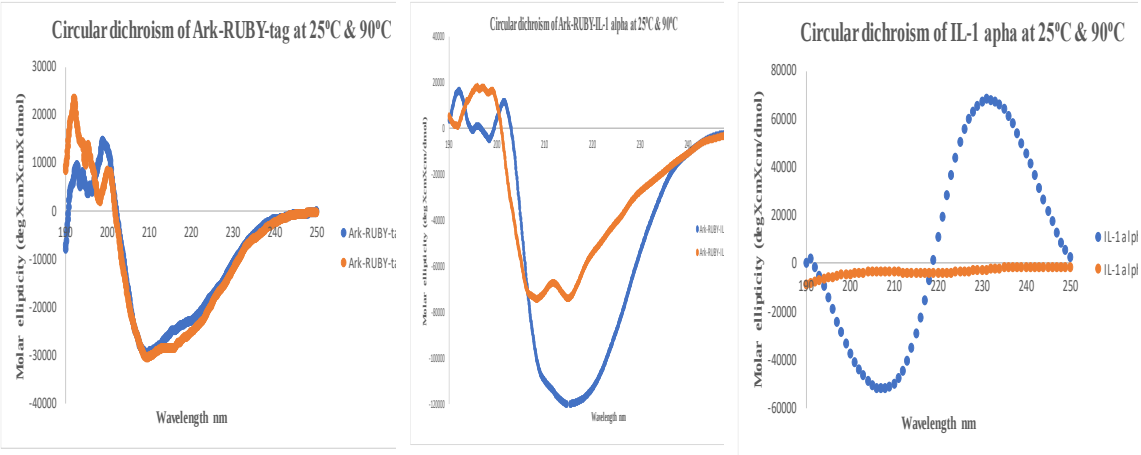

Figure 12: Represents the circular dichroism of Ark-RUBY-tag, Ark-RUBY-IL-1α, and IL-1α, and at 25°C & 90°C. The changes of the secondary structure monitored by recording the shifting of the positive peak at 228 nm and negative peak at 205nm for IL-1α. However, for both Ark-RUBY-IL1α and Ark-RUBY tag, the secondary structural changes were monitored by recording the shifting of the negative peak at 208 and 222 nm.

Interleukin 1 alpha that is expressed fused with the **Ark-RUBY-tag is biologically active** The biological activity was assessed to ensure that the purified recombinant IL-1α is in the biologically active conformation. IL-1α has a strong effect on splenocytes that are derived from C57BL/6Jmice. IL-1α is known to stimulate the secretion of IFN-γ from splenocytes[51]. Therefore, the secretion of IFN-γ was used as a measure of bioactivity of IL-1α. Splenocytes were plated on a 96-well plate in the presence and absence of IL-1α (0-50 ng/mL). The secreted IFN-γ activity in the supernatant was measured after 24 hours by using enzyme-linked immunosorbent assay (ELISA). The concentration of IFN-γ was found to increase significantly upon exposure to 0.0032 to 50 ng/mL of IL-1α (Figure 13). These results suggest that the purified recombinant IL-1α is biologically active.

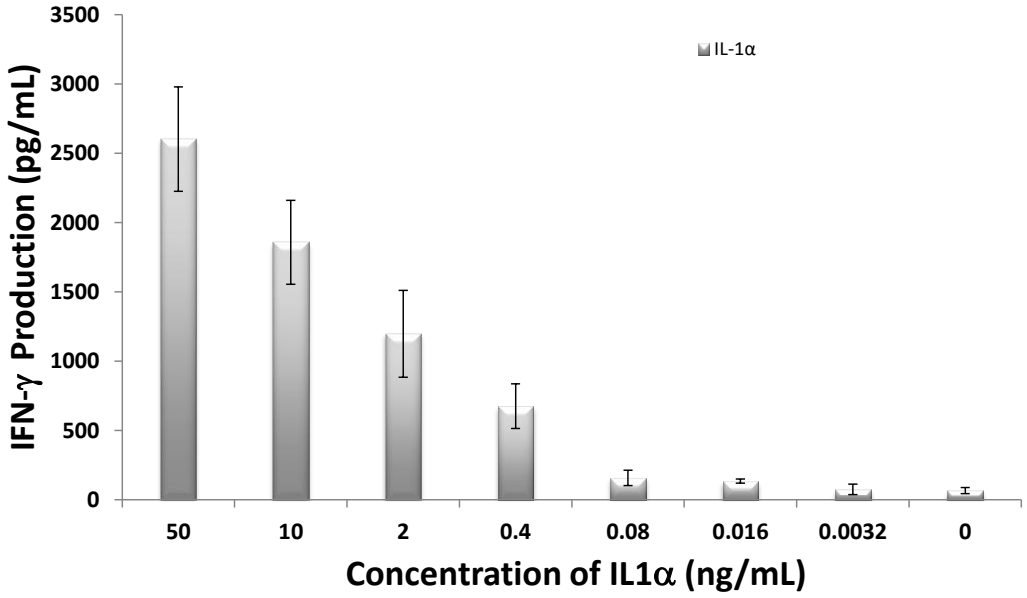

Figure 13: Represents the production of IFN-γ by splenocytes upon addition of IL-1α (0-50ng/mL). The calculated standard errors were derived from triplicate measurements.

Conclusions

Overexpression and purification of IL-1α in large quantities has been a challenge for performing detailed biophysical studies. IL-1α is very unstable, which leads to the degradation of the protein. Expressing IL-1α in a heterologous host such as *E. coli* was challenging. Herein, for the first time, recombinant IL-1α was produced in *E. coli* cells attached to rubredoxin using a simple IMAC Sepharose™ affinity chromatography. One of the most popular methods to purify recombinant proteins from a wide range of expression hosts is affinity chromatography. The method relies on the incorporation of selective protein or peptide affinity tags which are aligned in sequence to the target protein gene to produce the target fusion protein. This unique expression procedure

allowed for the acquisition of homogeneously pure IL-1α in order to perform various biophysical.

Rubredoxin (Rd) from Pyrococcus *furiosus has* unique and interesting properties which can be profitability exploited as an excellent recombinant protein purification tag. It exhibits a bright red color due to oxidation of the central iron atom in the iron-sulfur core. The red color of Rd will help to track the Rd-fused target recombinant protein during purification as it was shown in Ark-RUBY- IL-1α. The smaller molecular mass of Rd will reduce the possibility of its interference with the folding of the target protein. Rd proteins have an exceptionally high thermal stability (T_m > 90°C). The extraordinary thermal stability of Rd can likely be used to rapidly eliminate contaminating proteins from the expression host by heating the bacterial cell lysate. This aspect can be expected to significantly shorten the time duration required for the purification of Rd-fused recombinant proteins/peptides. Rd is known to be highly soluble protein. The high aqueous solubility of Rd can potentially facilitate the overexpression of the Rd-fused recombinant protein/peptide in their soluble form by preventing the formation of unproductive inclusion bodies. The advantage of using CNBr is that it eliminates the requirement of using expensive restriction proteases for separating the affinity/purification tag from the recombinant target protein. Another positive feature of the CNBr-induced cleavage of methionine-less Rd-fused target protein(s) is that it does not leave any extra amino acids, from the tag or the linker, on the target recombinant protein/peptide[52].

References

1. Gilsing, V.; Nooteboom, B., Exploration and exploitation in innovation systems: The case of pharmaceutical biotechnology. Research Policy 2006, 35 (1), 1-23.

2. Rosano, G. L.; Morales, E. S.; Ceccarelli, E. A., New tools for recombinant protein production in Escherichia coli: a 5-year update. Protein Science 2019.

3. Boi, C., Membrane Chromatography for Biomolecule Purification. In Current Trends and Future Developments on (Bio-) Membranes, Elsevier: 2019; pp 151-166.

4. Rosano, G. L.; Ceccarelli, E. A., Recombinant protein expression in Escherichia coli: advances and challenges. Frontiers in microbiology 2014, 5, 172.

5. Jia, B.; Jeon, C., High-throughput recombinant protein expression in Escherichia coli: current status and future perspectives. Open Biol. 2016; 6 (8).

6. Baumgarten, T.; Ytterberg, A. J.; Zubarev, R. A.; de Gier, J.-W., Optimizing recombinant protein production in the Escherichia coli periplasm alleviates stress. Appl. Environ. Microbiol. 2018, 84 (12), e00270-18.

7. Rinas, U.; Garcia-Fruitós, E.; Corchero, J. L.; Vázquez, E.; Seras-Franzoso, J.; Villaverde, A., Bacterial inclusion bodies: discovering their better half. Trends in biochemical sciences 2017, 42 (9), 726-737.

8. Peternel, S.; Gaberc-Porekar, V.; Komel, R., Bacterial growth conditions affect quality of GFP expressed inside inclusion bodies. Acta Chim Slov 2009, 56 (4), 860-7.

9. Zhu, S.; Gong, C.; Ren, L.; Li, X.; Song, D.; Zheng, G., A simple and effective strategy for solving the problem of inclusion bodies in recombinant protein technology: His-tag deletions enhance soluble expression. Applied microbiology and biotechnology 2013, 97 (2), 837-845.

10. Li, Y.; Oelkuct, M.; Gentz, R., Method of purifying protein from inclusion bodies. Google Patents: 2004.

11. Singh, A.; Upadhyay, V.; Upadhyay, A. K.; Singh, S. M.; Panda, A. K., Protein recovery from inclusion bodies of Escherichia coli using mild solubilization process. Microbial cell factories 2015, 14 (1), 1-10.

12. Hamidi, S. R.; Safdari, Y.; Arabi, M. S., Test bacterial inclusion body for activity prior to start denaturing and refolding processes to obtain active eukaryotic proteins. Protein expression and purification 2019, 154, 147-151.

13. Panda, A. K.; Sheikh, M. G.; Eshwari, A. N. S.; Garg, L. C., Process for solubilization of recombinant proteins expressed as inclusion body. Google Patents: 2007.

14. Kwon, S. B.; Yu, J. E.; Kim, J.; Oh, H.; Park, C.; Lee, J.; Seong, B. L., Quality Screening of Incorrectly Folded Soluble Aggregates from Functional Recombinant Proteins. International journal of molecular sciences 2019, 20 (4), 907.

15. Sadavarte, R.; Filipe, C. D.; Ghosh, R., Recovery of functionally-active protein from inclusion bodies using a thermal-cycling method. Biotechnology progress 2017, 33 (1), 133-139.

16. Hoffmann, D.; Ebrahimi, M.; Gerlach, D.; Salzig, D.; Czermak, P., Reassessment of inclusion body-based production as a versatile opportunity for difficult-to-express recombinant proteins. Critical reviews in biotechnology 2018, 38 (5), 729-744.

17. Young, C. L.; Britton, Z. T.; Robinson, A. S., Recombinant protein expression and purification: a comprehensive review of affinity tags and microbial applications. Biotechnology journal 2012, 7 (5), 620-634.

18. Raran-Kurussi, S.; Waugh, D. S., Expression and Purification of Recombinant Proteins in Escherichia coli with a His 6 or Dual His 6-MBP Tag. In Protein Crystallography, Springer: 2017; pp 1-15.

19. Block, H.; Maertens, B.; Spriestersbach, A.; Brinker, N.; Kubicek, J.; Fabis, R.; Labahn, J.; Schäfer, F., Immobilized-metal affinity chromatography (IMAC): a review. In Methods in enzymology, Elsevier: 2009; Vol. 463, pp 439-473.

20. Cheung, R. C. F.; Wong, J. H.; Ng, T. B., Immobilized metal ion affinity chromatography: a review on its applications. Applied microbiology and biotechnology 2012, 96 (6), 1411-1420.

21. Harper, S.; Speicher, D. W., Purification of proteins fused to glutathione S-transferase. In Protein Chromatography, Springer: 2011; pp 259-280.

22. LaVallie, E. R.; Lu, Z.; Diblasio-Smith, E. A.; Collins-Racie, L. A.; McCoy, J. M., [21] Thioredoxin as a fusion partner for production of soluble recombinant proteins in Escherichia coli. In Methods in enzymology, Elsevier: 2000; Vol. 326, pp 322-340.

23. Kapust, R. B.; Waugh, D. S., Escherichia coli maltose-binding protein is uncommonly effective at promoting the solubility of polypeptides to which it is fused. Protein Science 1999, 8 (8), 1668-1674.

24. Bornhorst, J. A.; Falke, J. J., [16] Purification of proteins using polyhistidine affinity tags. In Methods in enzymology, Elsevier: 2000; Vol. 326, pp 245-254.

25. Chalfie, M.; Kain, S. R., Green fluorescent protein: properties, applications and protocols. John Wiley & Sons: 2005; Vol. 47.

26. Skerra, A.; Schmidt, T. G., [18] Use of the Strep-tag and streptavidin for detection and purification of recombinant proteins. In Methods in enzymology, Elsevier: 2000; Vol. 326, pp 271-304.

27. Morris, J.; Jayanthi, S.; Langston, R.; Daily, A.; Kight, A.; McNabb, D. S.; Henry, R.; Kumar, T. K. S., Heparin-binding peptide as a novel affinity tag for purification of recombinant proteins. Protein Expression and Purification 2016, 126, 93-103.

28. Kimple, M. E.; Brill, A. L.; Pasker, R. L., Overview of affinity tags for protein purification. Current protocols in protein science 2013, 73 (1), 9.9. 1-9.9. 23.

29. Lichty, J. J.; Malecki, J. L.; Agnew, H. D.; Michelson-Horowitz, D. J.; Tan, S., Comparison of affinity tags for protein purification. Protein expression and purification 2005, 41 (1), 98-105.

30. Wingfield, P. T., Overview of the purification of recombinant proteins. Current protocols in protein science 2015, 80 (1), 6.1. 1-6.1. 35.

31. Bailon, P., Affinity chromatography: methods and protocols. Springer Science & Business Media: 2008; Vol. 421.

32. Mahajan, E.; George, A.; Wolk, B., Improving affinity chromatography resin efficiency using semi-continuous chromatography. Journal of chromatography A 2012, 1227, 154-162.

33. Zhao, M.; Vandersluis, M.; Stout, J.; Haupts, U.; Sanders, M.; Jacquemart, R., Affinity chromatography for vaccines manufacturing: Finally ready for prime time? Vaccine 2019, 37 (36), 5491-5503.

34. Lumppio, H. L.; Shenvi, N. V.; Summers, A. O.; Voordouw, G.; Kurtz, D. M., Rubrerythrin and rubredoxin oxidoreductase indesulfovibrio vulgaris: A novel oxidative stress protection system. Journal of Bacteriology 2001, 183 (1), 101-108.

35. Nanda, V.; Rosenblatt, M. M.; Osyczka, A.; Kono, H.; Getahun, Z.; Dutton, P. L.; Saven, J. G.; DeGrado, W. F., De novo design of a redox-active minimal rubredoxin mimic. Journal of the American Chemical Society 2005, 127 (16), 5804-5805.

36. Bonomi, F.; Burden, A. E.; Eidsness, M. K.; Fessas, D.; Iametti, S.; Kurtz, D. M.; Mazzini, S.; Scott, R. A.; Zeng, Q., Thermal stability of the [Fe (SCys) 4] site in Clostridiumpasteurianum rubredoxin: contributions of the local environment and Cys ligand protonation. JBIC Journal of Biological Inorganic Chemistry 2002, 7 (4-5), 427-436.

37. Blake, P. R.; Park, J. B.; Bryant, F. O.; Aono, S.; Magnuson, J. K.; Eccleston, E.; Howard, J. B.; Summers, M. F.; Adams, M. W., Determinants of protein hyperthermostability: purification and amino acid sequence of rubredoxin from the hyperthermophilic archaebacterium Pyrococcus furiosus and secondary structure of the zinc adduct by NMR. Biochemistry 1991, 30 (45), 10885-10895.

38. Grottesi, A.; Ceruso, M. A.; Colosimo, A.; Di Nola, A., Molecular dynamics study of a hyperthermophilic and a mesophilic rubredoxin. Proteins: Structure, Function, and Bioinformatics 2002, 46 (3), 287-294.

39. Sulpizi, M.; Raugei, S.; VandeVondele, J.; Carloni, P.; Sprik, M., Calculation of redox properties: Understanding short-and long-range effects in rubredoxin. The Journal of Physical Chemistry B 2007, 111 (15), 3969-3976.

40. Bau, R.; Rees, D. C.; Kurtz Jr, D. M.; Scott, R. A.; Huang, H.; Adams, M. W.; Eidsness, M. K., Crystal structure of rubredoxin from Pyrococcus furiosus at 0.95 Å resolution, and the structures of N-terminal methionine and formylmethionine variants of Pf Rd. Contributions of N-terminal interactions to thermostability. JBIC Journal of Biological Inorganic Chemistry 1998, 3 (5), 484-493.

41. Kohli, B. M.; Ostermeier, C., A Rubredoxin based system for screening of protein expression conditions and on-line monitoring of the purification process. Protein expression and purification 2003, 28 (2), 362-367.

42. Yurkiw, M. A.; Voordouw, J.; Voordouw, G., Contribution of rubredoxin: oxygen oxidoreductases and hybrid cluster proteins of D esulfovibrio vulgaris H ildenborough to survival under oxygen and nitrite stress. Environmental microbiology 2012, 14 (10), 2711-2725.

43. van Beilen, J. B.; Neuenschwander, M.; Smits, T. H.; Roth, C.; Balada, S. B.; Witholt, B., Rubredoxins involved in alkane oxidation. Journal of bacteriology 2002, 184 (6), 1722-1732.

44. Meyer, J.; Moulis, J. M., Rubredoxin. Handbook of metalloproteins 2006.

45. Block, H.; Maertens, B.; Spriestersbach, A.; Kubicek, J.; Schäfer, F., Proteolytic affinity tag cleavage. In Methods in enzymology, Elsevier: 2015; Vol. 559, pp 71-97.

46. Salimi, K.; Usta, D. D.; Koçer, İ.; Çelik, E.; Tuncel, A., Highly selective magnetic affinity purification of histidine-tagged proteins by Ni 2+ carrying monodisperse composite microspheres. RSC Advances 2017, 7 (14), 8718-8726.

47. Ryan, D. P.; Tremethick, D. J., A dual affinity-tag strategy for the expression and purification of human linker histone H1. 4 in Escherichia coli. Protein expression and purification 2016, 120, 160-168.

48. Hasenstab-Riedel, S.; Schmidt, B.; Schröder, B.; Sonnenberg, K.; Steinhauer, S., From Polyhalides to Polypseudohalides: Chemistry Based on Cyanogen Bromide. Angewandte Chemie 2019.

49. Dempsey, S. G.; Miller, C. H.; Hill, R. C.; Hansen, K. C.; May, B. C., Functional Insights from the Proteomic Inventory of Ovine Forestomach Matrix. Journal of proteome research 2019, 18 (4), 1657-1668.

50. ZHANG, C.; TIAN, L.-Y.; WENG, H.-B., Preparation of Thymosin-α1 Using a One-step Heat-treatment Method and CNBr Cleavage. Progress in Biochemistry and Biophysics 2019, 46 (5), 513-520.

51. Kyttaris, V. C., New treatments for systemic lupus erythematosus. In Systemic Lupus Erythematosus, Elsevier: 2016; pp 551-557.

52. Villa, S.; De Fazio, G.; Canosi, U., Cyanogen bromide cleavage at methionine residues of polypeptides containing disulfide bonds. Analytical biochemistry 1989, 177 (1), 161-164.

Chapter Three

Characterization of the copper-induced dimer of Interleukin 1-alpha

Abstract

Most secreted proteins have a hydrophobic cleavable signal peptide in their primary structure which guides their translocation into the lumen of the endoplasmic reticulum (ER). After vesicular transport through the ER-Golgi, secreted proteins are released into the extracellular compartment. This route of protein export is known as the classical secretion pathway. However, many extracellular proteins have shown to be secreted through ER-Golgi-independent (non-classical) pathways. A common feature of non-classically secreted proteins is the absence of a signal peptide. The prototype member of the interleukin 1 family, interleukin 1 alpha (IL1α) is a signal-less protein that is secreted *via* the non-classical secretory route. IL1α is a multifunctional pro-inflammatory cytokine. It is a key mediator in the cytokine network, regulating crucial functions in the immune response, inflammation, tissue remodeling, cell differentiation, and cell death. This study indicated that copper (Cu^{++}) binds to IL1α with high affinity and induced the formation of an IL1α dimer via the formation of an intermolecular disulfide bond. Also, the dimer formation did not alter the backbone conformation of the protein, although it displayed decreased bioactivity. Also, the dimer form as well as the monomer form of IL1α both exhibit high affinity to S100A13. The Cu^{2+} binding sites in IL1α were mapped by 2D HSQC spectroscopy. The HSQC data showed that many amino acids residues are perturbed by Cu^{++} binding.

Introduction

In living systems, many metals play crucial roles in cellular processes including inflammation, cells differentiation, anti-oxidant activities, and blood homeostasis[1, 2]. Calcium, zinc, copper and iron are co-factors which are involved in the activation of several biological reactions[3, 4]. Some of them have harmful effects on cells, but these metals are important for vital functions. Copper is involved in different biological processes including the production of neurotransmitters, connective tissue remodeling, anti-free radical reactions, and pigment development[5, 6]. Recent studies have demonstrated that copper acts as angiogenic molecules by regulating the secretion of FGF1 and IL-1α[7]. Also, some clinical data have suggested that using copper chelators helps in minimizing cancer progression[7-9]. Copper ions can have damaging effects on cells because it can easily exchange electrons leading to interference with cellular respiration, neuronal differentiation, and signal transmission. Many protein chaperons are involved in regulation of intracellular and extracellular copper trafficking[10]. In intracellular compartments, many proteins are known to bind to copper and serve as copper chaperons such as Atox1, CCS and Cox17, but still the mechanism of delivering copper for cellular processes is not clear[11]. In unconventional protein secretion of FGF1, copper plays an important role by binding to S10A13 and dimerizing FGF-1 by oxidizing cys30[12]. Copper induced FGF1 dimerization is crucial for non-classical protein secretion[13, 14]. Interestingly, IL-1α lacks the N-terminal signal peptide that mediates the secretion through the Endoplasmic-Golgi apparatus system (ER-Golgi system)[15, 16]. The ER-Golgi system is the route for moving proteins out the cells. The ER-Golgi transformation system needs a signal peptide that directs proteins to their final

destination[17]. IL-1α is secreted by unconventional protein secretion (UPS) into an extracellular compartment to exert its actions by binding to IL-1R1[18, 19]. UPS is induced but not exclusively by cellular stress such as inflammation, starvation, autoimmune diseases and ER stress. Even though many proteins like FGF1, FGF2, IL-1β, and calcium binding protein S100A13 are released by UPS, the mechanism(s) that triggers the release of signal peptide-less proteins is still not understood[20-22]. Many studies have shown that copper (Cu^{2+}) is involved in unconventional protein secretion of many proteins such as FGF1 in response to heat shock and hypoxia[23-25]. Also, using copper chelating agents for example, tetrathiomolybdate, decreases the release of FGF1 that helps in the suppression of tumor growth [26]. Many studies have confirmed that FGF1 and IL-1α share structural homology as well as being released by the UPS route[27, 28]. Surprisingly, S100A13, an important component of stressreleased FGF1, is also mandatory for unconventional protein secretion of IL-1α[29]. Also, S100A13 is known to bind to Cu^{2+} as well as calcium[30, 31]. It is believed that Cu^{2+} may be involved in unconventional protein secretion of IL-1α. Thus, it is important to define and understand the mechanism that underlies the export of IL-1α by unconventional protein secretion since it medically assists in the management of inflammatory and carcinogenic disorders that are caused by IL-1α. The results of this study revealed that IL-1α has high binding affinity for copper. Copper induced IL-1α dimerization is mediated by the oxidation of the lone Cys143. The dimeric form of IL-1α shows similar properties as the monomer but exhibits lower activity.

Materials and Methods

Materials VWR Scientific Inc, USA was the provider for all buffer components including Na_2HPO_4, NaH_2PO_4, NaCl. Lysogeny broth (LB) was purchased from EMD

Millipore, USA. Competent cells (DH5α and BL-21p-LysS (DE3)) were obtained from Novagen Inc., USA. DNA plasmid isolation kits were bought from Qiagen, USA and Quikchange II XL mutagenesis kits were purchased from Agilent. Nickel sepharose was acquired from GE Healthcare, USA.

Expression and Purification of Recombinant S100A13

For expression of S100A13, BL-21 Star (DE3) cells transformed with the expression vector pGEX-GST-S100A13 were grown at 37ºC in one liter of culture of Luria broth containing 100 µg/ml Ampicillin. The protein expression was induced with 1 mM isopropyl β-thiogalactoside for four hours after the optical density at Abs600 nm reached 0.4-0.6. Then, cells were harvested by centrifugation at 8000 rpm for 25 minutes, the pellet was suspended in 30 mls 10 mM phosphate buffer PH 7.2 and sonicated. GST-S100A13 was bound to glutathione Sepharose that was then washed successively with 10 mM phosphate buffer PH 7.2. Overnight cleavage on column was setup at room temperature on a rocker with thrombin protease for 16 hours. The cleavage product was washed with 10 mM phosphate buffer PH 7.2 to collect the cleavage product (S100A13). The GST tag was eluted using 10 mM L-Glutathione. The expression of GST-S100A13 and the cleavage product of S100A13 were checked by SDS-PAGE stained with Coomassie blue.

Far-UV Circular Dichroism Spectroscopy

Far-UV CD measurements were accomplished using Jasco 1500 spectropolarimeter at 25ₒC, and a protein concentration of 0.5 mg/mL in 10mM phosphate buffer (pH 7.2) using 0.1 mm bath length. All data were smoothed using the Savitzky-Golay algorithm.

Limited Trypsin Digestion (LTD)

LTD experiments were done by incubating protein samples with enzyme at pH 7.2 in 10 mM phosphate buffer at 37°C. The samples were collected after each ten minutes and the reactions were stopped immediately by adding 10% trichloroacetic acid. By running the samples on 15% SDS-PAGE, the results were analyzed by measuring the intensity of the digested protein by trypsin bands at different points of time using densitometric scan [UN-SCAN IT (Silk Scientific Inc., USA)]. Then the calculated values of bands intensities were compared with the zero-time Coomassie blue stained protein band.

Isothermal titration calorimetry (ITC)

ITC (iTC-200, Malvern Inc.) was used to determine the IL-1α (monomer or dimer form)-S100A13 and IL-1α-$CuCl_2$, and different metals binding affinity. By titrating the ligand (loaded in the syringe) into protein solution in the reaction cell, heat changes were measured. All protein and metals samples were prepared in solution containing 10 mM HEPES buffer (pH 7.2) then all samples were degassed prior to titration. ITC experiment parameters performed were 30 titration injections, at 25°C with a stirring speed of 750 rpm. ITC binding curves were best fits using one set of binding models followed by appropriate corrections to eliminate the heats that were generated from the dilution.

Extrinsic Fluorescence Spectroscopy

Extrinsic fluorescence experiments (ANS binding assays) were performed using a Hitachi F-2500 fluorescence spectrophotometer at 25°C. A protein concentration of 0.5 mg/mL in 10 mM phosphate buffer, pH 7.2 was used in all fluorescence experiments. All fluorescence measurements were recorded using the slit width set to 2.5 nm, excitation

wavelength of 280 nm, and emission wavelength range from 300-450 nm. Performing ANS binding assays, the titrations were carried out by adding 1μL of ANS. The relative fluorescence intensity records were made at 510 nm.

Equilibrium unfolding of Proteins

Far-UV Circular dichroism (Jasco-1500) was used to study thermal and chemical denaturation experiments. In thermal unfolding studies, the protein concentration of the samples was 0.5 mg/ml in 10 mM phosphate buffer, pH 7.2. Spectra were collected from 25°C to 90°C at five-degree intervals. To calculate Tm value where 50% of protein population is in the unfolded state(s), a plot was generated from fraction unfolded protein population *versus* temperature. The Cm where 50% of protein population was in unfolded state(s) was calculated by plotting each spectrum verses urea concentrations. Urea-induced equilibrium unfolding of protein samples was analyzed using the fluorescence mode of Jasco-1500 spectrometry. Protein concentration of the sample was 0.5 mg/ml in 10 mM phosphate buffer at pH 7.2.

Nuclear Magnetic Spectroscopy

^{1}H-^{15}N heteronuclear signal quantum coherence (HSQC) were performed on Bruker 700 MHz NMR, at 25°C. The protein concentration was 350 μM in 10 mM phosphate buffer (pH 7.2). M9 media was used to grow the bacterial hosts of IL-1α in which the nitrogen source was isotopes $^{15}NH_4Cl$. Sparky 3.114 software was used to analyze 2D NMR data of labeled IL-1α.

Bioactivity assay

HEK-Blue™ IL-1α/IL-1β cells (Invivogen) allow monitoring the bioactivity of IL-1α and IL-1β by activation of the NF-κB and AP-1 pathways. The response to TNF- α

is blocked, so the cells are responsive only to IL-1. The binding of IL-1 to cell surface receptors triggers specifically the NF-kB cascade leading to producing the secreted embryonic alkaline phosphatase (SEAP). A 96-well plate was seeded with 50,000 cells/well of HEK-Blue™ IL-1α/IL-1β cells, then the cells were treated with media containing 0.4 to 10 ng/ml IL-1α or copper induced IL-1α dimerization. Supernatant SEAP concentrations were detected by quantifying Quanti-Blue™ (Invivogen) via reading the wells at 650 nm.

Results and discussion

Copper dimerizes Interleukin-1 alpha

In order to examine the effects of copper on IL-1α, $CuCl_2$ was incubated with IL-1α at room temperature. One migrating band resolved when IL-1α in the absence of copper was run and two bands of IL-1α-copper complex were migrated through non-reduced SDS-PAGE representing the monomer and the dimer (Figure 1). In contrast to the monomer, double bands appeared when the same concentration of IL-1α was treated with 30 μM $CuCl_2$. For calculating the copper concentration that induces complete protein dimerization, IL-1α was treated with different concentrations of $CuCl_2$. Then, IL-1α was electrophoresed in non-reduced SDS-PAGE. Dimer band of IL-1α appeared even at a low concentration of $CuCl_2$. The intensity of dimer bands increased while the concentration of $CuCl_2$ increased. Compete dimer band displayed with no monomer band left at 46 μM $CuCl_2$ (Figure 2).

Figure 1: illustrates Non-reduced SDS-PAGE that revealed the dimer formation of IL-1α after treating it with $CuCl_2$. Uncompleted dimerization of IL-1α under influence of particular concentration of $CuCl_2$ indicates that some proteins were at monomer form.

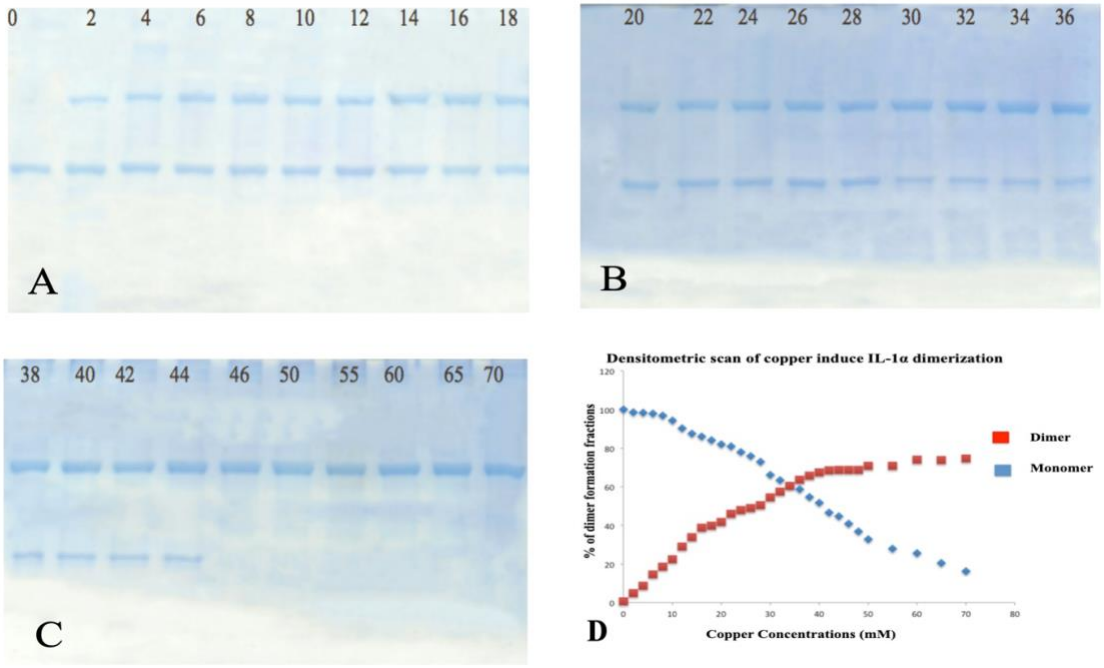

Figure 2: demostrates the dimer formation and monomer reduction of IL-1α while $CuCl_2$ concentrations are increasing. The concentrations of $CuCl_2$ in (μM) are shown above each band. A: The dimer form of IL-1α appeared at a low concentration of $CuCl_2$. C: Both monomer and dimer form of IL-1α appeared on the non-reduced SDS-PAGE. C: The maximum concentration of $CuCl_2$ for complete dimerization is 46 μM $CuCl_2$. D: the densitometric scan of the SDS-PAGE gel that shows the dimer formation versus the monomer form of IL-1α in presence of different concentrations of $CuCl_2$.

These results indicated that specific disulfide bands were formed between two cysteine amino acids of different monomers of IL-1α. We propose that forming the dimer form of IL-1α is relatively important for some biological activities. It may explain that the IL-1α might be released at high volume to reach maximum effects.

Secondary structure of IL-1alpha does not alter upon copper-induced dimerization

The secondary structure of IL-1α belongs to β-trefoil family that is one of the ten of protein super families32. Several proteins types that are included in this family such as FGF-1, FGF-2, IL-1β, and soybean trypsin inhibitors33. IL-1α consists of twelve β strands that are arranged into trefoil units called hairpin. The twelve β-strands are folded into three similar trefoil units of β-β-β-loop-β32. Circular dichroism is a valuable technique for examining the secondary structure changes induced in protein-protein interaction. CD spectra of the dimer form of IL-1α gets overlaid well (Figure 3)

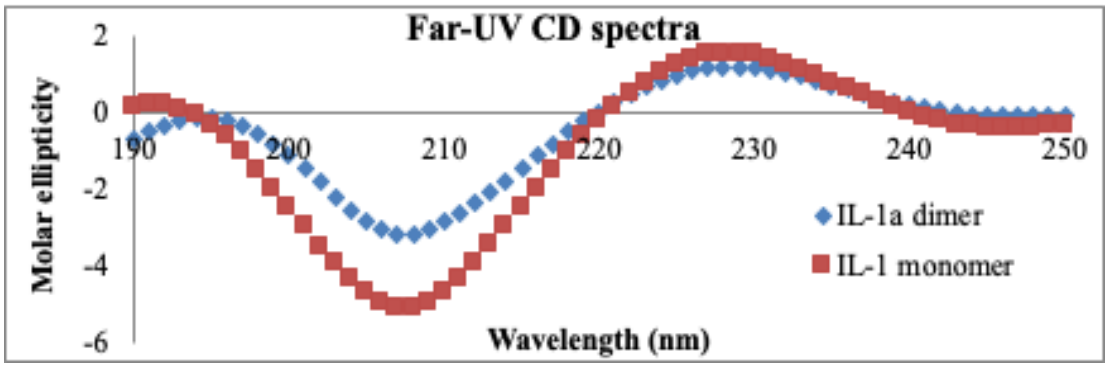

Figure 3: Far-UV spectra of the monomer form of IL-1 α (orange dots) and the dimer form of IL-1 α (blue dots).

with the monomer type, displaying the quality feature of the positive ellipticity shoulder in the wavelength range 220-240 nm, and a negative shoulder in the region of 200-210 nm. These spectral characters indicate that the native β-trefoil conformation is not significantly disturbed because of the dimer formation.

No conformational changes in three-dimensional structure upon copper induced dimerization of IL-1α monitored by (ANS) binding assay

The tertiary structural changes of proteins were examined by using the ANS binding assay. ANS is hydrophobic, non-polar dye that has been used to study proteins conformational changes. Polar amino acids make hydrogen bonds with water whereas non-polar and aromatic amino acids are hydrophobic and are usually buried inside the core of the protein(s)[34]. Upon protein-protein interaction, hydrogen bonds are formed between two reactants that cause conformational changes. Monitoring ANS binding, conformational changes can be analyzed. The extrinsic fluorescent probe of ANS binds to solvent accessible hydrophobic surface(s) in the proteins[35]. In this context, measuring the changes of ANS fluorescence helps to study structural differences between the monomer and the dimer form of IL-1α (Figure 4).

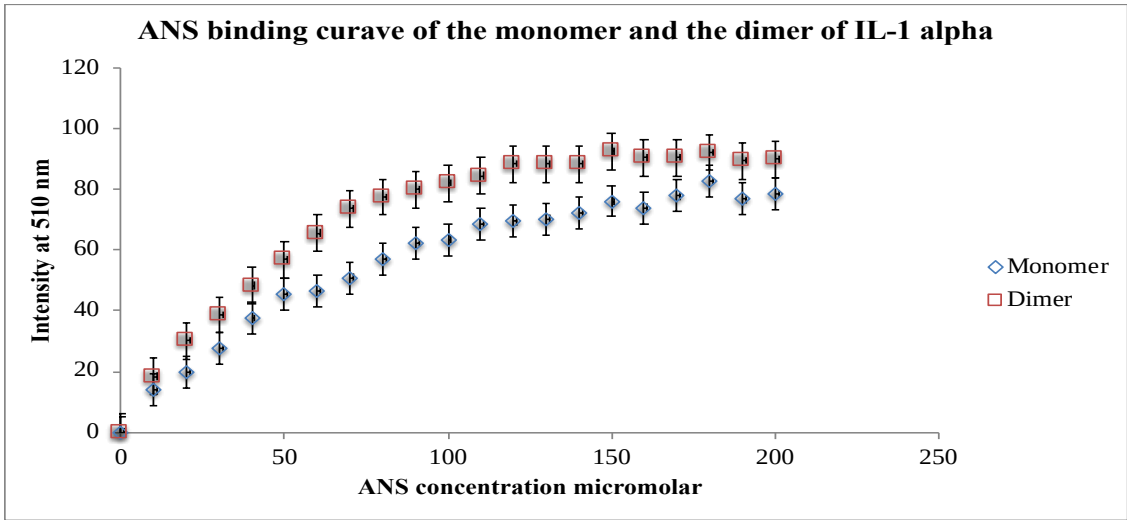

Figure 4: ANS binding curve of the monomer form of IL-1 α & the dimer form of IL-1 α

Typically, hydrophobic portion(s) of proteins are buried in the protein core, so increasing ANS fluorescence suggests more solvent accessible hydrophobic surface(s)

are present. The emission intensity of ANS binding to the dimer form of IL-1α is higher than the monomer form when it binds to ANS. This indicates that induced dimerization encourages a modest conformational change causing an increase in the solvent-exposure of the hydrophobic surfaces(s).

No conformational changes upon copper induced IL-1α dimerization detected by Limited Trypsin Digestion (LTD)

Trypsin is a serine protease that cleaves at the carboxyl terminal end of lysine and arginine residues. Many factors affect the rate of the protease-substrate cleavage reaction including number of hydrogen bonds between the cleavage sites, the degree of protease accessible to the cleavage site, degree of protein folding, and flexibility of the substrate[36]. In this context, the LTD assay is a useful technique to study protein flexibility and possible structural changes in the protein backbone caused by protein dimerization. LTD was performed on the monomer and the dimer form of IL-1α to determine any conformational and flexibility changes of the dimer form compared to the monomer form. The progress of the cleavage reaction of the substrates was determined by comparing the measurements of the intensity of the zero trypsin, non-cleaved band at 19 kDa (monomer) and 38 kDa (dimer) Coomassie blue stained bands on SDS-PAGE with trypsin-substrates bands at different time periods. Based on the digestion rate of the monomer and the dimer form of IL-1α, both showed higher susceptibility to trypsin (Figure 5). The monomer form of IL-1α began cleavage by trypsin after five minutes of incubation until fifty percent of Cu^{2+} free IL-1α was cleaved after 30 minutes from the initiation time. Copper induced IL-1α dimerization showed better stability than the monomer form. The dimer was stable till twenty minutes of incubation then cleavage

started gradually after 30 minutes until fifty percent of the dimer became cleaved after 50 minutes.

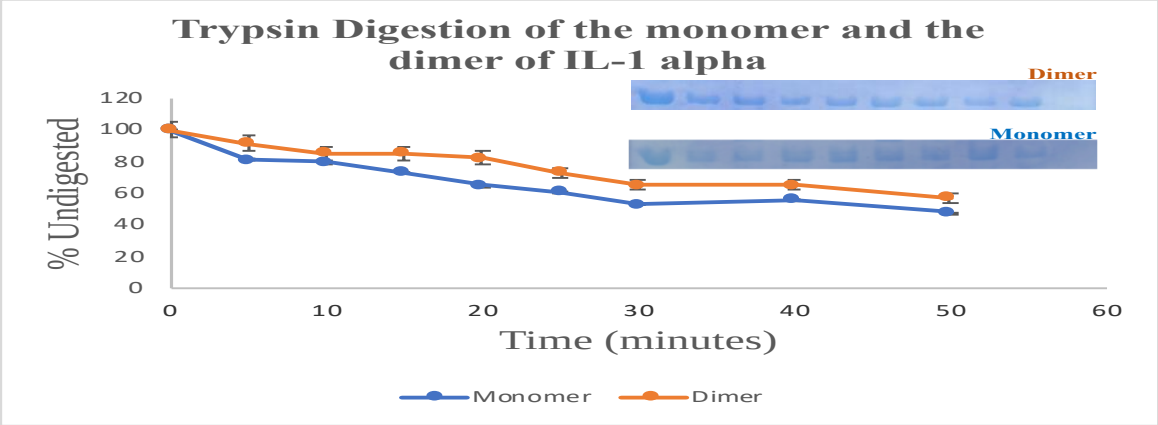

Figure 5: Densitometric analysis of the SDS-PAGE gel analyzing the flexibility of the monomer and the dimer form of IL-1α.

The monomer form of IL-1α showed higher vulnerability to trypsin than the dimer form which suggests that the dimer form is more tightly packed. These results indicate that the dimer formation of IL-1α has better stability effects on the flexibility of the backbone.

Copper induced IL-1α dimerization alters the stability of the protein

Metal binding induces conformational changes that alter the stability of the protein. It is important to investigate the properties of metal binding effects in order to understand the physiological role(s) that are changing the functional characteristics of the proteins. In this context, thermal denaturation was performed to analyze the effects of copper on thermodynamic stability of protein dimerization. Far UV CD spectroscopy was used to measure the thermal stability of the monomer and the dimer forms of IL-1α. The thermal denaturation of the monomer form of IL-1α was examined by analyzing the fraction unfolded at 228 nm (Figure 6).

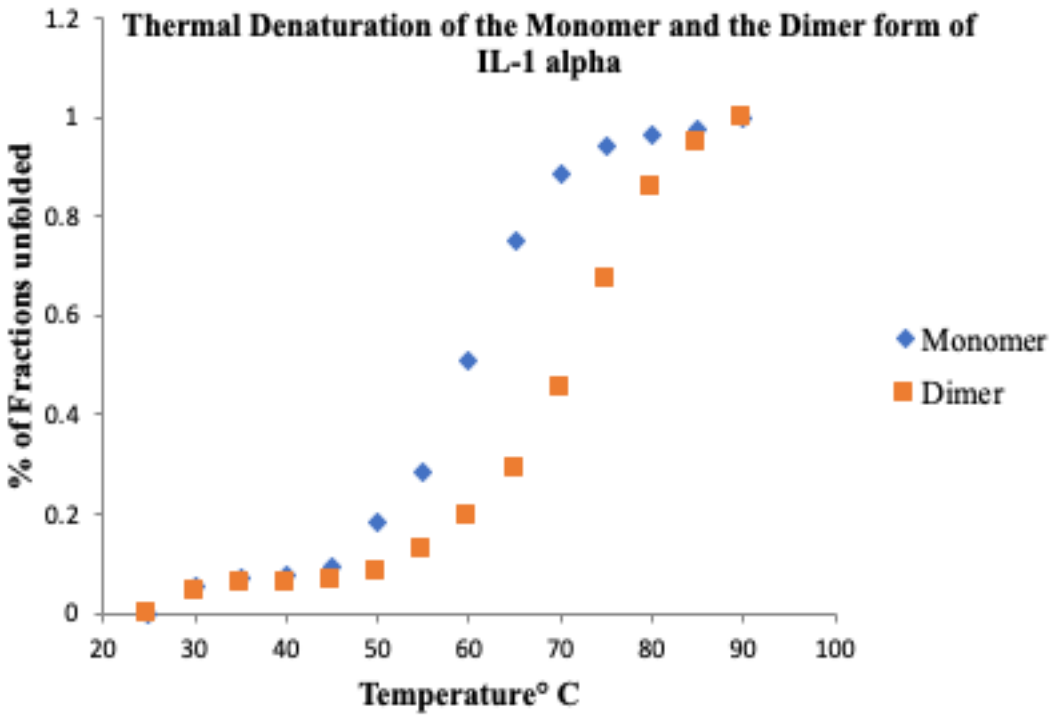

Figure 6: shows thermal stability of IL-1α forms (monomer and dimer).

The monomer form of IL-1α began unfolding at temperature 50°C and it was completely unfolded at 90°C. In order to analyze the denaturation temperature, the melting point (Tm) value should be determined. Tm is the temperature at where 50% of the protein population exists in the denatured state. The Tm value of the IL-1α in monomer states is at 60°C. Interestingly, the copper induced IL-1α dimerization form shows remarkable thermal stability. The thermal stability of the dimer form increases to which the protein starts unfolding at 60°C. The melting point of the dimer form is 70°C. The results suggest that the compact protein structure of the dimer form improved leading to increase the stability of the protein. Also, the formation of disulfide bonds helps in increasing the stability of the dimer form of IL-1α.

Copper induced IL-1α dimerization increases protein chemical stability

In order to complete the protein stability investigation, chemical denaturation was monitored to study the influence of metal binding on protein conformation. It is known that metals alter the mass of hydrogen bonds across the protein core. The Chemical stability was also measured using Far UV CD spectroscopy for the monomer and the dimer forms of IL-1α. The metal binding conformational changes were analyzed by measuring the fractions unfolded for both IL-1α forms to calculate chemical denaturant melting point (Cm). Cm is the concentrations at which 50% of the proteins are in denatured state. Urea was used to study the effect of metal binding on the chemical stability of proteins (Figure 7).

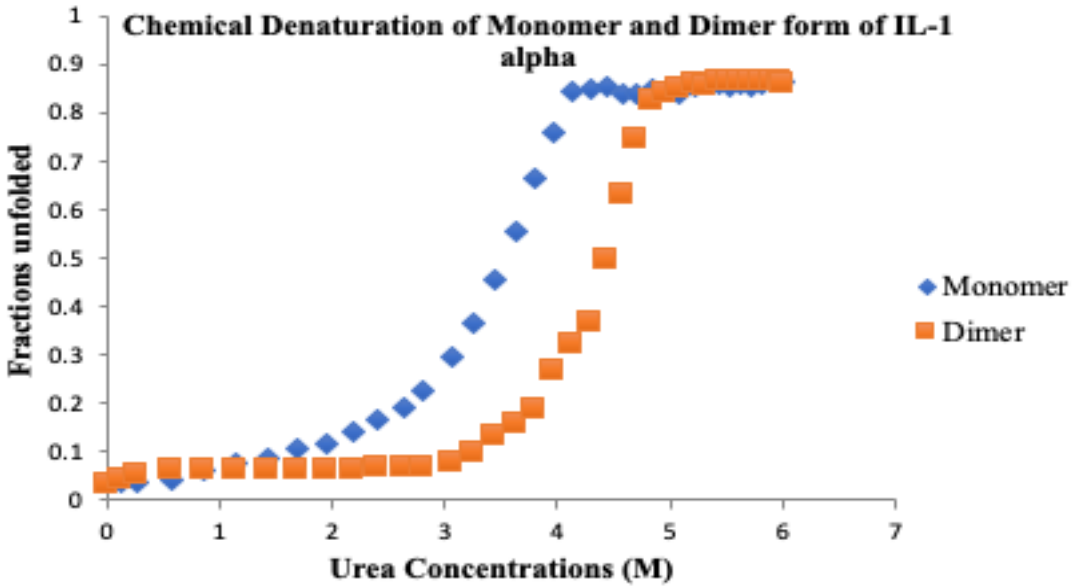

Figure 7: displays the chemical stability of IL-1α in two forms (monomer and dimer).

Urea is known as a non-ionic denaturant salt which breaks hydrogen bonds. The unfolding state of the monomer form of IL-1α began at a urea concentration of 2.18 M and the protein was completely unfolded at a urea concentration of 4.29 M. The Cm

value of the monomer form was 3.5 M. Interestingly, the copper induced IL-1α dimerization showed that the unfolded state started at a concentration of 3.5 M urea and it was entirely unfolded at 4.85 M. The Cm value of the dimer form was 4.5 M. This result indicates that copper binding to the protein stabilizes the protein by increasing the hydrogen bonds and decreasing the protein surface exposed to the solvent.

Cysteine 143 mediates disulfide-liked dimerization of IL-1α

FGF1 is released from NIH 3T3 cells as a biologically inactive homodimeric form in response to heat shock. During heat shock, the cysteine residues of FGF1 are important in the non-classical secretion mechanism since FGF1 free cysteine residues are not released in response to stress[37]. Also, in non-classical secretion of peroxiredoxine 1 and 2 that do not have signal peptides, cysteine residues mediate the protein dimerization in the cytoplasm and during the protein translocation outside of the cells[38]. To gain further insight into understanding the non-classical protein secretion of IL-1α, and since IL-1α has only one cysteine; we attempted to determine whether or not Cys143 is essential in protein dimerization. The cysteine residue was mutated to serine, as both amino acids are similar except the sulfur thiol atom in cysteine is replaced with oxygen in serine. The single IL-1α C143S mutant was overexpressed using the same conditions that were applied in producing the wild type of IL-1α. The IL-1α C143S mutant was successfully overexpressed and the secondary structure of the mutant IL-1α matched that of the wild type. Treating the mutant IL-1α with $CuCl_2$ did induce IL-1α dimerization. The results suggested that cysteine oxidation mediates the formation of a disulfide linked dimer of the wild type IL-1α whereas IL-1α free cysteine failed to present the dimer form.

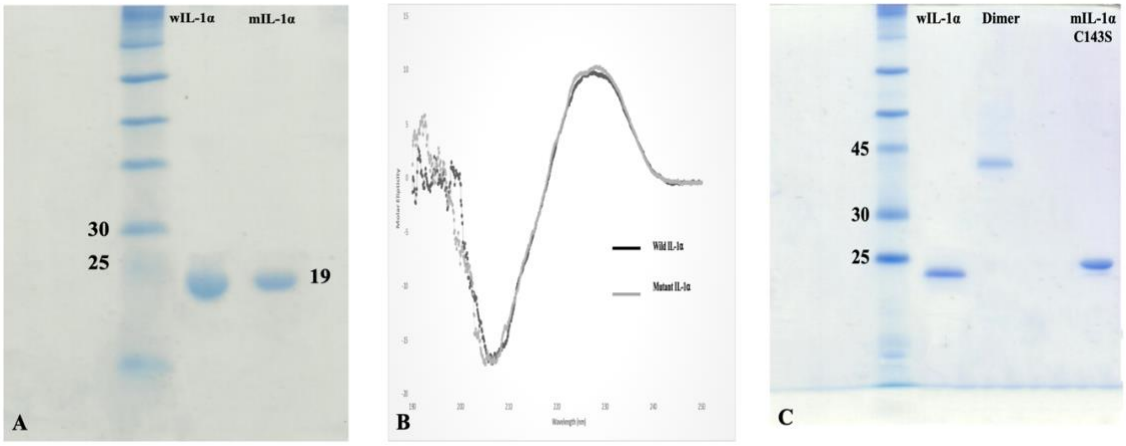

Figure 9: SDS-PAGE showed A: the wild and the mutant proteins have the same molecular weight. B: The secondary structure of the mutant overlays on the wild type of IL-1α. C: Copper induced wild type of IL-1α whereas the copper did not dimerize the mutant.

Interleukin 1 alpha is a copper binding protein as monitored by isothermal titration calorimetry (ITC)

In this study, ITC was used to examine the affinity of IL-1α not only to $CuCl_2$ but also to different metals such as $CaCl_2$, $FeCl_2$, $NiCl_2$, CuCl, $MnCl_2$, ZnCl2, CoCl2, CdCl2 and $MgCl_2$ (Figure 10). ITC revealed that the type of interaction of IL-1α and CuCl2 is exothermic and the reaction has negative enthalpy. The binding curve of the IL-1α and CuCl2 is hyperbolic. The binding constant (Kd) was calculated after applying a best-fit model. The Kd value of the IL-1α to CuCl2 was 1.9 μM. ITC results demonstrate that copper interacts with IL-1α at high affinity which causes conformational changes. These data are in good agreement with copper induced IL-1α dimerization, and protein stability experiments as well as ANS binding assays and trypsin digestion. To determine the specificity of copper binding, ITC was used to titrate IL-1α with various metals. Some metals like MgCl2, NiCl2, CdCl2, and FeCl2 showed weak binding, but the binding did not induce IL-1α dimerization. This means the reaction of these metals with IL-1α were not specific.

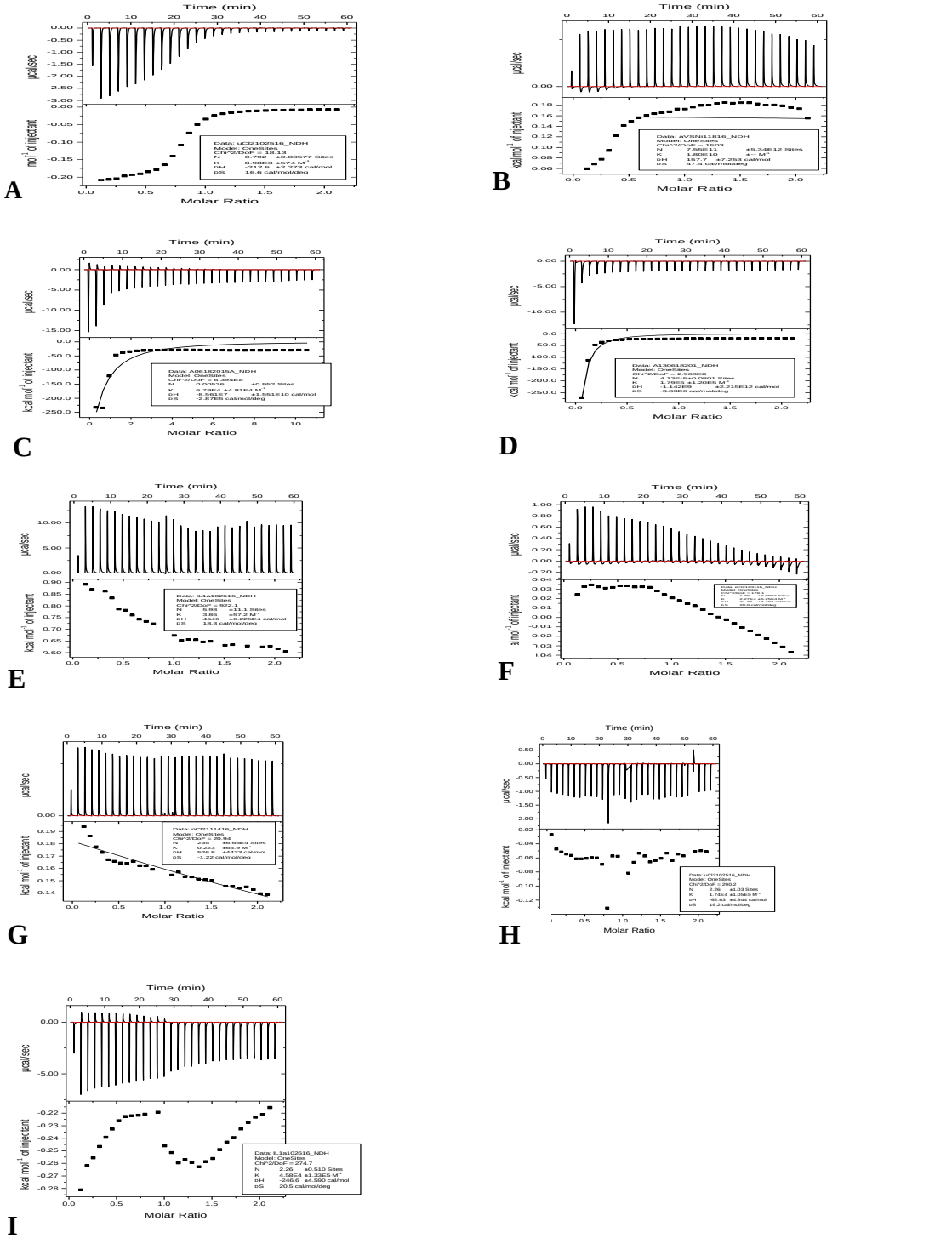

Figure 10: Illustration of the ITC data of IL-1α titrated with different metals. A: Copper shows strong binding affinity to IL-1α. B, C, D, E, F, G, H, and I: illustrate IL-1α has no binding affinity to $NiCl_2$, $MgCl_2$, $CdCl_2$, $CoCl_2$, $FeCl_2$, $MnCl_2$, $ZnCl_2$, and $CaCl_2$. The upper panels of each data represent the raw data and the bottom panels are the best fits of the raw data. The protein concentration was made of 100 µM in 10 mM phosphate buffer at PH 7.2. All ligands concentrations were made of 500 µM.

In order to examine the dimerization effects of all tested metals, SDS-PAGE of interleukin 1 alpha incubated with different metals revealed that only the cupric form of copper had the dimerization effect in interleukin 1 alpha (Figure11).

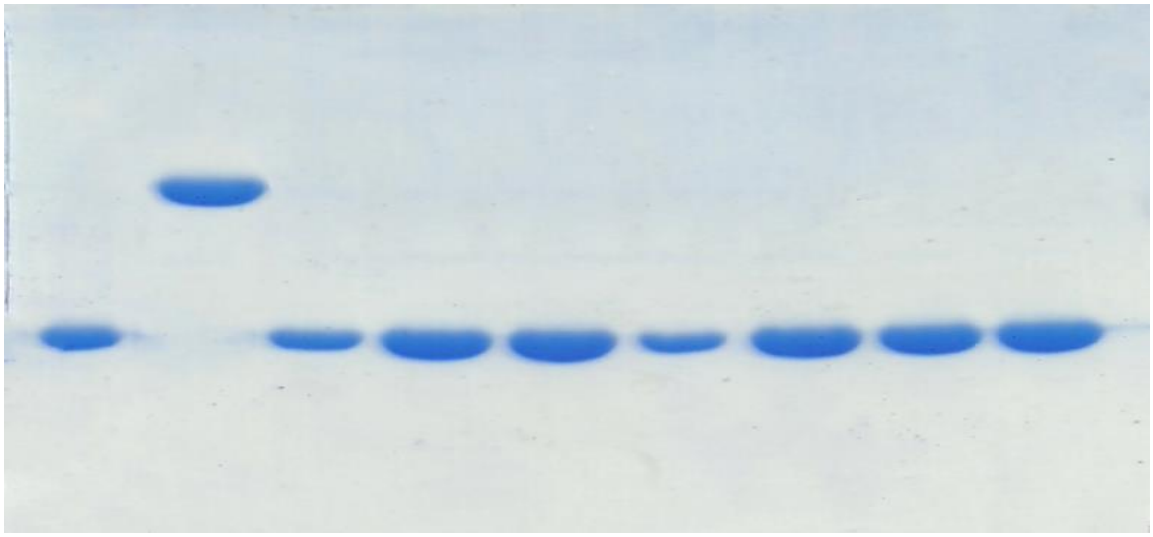

Figure 11 shows the dimerization effect of copper(II) comparing to different metals.

Monomer and dimer forms of IL-1α are S100A13 binding proteins

Studying protein-protein interactions is critical to elucidate the mechanism of IL-1α export. The S100A13 protein is an important partner for signal-less proteins export by the non-classical pathway. The unconventional secretion of FGF1 involves multiprotein complex formation including FGF1, S100A13, and C2A of synaptotagmin 1(Syt1)[29]. S100A13 is a member of the S100 proteins family which play key roles in cellular functions with some indication of participating in tumor progression[39]. S100A13 is calcium-binding protein because of the presence of the EF-hand domains[40]. Due to the absence of a signal peptide, S100A13 is exported by a non-classical mechanism[41]. ITC has shown that the IL-1α (monomer) is binding to S100A13 with a high affinity, so that in this study, ITC is used to determine whether or not the copper induced IL-1α dimeric form binds to S100A13. The data illustrates that the dimeric form of IL-1α has high

binding affinity to S100A13 which suggests that the dimer formation is important for the non-classical protein secretion of IL-1α. Also, the conformational change upon copper binding that was monitored by the ANS binding assay does not alter the binding site where S100A13 interacts.

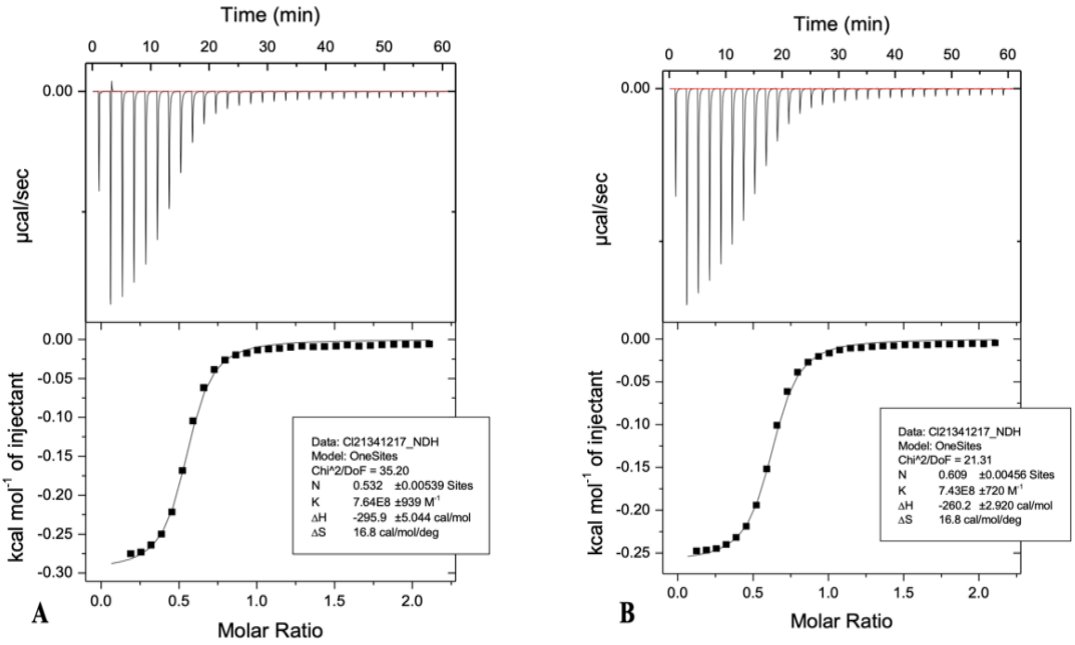

Figure 11*:* A) ITC of the monomer form of IL-1α versus S100A13. B) ITC of copper induced IL-1α dimerization versus S100A13. S100A13 shows strong binding affinity to the dimer form of IL-1α in both conditions. The upper panels of each data represent the raw data and the bottom panels are the best fits of the raw data. The protein concentration was made of 100 µM versus 500 µM of S100A13 in 10 mM phosphate buffer at pH 7.2.

The type of interaction of copper induced IL-1α dimerization and S100A13 and the monomer form of IL-1α that was titrated with S100A13 was exothermic with negative enthalpy. The binding curve for both was hyperbolic. The binding constant (Kd) was calculated after applying the best-fit model. The Kd value of monomer form of IL-1α to S100A13 was 1.3 µM. Interestingly, the Kd of binding was 1.34 µM for copper induced IL-1α dimerization.

Copper induces several chemical shifts

Monitoring backbone conformational changes of proteins can be done using ^{1}H-^{15}N heteronuclear single quantum coherence (HSQC) spectroscopy[42]. Studying ^{1}H-^{15}N crosspeaks, the microenvironment of the amino acids can be examined upon addition of metals or any ligand by analyzing the chemical shift perturbation[43]. Due to the fact that Cu^{++} is paramagnetic, the resonances of the amino acid residues were beyond the detection limit upon binding to Cu^{++}[44]. Therefore, in this study, corpus chloride is used to study the backbone conformation of the protein for two reasons. Firstly, Cu(I) is diamagnetic, so that ^{1}H-^{15}N spectra are not broadened upon binding. Secondly, ITC data showed Cu(I) binds to IL-1α, but it does not cause dimerization (Figure 12).

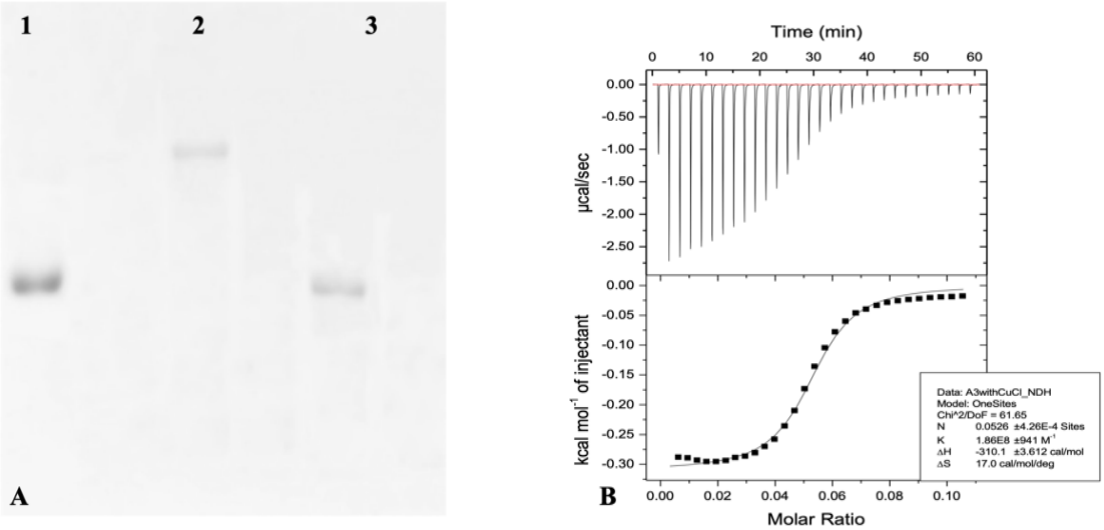

Figure 12: Panel A) Non reduced 15% SDS-PAGE that showed IL-1α without Cu(II) (lane number 1), Cu(II) induced IL-1α dimerization (lane number 2), & IL-1α with Cu(I) with no dimerization (lane number 3) Panel B) ITC of IL-1α titrated with Cu(I)

Upon treating with copper(I), the analysis of superimposition of the ^{1}H-^{15}N HSQC spectra of treated and non-treated IL-1α on the chemical shift perturbation plot showed that copper induces drastic crosspeak shifts corresponding to where copper is binding (Figure 13).

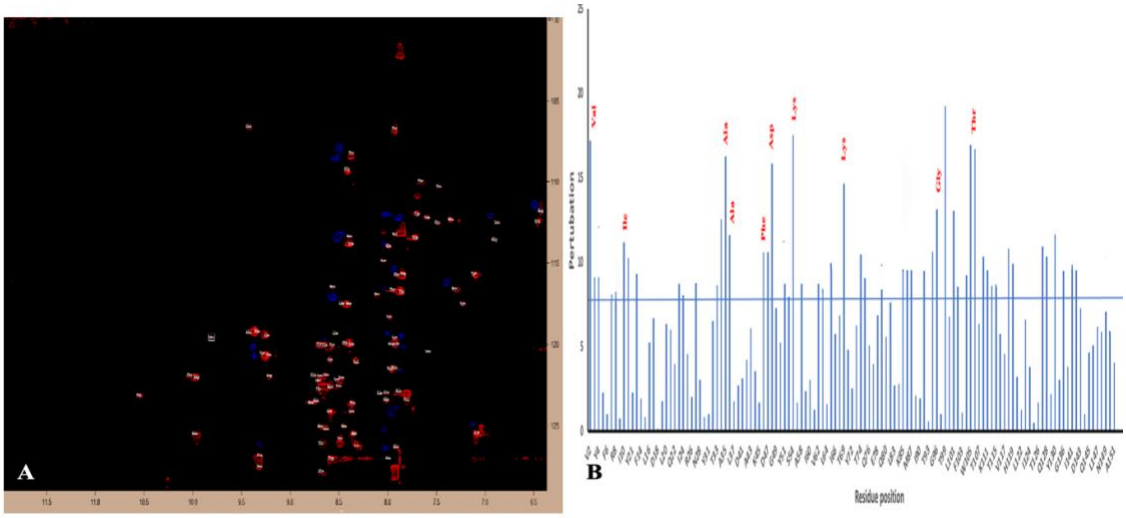

Figure 13: Panel-A) The $^{1}H^{15}N$ HSQC of IL-1 (red) is superimposed onto IL-1α treated with copper (I) (blue). Panel-B) The chemical shift perturbation plot of the IL-1α treated with copper.

In addition, residues Val2, Ile10, Lys11, Lys61, and Arg8, Ser54 that are located in strand one undergoes drastic crosspeak shifts. Also, amino acid residues that are located in strand two including Ala27, Ala34, and Ala35 had significant ^{1}H-^{15}N chemical shift perturbation. Strand three was also perturbed as Gly96, Phe46, and Lys69 displayed chemical shifts. Amino acids residues Asp45, Ser53, and Thr107 that are located in strand four were also perturbed. Unfortunately, cysteine was not assigned in the data of BMRB number 16379, so that it was not possible to calculate the chemical shift. However, cysteine was involved in copper induced dimerization as the study showed that

mIL-1α (C143S) was not induced to build a homodimeric form of IL-1α. ^{1}H-^{15}N data analysis is consistence with the ITC data showing that IL-1α has good binding affinity to copper as many amino acids residues are binding to copper.

Cooper induced IL-1α dimerization is less biologically active than the monomer

The level of secreted embryonic alkaline phosphatase (SEAP) produced by HEK-blue™ was reduced when the cells were exposed to the media that contained copper induced IL-1α dimerization (Figure 14). At high concentration, the dimer form shows some activity because the media is in reduced environment that may break the disulfide bonds producing some monomer form of IL-1α.

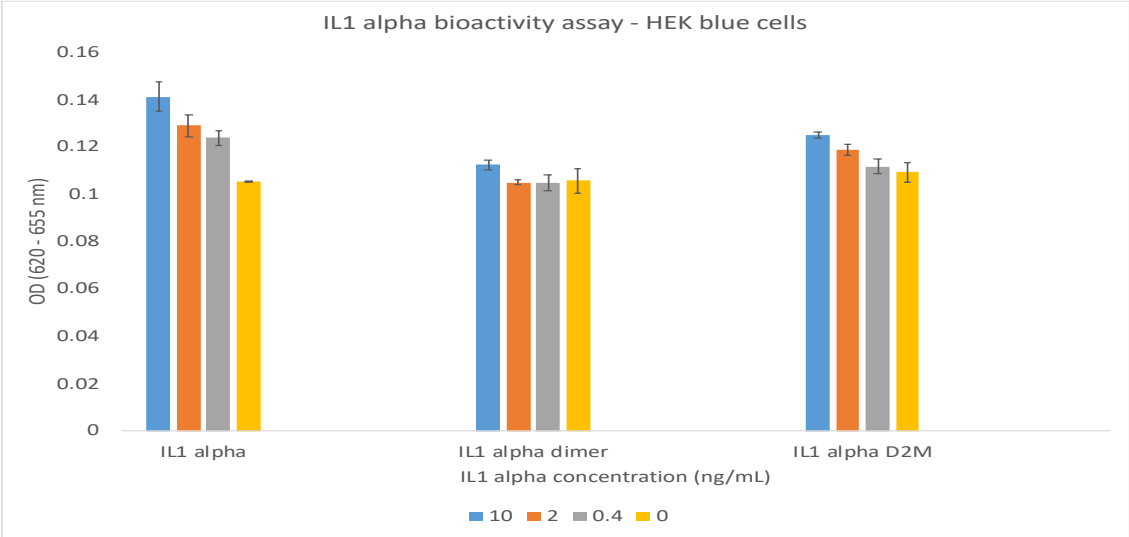

Figure 14: Represents the production of SAEP by HEK-blue cells upon addition of IL-1α (0-50 ng/mL). The calculated standard errors were derived from triplicate measurements.

The monomer form of IL-1α showed significant activity as the concentrations of SEAP increased with the concentration of IL-1α. Also, the activity of the reduced form of copper induced IL-1α dimerization showed similar results as the monomeric form that suggests that the breaking of disulfide bonds has no effects on the protein confirmation

and protein bioactivity.

It is known that copper has a role in non-classical protein secretion of IL1α. However, many questions related to the mechanism which is involved in protein export are still unanswered. Upon binding to copper, conformational changes have occurred to IL1α. Copper induces IL1α dimerization which increases protein stability that has been monitored by thermal and chemical stability of the protein. Increasing the compact nature of the protein is correlated with the results of the limited trypsin digestion which enhances the stability of the dimer form. In the presence and absence of copper, the dimer form of IL1α showed high binding affinity to S100A13 that suggests the involvement of copper in non-classical secretion of IL1α is mediated by inducing the dimerization. It looks like S100A13 is a Cu^{++} provider for inducing IL1α dimerization. This study should be extended further to investigate another partner of S100A13- IL1α (monomer and/or dimer) that helps to make the membrane to flip out and make the delivery such as in the case of annexinII.

Conclusions

Understanding the mechanism of non-classical protein secretion of IL1α helps in designing a treatment for several IL1α related pathological conditions such as cancer and rheumatoid arthritis. We were able to successfully demonstrate the copper induced dimerization of IL1α under *in vitro* conditions. At approximately 46 µM of $CuCl_2$, the monomeric form of IL1α transforms into a dimer. We have identified the Cu^{2+} mediated mechanism of dimerization where the single cysteine at position 143 becomes oxidized resulting in the formation of an inter-disulfide bond leading to the generation of the

homodimer. Also, the result that was gained from this study found that the dimer form of IL1α has binding affinity to S100A13 as well as the monomeric form.

References

1. Chen, L.; Deng, H.; Cui, H.; Fang, J.; Zuo, Z.; Deng, J.; Li, Y.; Wang, X.; Zhao, L., Inflammatory responses and inflammation-associated diseases in organs. Oncotarget 2018, 9 (6), 7204.

2. Kurutas, E. B., The importance of antioxidants which play the role in cellular response against oxidative/nitrosative stress: current state. Nutrition journal 2015, 15 (1), 71.

3. Soetan, K.; Olaiya, C.; Oyewole, O., The importance of mineral elements for humans, domestic animals and plants-A review. African journal of food science 2010, 4 (5), 200-222.

4. Forte, G.; Alimonti, A.; Violante, N.; Di Gregorio, M.; Senofonte, O.; Petrucci, F.; Sancesario, G.; Bocca, B., Calcium, copper, iron, magnesium, silicon and zinc content of hair in Parkinson's disease. Journal of Trace Elements in Medicine and Biology 2005, 19 (2-3), 195-201.

5. Valko, M.; Jomova, K.; Rhodes, C. J.; Kuča, K.; Musilek, K., Redox-and non-redox-metal-induced formation of free radicals and their role in human disease. Archives of toxicology 2016, 90 (1), 1-37.

6. Zlatic, S. A.; Vrailas-Mortimer, A.; Gokhale, A.; Carey, L. J.; Scott, E.; Burch, R.; McCall, M. M.; Rudin-Rush, S.; Davis, J. B.; Hartwig, C., Rare disease mechanisms identified by genealogical proteomics of copper homeostasis mutant pedigrees. Cell systems 2018, 6 (3), 368-380. e6.

7. Denoyer, D.; Masaldan, S.; La Fontaine, S.; Cater, M. A., Targeting copper in cancer therapy:'Copper That Cancer'. Metallomics 2015, 7 (11), 1459-1476.

8. Lopez, J.; Ramchandani, D.; Vahdat, L., Copper Depletion as a Therapeutic Strategy in Cancer. Essential Metals in Medicine: Therapeutic Use and Toxicity of Metal Ions in the Clinic 2019, 19, 303.

9. Vimalraj, S.; Rajalakshmi, S.; Preeth, D. R.; Kumar, S. V.; Deepak, T.; Gopinath, V.; Murugan, K.; Chatterjee, S., Mixed-ligand copper (II) complex of quercetin regulate osteogenesis and angiogenesis. Materials Science and Engineering: C 2018, 83, 187-194.

10. Kardos, J.; Héja, L.; Simon, Á.; Jablonkai, I.; Kovács, R.; Jemnitz, K., Copper signalling: causes and consequences. Cell Communication and Signaling 2018, 16 (1), 71.

11. Hatori, Y.; Lutsenko, S., The role of copper chaperone Atox1 in coupling redox homeostasis to intracellular copper distribution. Antioxidants 2016, 5 (3), 25.

12. Rajalingam, D.; Kumar, T. K. S.; Yu, C., The C2A domain of synaptotagmin exhibits a high binding affinity for copper: implications in the formation of the multiprotein FGF release complex. Biochemistry 2005, 44 (44), 14431-14442.

13. Rajalingam, D.; Kumar, T. K. S.; Soldi, R.; Graziani, I.; Prudovsky, I.; Yu, C., Molecular mechanism of inhibition of nonclassical FGF-1 export. Biochemistry 2005, 44 (47), 15472-15479.

14. Pan, Q.; Kleer, C. G.; Van Golen, K. L.; Irani, J.; Bottema, K. M.; Bias, C.; De Carvalho, M.; Mesri, E. A.; Robins, D. M.; Dick, R. D., Copper deficiency induced by tetrathiomolybdate suppresses tumor growth and angiogenesis. Cancer research 2002, 62 (17), 4854-4859.

15. Daniels, M.; Brough, D., Unconventional pathways of secretion contribute to inflammation. International journal of molecular sciences 2017, 18 (1), 102.

16. Lee, M. C.; Miller, E. A.; Goldberg, J.; Orci, L.; Schekman, R., Bi-directional protein transport between the ER and Golgi. Annu. Rev. Cell Dev. Biol. 2004, 20, 87-123.

17. Viotti, C., ER to golgi-dependent protein secretion: the conventional pathway. In Unconventional Protein Secretion, Springer: 2016; pp 3-29.

18. Dupont, N.; Jiang, S.; Pilli, M.; Ornatowski, W.; Bhattacharya, D.; Deretic, V., Autophagy-based unconventional secretory pathway for extracellular delivery of IL-1β. The EMBO journal 2011, 30 (23), 4701-4711.

19. Prudovsky, I.; Mandinova, A.; Soldi, R.; Bagala, C.; Graziani, I.; Landriscina, M.; Tarantini, F.; Duarte, M.; Bellum, S.; Doherty, H., The non-classical export routes: FGF1 and IL-1α point the way. Journal of Cell Science 2003, 116 (24), 4871-4881.

20. Nickel, W., Pathways of unconventional protein secretion. Current opinion in biotechnology 2010, 21 (5), 621-626.

21. Martín-Sánchez, F.; Diamond, C.; Zeitler, M.; Gomez, A.; Baroja-Mazo, A.; Bagnall, J.; Spiller, D.; White, M.; Daniels, M.; Mortellaro, A., Inflammasome-dependent IL-1β release depends upon membrane permeabilisation. Cell death and differentiation 2016, 23 (7), 1219.

22. Laberge, R.-M.; Sun, Y.; Orjalo, A. V.; Patil, C. K.; Freund, A.; Zhou, L.; Curran, S. C.; Davalos, A. R.; Wilson-Edell, K. A.; Liu, S., MTOR regulates the pro-tumorigenic senescence-associated secretory phenotype by promoting IL1A translation. Nature cell biology 2015, 17 (8), 1049.

23. Landriscina, M.; Soldi, R.; Bagalá, C.; Micucci, I.; Bellum, S.; Tarantini, F.; Prudovsky, I.; Maciag, T., S100A13 participates in the release of fibroblast growth

factor 1 in response to heat shock in vitro. Journal of Biological Chemistry 2001, 276 (25), 22544-22552.

24. Landriscina, M.; Bagalá, C.; Mandinova, A.; Soldi, R.; Micucci, I.; Bellum, S.; Prudovsky, I.; Maciag, T., Copper induces the assembly of a multiprotein aggregate implicated in the release of fibroblast growth factor 1 in response to stress. Journal of Biological Chemistry 2001, 276 (27), 25549-25557.

25. Kathir, K. M.; Gao, L.; Rajalingam, D.; Daily, A. E.; Brixey, S.; Liu, H.; Davis, D.; Adams, P.; Prudovsky, I.; Kumar, T. K. S., NMR characterization of copper and lipid interactions of the C2B domain of synaptotagmin I—relevance to the non-classical secretion of the human acidic fibroblast growth factor (hFGF-1). Biochimica et Biophysica Acta (BBA)-Biomembranes 2010, 1798 (2), 297-302.

26. Brewer, G. J.; Dick, R. D.; Grover, D. K.; LeClaire, V.; Tseng, M.; Wicha, M.; Pienta, K.; Redman, B. G.; Jahan, T.; Sondak, V. K., Treatment of metastatic cancer with tetrathiomolybdate, an anticopper, antiangiogenic agent: Phase I study. Clinical Cancer Research 2000, 6 (1), 1-10.

27. Zhang, J.; Cousens, L. S.; Barr, P. J.; Sprang, S. R., Three-dimensional structure of human basic fibroblast growth factor, a structural homolog of interleukin 1 beta. Proceedings of the National Academy of Sciences 1991, 88 (8), 3446-3450.

28. Prudovsky, I.; Tarantini, F.; Landriscina, M.; Neivandt, D.; Soldi, R.; Kirov, A.; Small, D.; Kathir, K. M.; Rajalingam, D.; Kumar, T. K. S., Secretion without golgi. Journal of cellular biochemistry 2008, 103 (5), 1327-1343.

29. Kathir, K. M.; Ibrahim, K.; Rajalingam, D.; Prudovsky, I.; Yu, C.; Kumar, T. K. S., S100A13–lipid interactions—role in the non-classical release of the acidic fibroblast growth factor. Biochimica et Biophysica Acta (BBA)-Biomembranes 2007, 1768 (12), 3080-3089.

30. Sivaraja, V.; Kumar, T. K. S.; Rajalingam, D.; Graziani, I.; Prudovsky, I.; Yu, C., Copper binding affinity of S100A13, a key component of the FGF-1 nonclassical copper-dependent release complex. Biophysical journal 2006, 91 (5), 1832-1843.

31. Heizmann, C. W.; Cox, J. A., New perspectives on S100 proteins: a multi-functional Ca 2+-, Zn 2+-and Cu 2+-binding protein family. Biometals 1998, 11 (4), 383-397.

32. Gosavi, S.; Whitford, P. C.; Jennings, P. A.; Onuchic, J. N., Extracting function from a β-trefoil folding motif. Proceedings of the National Academy of Sciences 2008, 105 (30), 10384-10389.

33. Priestle, J. P.; Schär, H.-P.; Grütter, M., Crystal structure of the cytokine interleukin-1 beta. The EMBO journal 1988, 7 (2), 339.

34. Goh, C.-S.; Milburn, D.; Gerstein, M., Conformational changes associated with protein–protein interactions. Current opinion in structural biology 2004, 14 (1), 104-109.

35. Gabellieri, E.; Strambini, G. B., Perturbation of protein tertiary structure in frozen solutions revealed by 1-anilino-8-naphthalene sulfonate fluorescence. Biophysical journal 2003, 85 (5), 3214-3220.

36. Lindh, E., Increased resistance of immunoglobulin A dimers to proteolytic degradation after binding of secretory component. The journal of immunology 1975, 114 (1 Part 2), 284-286.

37. Tarantini, F.; Gamble, S.; Jackson, A.; Maciag, T., The cysteine residue responsible for the release of fibroblast growth factor-1 resides in a domain independent of the domain for phosphatidylserine binding. Journal of Biological Chemistry 1995, 270 (49), 29039-29042.

38. Mullen, L.; Hanschmann, E.-M.; Lillig, C. H.; Herzenberg, L. A.; Ghezzi, P., Cysteine oxidation targets peroxiredoxins 1 and 2 for exosomal release through a novel mechanism of redox-dependent secretion. Molecular Medicine 2015, 21 (1), 98-108.

39. Miao, S.; Qiu, T.; Zhao, Y.; Wang, H.; Sun, X.; Wang, Y.; Xuan, Y.; Qin, Y.; Jiao, W., Overexpression of S100A13 protein is associated with tumor angiogenesis and poor survival in patients with early-stage non-small cell lung cancer. Thoracic cancer 2018, 9 (9), 1136-1144.

40. Ridinger, K.; Schäfer, B. W.; Durussel, I.; Cox, J. A.; Heizmann, C. W., S100A13 biochemical characterization and subcellular localization in different cell lines. Journal of Biological Chemistry 2000, 275 (12), 8686-8694.

41. Gilston, B. A.; Skaar, E. P.; Chazin, W. J., Binding of transition metals to S100 proteins. Science China Life Sciences 2016, 59 (8), 792-801.

42. Clarkson, J.; Campbell, I., Studies of protein–ligand interactions by NMR. Portland Press Ltd.: 2003.

43. Airoldi, C.; Merlo, S.; Sironi, E., NMR Molecular Recognition Studies for the Elucidation of Protein and Nucleic Acid Structure and Function. In Applications of NMR Spectroscopy, Elsevier: 2015; pp 147-219.

44. Sengupta, I.; Gao, M.; Arachchige, R. J.; Nadaud, P. S.; Cunningham, T. F.; Saxena, S.; Schwieters, C. D.; Jaroniec, C. P., Protein structural studies by paramagnetic solid-state NMR spectroscopy aided by a compact cyclen-type Cu (II) binding tag. Journal of biomolecular NMR 2015, 61 (1), 1-6.

Chapter Four

Investigation the Role of Amlexanox in Non-Classical Secretion of Interleukin 1 alpha

Abstract

The interleukin-1 (IL-1) family of pro-inflammatory cytokines is known to amplify cancer metastasis, making them potential targets for treatment. Non-classical secretion of IL-1α appears to be mediated by a Cu^{2+} binding. Hence, development of drugs to inhibit the Cu^{2+} mediated oligomerization and resultant multiprotein complex interactions could block tumor angiogenesis. This study focused on elucidating the underlying molecular effects of non-classical release of IL-1α upon treatment with the drug amlexanox (AMX). AMX has low solubility below pH 8.2. This finding is characteristic of metal chelators such as ethylenediamine tetraacetic acid (EDTA), nitrilotriacetic acid (NTA), and iminodiacetic acid. Also, AMX can bind to copper as well as IL-1α that may interfere with the non-classical secretion of the protein. Binding of IL-1α to AMX may induce conformational changes, which interfere with the flexibility and stability of IL-1α. This study shed light in identifying the cause and plausible mechanism involved in the secretion of these intriguing cytokines, which could pave the way towards development of potent cancer drugs.

Introduction

IL-1α is a key member of the IL-1 family[1, 2]. It is unique in certain properties compared to the other members of the cytokine family[3, 4]. IL-1α expression is significantly responsive to wide range of external stimuli[5-7]. IL-1α plays a key role in many cellular processes such as inflammation, proliferation, and immunological reactions against many microbial infections[8, 9]. IL-1α also plays key roles in molecular decisions during infections and stress conditions[10, 11]. Cellular reposes to IL-1α actions represents through the inflammatory mechanism that activates inflammatory cells[12, 13]. Also, many studies have linked IL-1α to wound healing, rheumatoid arthritis, cancer metastasis, and Alzheimer's disease[12, 14]. IL-1α lacks the signal segment that guides protein secretion through the endoplasmic reticulum-Golgi apparatus complex[15, 16]. In non-classical secretion of IL-1α, multiprotein complex formation takes place that acts as a cargo targeting IL-1α to be exported outside the cells[15, 17]. The underlying mechanisms governing IL-1α export from cells requires further investigation. Also, the mechanism of multiprotein complex formation of IL-1α and S100A13 inside cells needs to be deciphered. S100A13 is a member of S100 protein family that binds to calcium[18, 19]. The S100 protein family is characterized by forming two EF segments that are classified into a C-terminal hand and an N-terminal hand[20-22]. S100A13, a Ca^{2+} binding protein, is a small protein that exhibits ubiquitously in different tissues such as intestine, heart, kidney, ovary, and muscles[23-25]. S100A13 regulates a wide range of cellular functions including cellular proliferation, muscle contraction, and protein export[26-28]. In fact, S100A13 is the only S100 member that is involved in protein translocation of signal-less proteins by non-classical protein secretion during cellular stress[29-31]. IL-1α is well known

as an angiogenic cytokine that secretes into the extracellular compartment under stress conditions without a signal peptide[32, 33]. Uncontrolled release of IL-1α is responsible for various pathological conditions such as autoimmune disorders and tumor angiogenesis[8, 34]. Several reports confirmed the role of IL-1α in the growth progress of breast and intestinal cancer[9, 35]. Several studies have shown copper (Cu^{2+}) is involved in non-classical secretion of signal-less proteins[36-38]. Cu^{2+} plays a crucial role in forming multiprotein complex release of FGF1[39, 40]. It was demonstrated that amlexanox (AMX) (Figure 1), the anti-allergic and anti-inflammatory drug[41], can inhibit non-classical secretion of FGF1[42]. The mechanism that involves the inhibition of FGF1 secretion by AMX includes different processes. Some scientists confirmed that AMX binds to S100A13, which in return prevents multiprotein complex formation that includes FGF1 and S100A13[43, 44]. Also, some studies showed that AMX is used to treat aphthous ulcers, inflammation of gums or tongue, because it inhibits the release of inflammatory mediators[45, 46]. Studying the role of AMX in exporting IL-1α paves the way for developing a new drug that inhibits the non-classical secretion of IL-1α.

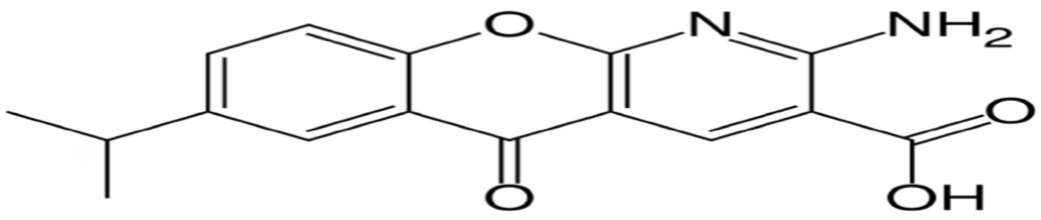

Figure 1: depicts the chemical structure of amlexanox[47].

The main objective of the present study is to shed light on how AMX binds to IL-1α and stops non-classical secretion of the protein. This investigation includes several

physical experiments to elucidate the role of AMX on the monomer/dimer form of IL-1α and to investigate if AMX may be involved in regulating copper involvement.

Materials and Methods

Materials All buffer components including Na_2HPO_4, NaH_2PO_4, and NaCl were purchased from VWR Scientific Inc, USA. Lysogeny broth (LB) and urea were bought from EMD Millipore, USA. 1-anilino-8-naphthalene sulfonate and Trypsin were obtained from Sigma. Nickel sepharose was obtained from GE Healthcare, USA.

Far-UV Circular Dichroism Spectroscopy Far-UV CD measurements were accomplished using Jasco 1500 spectrometer to determine the secondary structure changes. To obtain the CD spectrum, the machine was setup to scan the protein samples at a speed of 20 nm/min using wavelength of 190-250 nm at 25°C or at specific temperature when it was required. The protein concentration of 0.5 mg/mL in 10mM phosphate buffer (pH 7.2) was examined. All data were smoothed using the Savitzky-Golay algorithm for the best fit. Far-CD was used for studying the following experiments

A: Thermal Denaturation Thermal denaturation studies were performed on the JASCO-1500 spectrometer to reveal how temperature affects the stability of IL-1 in presence and absence of AMX. Spectra were collected from 25°C to 90°C in five-degree intervals.

B: Chemical Denaturation (Urea denaturation) For the chemical denaturation studies, 8M urea was used to induce protein denaturation. This process was monitored using JASCO-1500 s spectrometer. Data of samples of 0.5 mg/ml proteins in 10 mM PB were each over the titration of urea. Samples of 0.5 mg/ml protein in 10 mM PB were used for titration with urea. These experiments revealed information about the stability of the protein in the presence and absence of AMX.

Extrinsic Fluorescence experiment Extrinsic fluorescence experiments (ANS binding assays) were performed using a Hitachi F-2500 fluorescence spectrophotometer at 25°C to provide information regarding the protein's tertiary structure. ANS (8-anilinonaphthalene-1-sulfonic acid) is an extrinsic fluorophore that fluoresces when it binds to solvent exposed hydrophobic regions of a protein. A protein concentration of 0.5 mg/mL in 10 mM phosphate buffer, pH 7.2 was used. All fluorescence measurements were recorded using the slit width set to 2.5 nm, excitation wavelength of 280 nm, and emission wavelength range from 300-450 nm. Performing ANS binding assays, the titrations were carried out by adding 1μL of ANS per interval. The relative fluorescence intensity was recorded at 510 nm.

Limited Trypsin Digestion (LTD) Proteolytic trypsin digestion was performed to determine the structural flexibility of the protein with and without the ligand. Trypsin cleaves peptide bonds at the C-terminal end of lysine and arginine amino acids residues. The water bath was used to incubate the samples immediately at 37 °C. After the samples were removed from the water bath, TCA preparation was performed on each sample to stop the trypsin reaction. Samples were then assessed using 15% SDS-PAGE analyzed with UN-SCAN-IT gel software (Silk Scientific Inc., USA). The intensity of the bands in the gel stained with Coomassie blue were compared to control bands containing pure protein with or without the ligand.

Isothermal titration calorimetry (ITC) Isothermal calorimetry (ITC) is a great thermodynamic technique used to study the binding affinity of interacting macromolecules, by measuring changes in entropy and enthalpy in this case, the binding of AMX and IL-1α. The ITC system consists of two adjacent cells (reference cell and

sample cell) in an adiabatic jacket, which prevents heat transfer between the environment and the cells. Protein samples were prepared in 10 mM phosphate buffer pH 7.2. The protein sample was degassed at 25ºC before titration. During the titration, the generated heat from the binding of ligands to the protein was measured. Then, the data was processed using Origin software provided by the manufacturer to get the best fit. Kd value, the equilibrium dissociation constant of the reaction, was calculated for each ligand.

Results and Discussion

AMX behaves as copper chelator molecules

Amlexanox needs high pH to be dissolved completely. It dissolves at pH 8.8, 10 mM phosphate buffer. Dissolving at high pH is characteristics for metals chelators such as EDTA[48]. This finding may suggest that AMX can be used as copper chelators. In this context, ITC was performed to confirm whether or not AMX binds to copper (Figure 2).

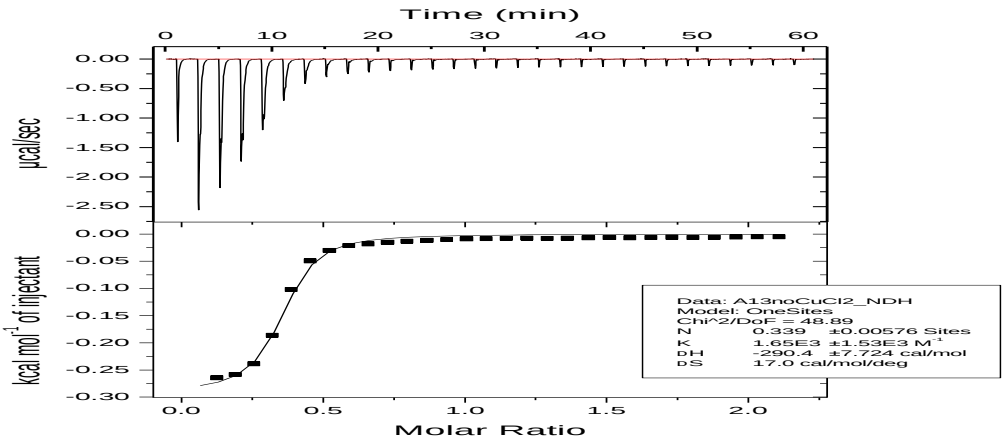

Figure 2: Isothermogram representing the binding of AMX to copper. The data represented the best curve fit using ITC software.

The calculated Kd value calculated from the ITC data was 1.6 µM. This finding indicates that AMX can regulate the involvements of copper in many biological processes.

AMX prevents copper induced IL-1α dimerization

The previous results may indicate that AMX could stop copper induced IL-1α dimerization. The homodimer of IL-1α is mediated by the oxidation of the thiol group of cysteine 143. In order to examine this theory, IL-1α was incubated with different concentrations of AMX followed by addition of 46 µM of CuCl2, the concentration required to induce dimerization to 100 µM of IL-1α completely. 15% SDS-PAGE was used to reveal the results (Figure 3 A & B). It seems that AMX prevents oxidation of Cys143's thiol group by copper, so that inter-disulfide bond formation was blocked.

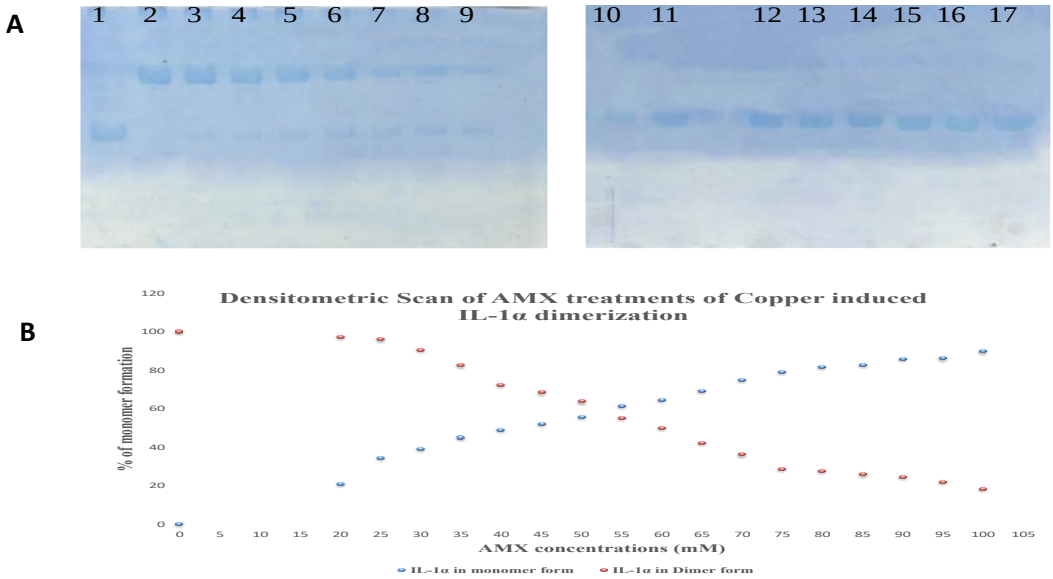

Figure 3: A) AMX interferes with Cu^{++} induced IL-1α dimerization. The protein samples were first incubated with different concentrations of AMX and then $CuCl_2$ was added. The numbers above the gels represent the protein samples based on AMX concentrations: 1) IL-1α monomer, 2) 20µM AMX, 3) 25µM AMX, 4) 30µM AMX, 5) 35µM AMX, 6) 40µM AMX, 7) 45µM AMX. 8) 50µM AMX, 9) 55µM AMX, 10) 60µM AMX, 11) 65µM AMX, 12) 70µM AMX, 13) 75µM AMX, 14) 80µM AMX, 15) 85µM AMX. 16) 90µM AMX. 17) 100µM AMX. B) Densitometric scan of the monomer formation of IL-1α that induce at different concentrations of AMX.

AMX binds to IL-1α

ITC was used to determine AMX binding affinity of IL-1α. The binding affinity is represented by the dissociation constant (Kd) value that is the reciprocal of the association constant (Ka) value. Ka value is obtained from ITC data. A small Kd value correlates to high binding affinity. The Kd value for AMX binding to IL-1α was 1.9 µM as shown (Figure 4). This indicates AMX has high binding affinity to the protein. These results may confirm that AMX might be used for inhibiting non-classical release of IL-1α.

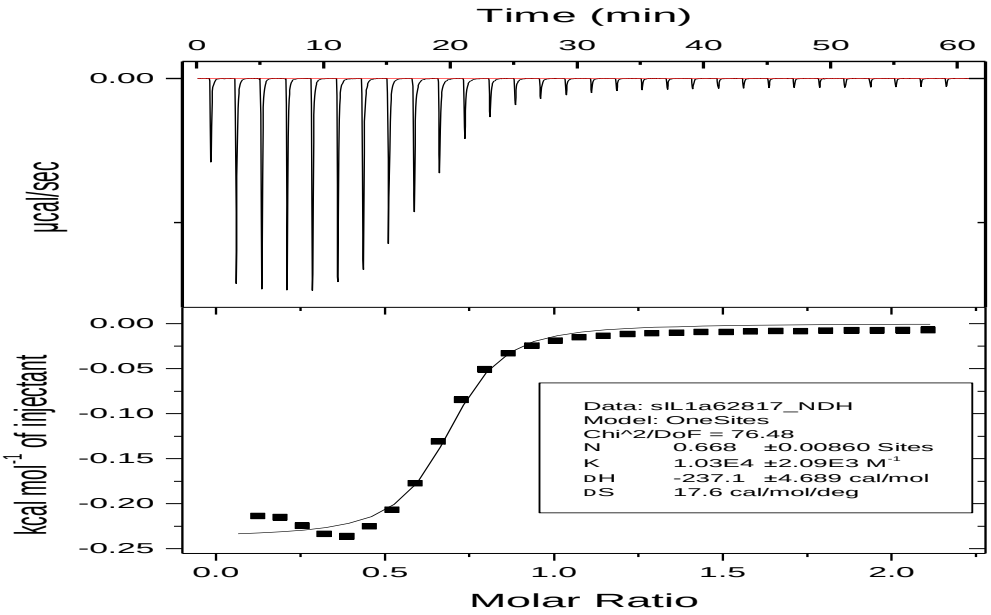

Figure 4: Isothermogram representing the binding of AMX to IL-1α. Protein concentration was 100 µM and AMX was 50 µM. All samples were prepared in phosphate buffer.

AMX decreases IL-1α affinity to copper

Copper induced IL-1α dimerization is mediated by cysteine 143. Copper oxidizes the thiol group to convert cysteine to cystine. Forming a disulfide bridge between two

protein molecules. AMX prevents IL-1α dimerization by copper and also it chelates copper. AMX prevents copper-induced IL-1α dimerization by chelating copper. In order to confirm that AMX and copper bind in the same site, ITC was performed with IL-1α mixed first with AMX then titrated with copper chloride (Figure 5). ITC data showed that copper lost its affinity to IL-1α in presence of AMX.

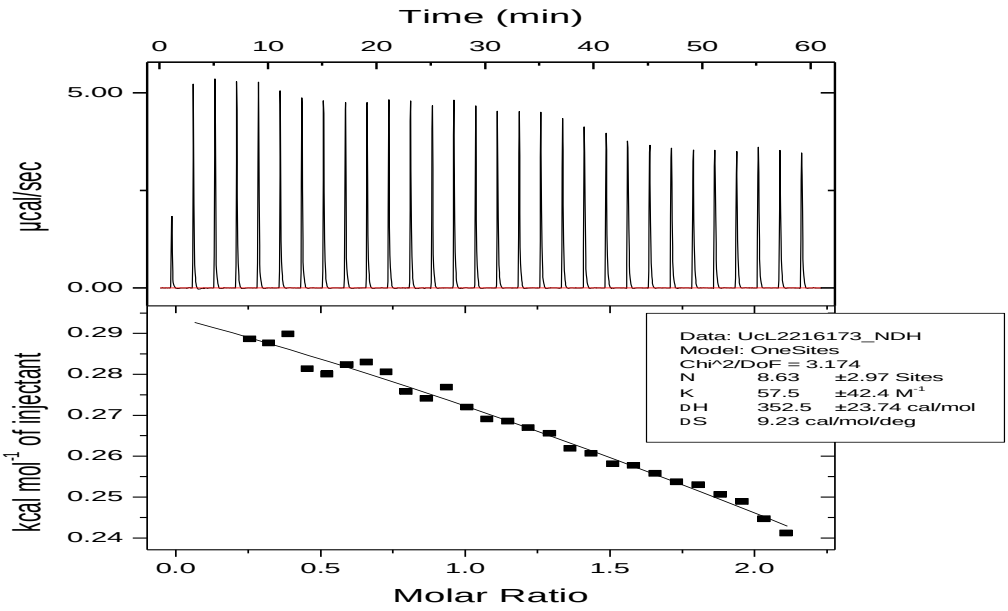

Figure 5: ITC data is showing the binding of copper to AMX bound IL-1α. After AMX binding, the bound form was dialyzed to remove all AMX that can bind to copper. All samples were prepared in phosphate buffer.

AMX binding alters IL-1α conformation

Anilino naphthalene 8-sulfonate (ANS) is a non-polar reagent used to examine the flexibility of solvent-exposed hydrophobic surfaces in proteins. Upon binding to hydrophobic pocket within the protein, ANS fluoresces which helps examine the structural rigidity of proteins. Hydrophobic interactions of proteins are important in protein folding and stability. Upon binding to ANS, IL-1α shows an emission maximum

at 510 nm and the surface exposed hydrophobic regions of protein in presence of AMX were saturated at ANS concentration of 150 µM (Figure 6). Whereas the ANS saturation curves of IL-1α without AMX were saturated at ANS concentration 115 µM. These finding suggest that in presence of AMX, the protein is more structurally flexible in which the solvent exposed hydrophobic surfaces are reduced in presence of AMX, indicating that AMX helps shift the protein to a more compact state.

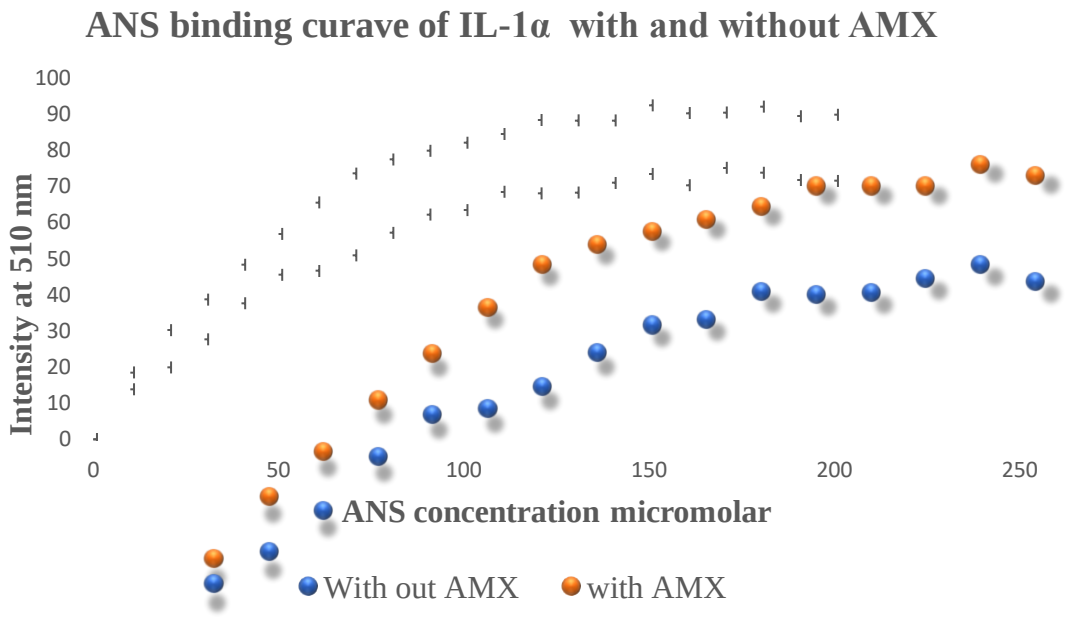

Figure 6: ANS binding curve of IL-1α with and without AMX.

AMX increase IL-1α flexibility

Limited proteolytic digestion experiment investigates the mode of action between the protein and the ligand. In general, protein-ligand binding can mask the potential cleavage sites of the substrate. The masking will delay the proteolytic enzyme to reach the cleavage sites. This delay can be detected by analyzing the differences in the cleavage

pattern between the free protein and the protein-ligand bound forms on the SDS-PAGE gel. In order to study the effects of AMX on the conformational flexibility of IL-1α, limited trypsin digestion was used. Trypsin cleaves at the carboxyl end of the amino acids lysine and arginine unless proline comes after either one of them. IL-1α has four arginine residues and eleven lysine residues and both are not followed by proline, so there are fifteen potential trypsin cleavage sites. In time dependent trypsin digestion, protein samples were incubated at 37 °C using water bath. Then, the results were revealed using 15% SDS-PAGE gel followed by measuring the bands intensity using densitometric scan. With no AMX, IL-1α was more susceptible to trypsin in which trypsin cleaved 50% of the proteins after 25 minutes whereas IL-1α in presence of AMX got cleaved after 35 minutes (Figure 7). It seems that binding to AMX, IL-1α has enhanced resistance to trypsin action. This indicates that AMX binds where trypsin cleavage sites are located. This decreased susceptibility to trypsin digestion suggests that the backbone of IL-1α mixed with AMX is more flexible than IL-1α alone.

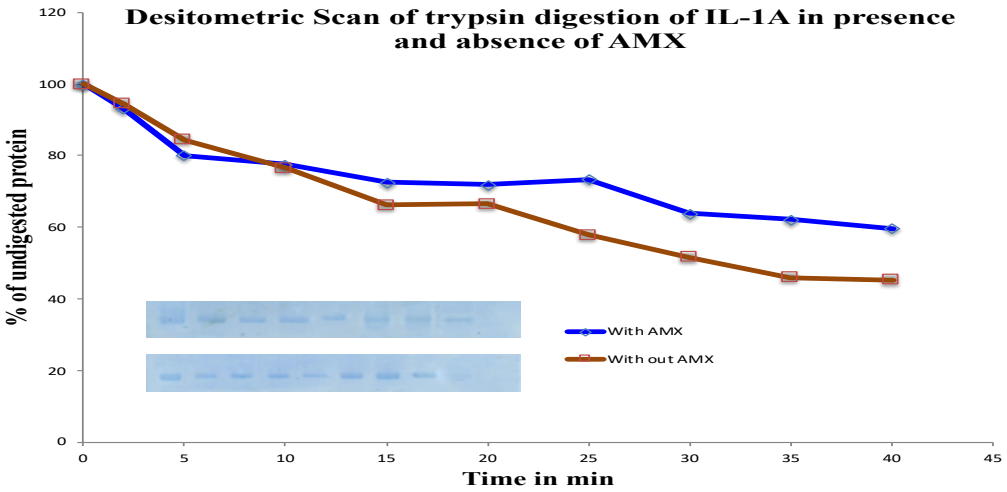

Figure 7: Densitometric plot of limited time trypsin digestion showing the rate of cleavage of IL-1α, incubated at 37ºC. The insert shows the 15% SDS-PAGE with lanes 1-9 representing 5, 10, 15, 20, 25, 30, 35, 40, and 45 minutes.

IL-1α is stabilized by AMX

Thermal denaturation of IL-1α was examined by circular dichroism from 25-90°C at 5°C increments. Unfolding of the proteins under different temperatures was monitored by the change in secondary structure of IL-1α at 208 nm and 215 nm. The temperature-induced unfolding curves of the IL-1α with no AMX and IL-1α with AMX show that IL-1α with AMX is more stable at higher temperatures than the protein alone, shown in (Figure 8). Denaturation midpoint (Tm) where 50% of the proteins are in the folded state was 65 °C in presence of AMX whereas with no AMX the Tm was 60°C. These results indicate that AMX has good affinity to IL-1α.

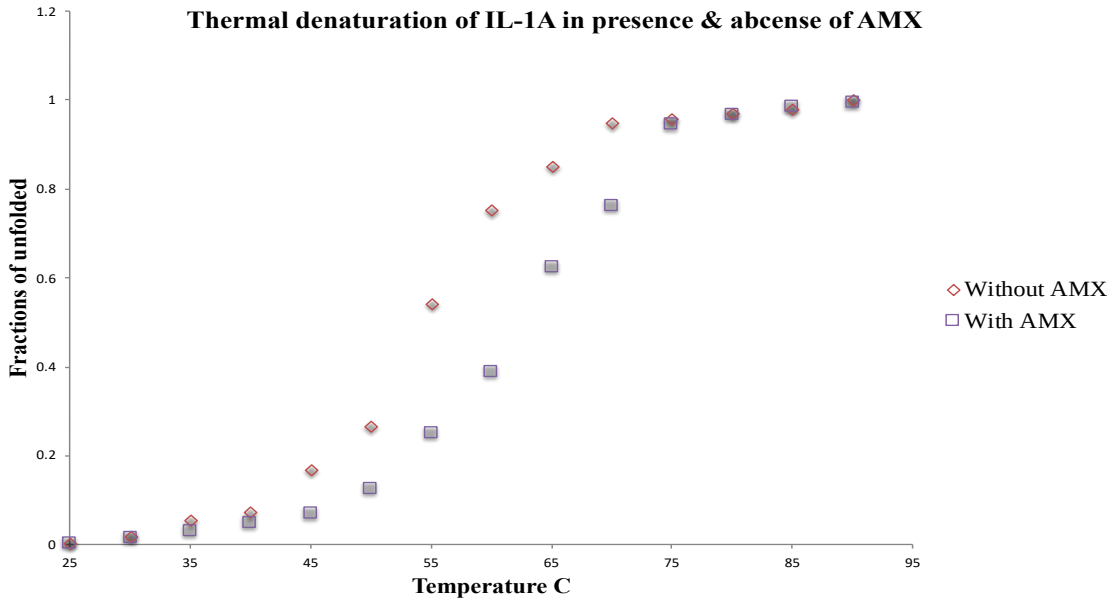

Figure 8: Thermal denaturation of IL-1α in presence of AMX (purple squares) and absence of AMX (red rhomboids). Far-CD was probed to examine of the protein at different temperature from 25-90°C within 5°C increments.

The chemical stability of IL-1α without and with AMX was examined by urea-induced protein unfolding experiment using Far-CD spectroscopy (Figure 9).

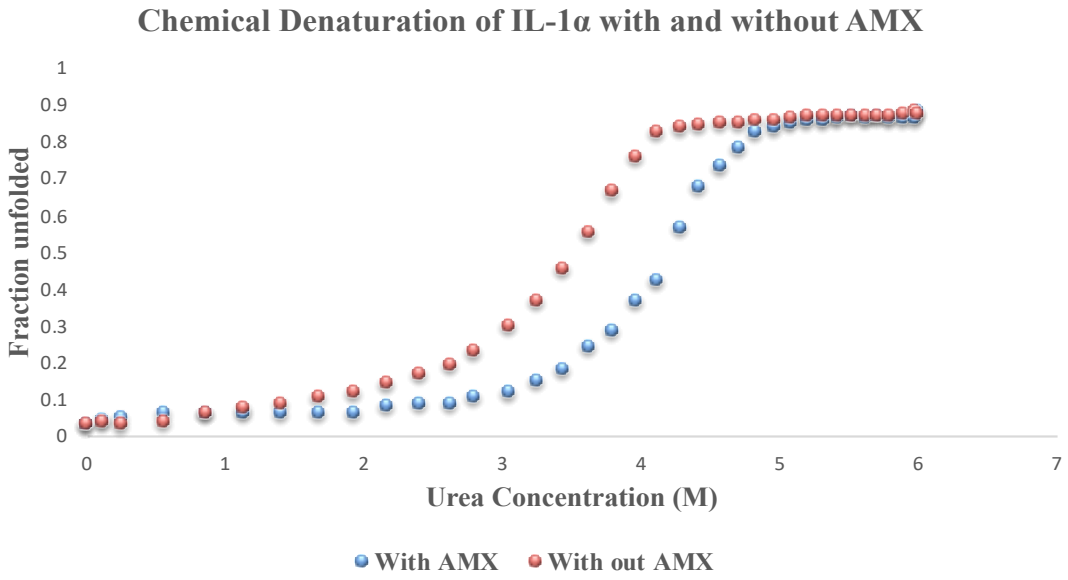

Figure 9: Chemical denaturation of IL-1α in presence and absence of AMX. Far-CD was probed to examine of the protein stability in urea.

In presence and absence of AMX, the protein exists in the native conformation at zero concentration of urea. During titration with urea, the unfolded states of the protein molecules are monitored. The Cm values where 50% of the proteins exist in folded state were calculated from urea unfolding curve. The Cm value of IL-1α with AMX was 4.3 M urea whereas without AMX the Cm a value was 3.3 M urea. The results indicated that as urea is neutral denaturant that disturbs hydrogen bonds within the protein molecules, so in presence of AMX, urea interfered with the hydrogen binds occurred at high concentration. As urea is a neutral denaturant that disturbs hydrogen bonds within protein molecules, these results indicate that in the presence of AMX urea interferes with the hydrogen bonds at high concentrations. These results of protein stability are consistent with the findings of limited trypsin digestion and ANS binding assay that showed conformational changes may increase protein compact structure.

Conclusions

The non-classical secretion of signal-less protein involves protein cargo that is made from multiprotein complex. The non-classical secretion of signal-less proteins involves a multiprotein complex for transport. In the case of IL-1α, S100A13 is involved in protein export in presence of copper. The results of this study showed that AMX can bind to IL-1α and also chelates copper. AMX binds to cysteine 143 of IL-1α where copper can bind and form a homodimer of IL-1α. Therefore, AMX can mask the thiol group and protect it from copper oxidation. Upon binding to AMX, IL-1α showed some conformational changes that stabilized the protein in some ways. For future work, NMR would be beneficial for examining other amino acid residues in the AMX binding site of IL-1α. In vivo study could help to determine whether or not AMX can inhibit non-classical secretion of IL-1α by binding to it, by chelating copper, or both.

References

1. Sims, J. E.; Smith, D. E., The IL-1 family: regulators of immunity. Nature Reviews Immunology 2010, 10 (2), 89.

2. Sarajlic, M.; Neuper, T.; Quiroz, F.; Tamara, K.; Michelini, S.; Vetter, J.; Schaller, S.; Horejs-Hoeck, J., IL-1β Induces SOCS2 Expression in Human Dendritic Cells. International journal of molecular sciences 2019, 20 (23), 5931.

3. Dinarello, C.; Arend, W.; Sims, J.; Smith, D.; Blumberg, H.; O'Neill, L.; Goldbach-Mansky, R.; Pizarro, T.; Hoffman, H.; Bufler, P., IL-1 family nomenclature. Nature immunology 2010, 11 (11), 973.

4. Hou, Z.; Zhou, J.; Ma, X.; Fan, L.; Liao, L.; Liu, J., Role of interleukin-1 receptor type II in the pathogenesis of endometriosis. Fertility and sterility 2008, 89 (1), 42-51.

5. Netea, M. G.; van de Veerdonk, F. L.; van der Meer, J. W.; Dinarello, C. A.; Joosten, L. A., Inflammasome-independent regulation of IL-1-family cytokines. Annual review of immunology 2015, 33, 49-77.

6. Orjalo, A. V.; Bhaumik, D.; Gengler, B. K.; Scott, G. K.; Campisi, J., Cell surface-bound IL-1α is an upstream regulator of the senescence-associated IL-6/IL-8 cytokine network. Proceedings of the National Academy of Sciences 2009, 106 (40), 17031-17036.

7. Rider, P.; Carmi, Y.; Guttman, O.; Braiman, A.; Cohen, I.; Voronov, E.; White, M. R.; Dinarello, C. A.; Apte, R. N., IL-1α and IL-1β recruit different myeloid cells and promote different stages of sterile inflammation. The Journal of Immunology 2011, 187 (9), 4835-4843.

8. Dinarello, C., The IL-1 family and inflammatory diseases. Clinical and experimental rheumatology 2002, 20 (5; SUPP/27), S1-S13.

9. Voronov, E.; Apte, R. N., IL-1 in colon inflammation, colon carcinogenesis and invasiveness of colon cancer. Cancer microenvironment 2015, 8 (3), 187-200.

10. Bertheloot, D.; Latz, E., HMGB1, IL-1α, IL-33 and S100 proteins: dual-function alarmins. Cellular & molecular immunology 2017, 14 (1), 43.

11. Mayer-Barber, K. D.; Andrade, B. B.; Barber, D. L.; Hieny, S.; Feng, C. G.; Caspar, P.; Oland, S.; Gordon, S.; Sher, A., Innate and adaptive interferons suppress IL-1α and IL-1β production by distinct pulmonary myeloid subsets during Mycobacterium tuberculosis infection. Immunity 2011, 35 (6), 1023-1034.

12. Dinarello, C. A., Overview of the IL-1 family in innate inflammation and acquired immunity. Immunological reviews 2018, 281 (1), 8-27.

13. Fettelschoss, A.; Kistowska, M.; LeibundGut-Landmann, S.; Beer, H.-D.; Johansen, P.; Senti, G.; Contassot, E.; Bachmann, M. F.; French, L. E.; Oxenius, A., Inflammasome activation and IL-1β target IL-1α for secretion as opposed to surface expression. Proceedings of the National Academy of Sciences 2011, 108 (44), 18055-18060.

14. Mantovani, A.; Barajon, I.; Garlanda, C., IL-1 and IL-1 regulatory pathways in cancer progression and therapy. Immunological reviews 2018, 281 (1), 57-61.

15. Monteleone, M.; Stow, J. L.; Schroder, K., Mechanisms of unconventional secretion of IL-1 family cytokines. Cytokine 2015, 74 (2), 213-218.

16. Prudovsky, I.; Kumar, T. K. S.; Sterling, S.; Neivandt, D., Protein-phospholipid interactions in nonclassical protein secretion: problem and methods of study. International journal of molecular sciences 2013, 14 (2), 3734-3772.

17. Omer, S.; Meredith, D.; Morris, J. F.; Christian, H. C., Evidence for the role of adenosine 5′-triphosphate-binding cassette (ABC)-A1 in the externalization of annexin 1 from pituitary folliculostellate cells and ABCA1-transfected cell models. Endocrinology 2006, 147 (7), 3219-3227.

18. Donato, R.; Sorci, G.; Giambanco, I., S100A6 protein: functional roles. Cellular and Molecular Life Sciences 2017, 74 (15), 2749-2760.

19. Heizmann, C. W.; Cox, J. A., New perspectives on S100 proteins: a multi-functional Ca 2+-, Zn 2+-and Cu 2+-binding protein family. Biometals 1998, 11 (4), 383-397.

20. Bresnick, A. R.; Weber, D. J.; Zimmer, D. B., S100 proteins in cancer. Nature Reviews Cancer 2015, 15 (2), 96-109.

21. Kiss, B.; Ecsédi, P.; Simon, M.; Nyitray, L., Isolation and Characterization of S100 Protein-Protein Complexes. In Calcium-Binding Proteins of the EF-Hand Superfamily, Springer: 2019; pp 325-338.

22. Wicki, R.; Schäfer, B. W.; Erne, P.; Heizmann, C. W., Characterization of the Human and Mouse cDNAsCoding for S100A13, a New Member of the S100 Protein Family. Biochemical and biophysical research communications 1996, 227 (2), 594-599.

23. Garcia, V.; Chazin, W. J., A new approach to discovery of S100 protein heterodimers. The FEBS journal 2019, 286 (10), 1838-1840.

24. Viotti, C., ER to golgi-dependent protein secretion: the conventional pathway. In Unconventional Protein Secretion, Springer: 2016; pp 3-29.

25. Yao, R.; Lopez-Beltran, A.; Maclennan, G. T.; Montironi, R.; Eble, J. N.; Cheng, L., Expression of S100 protein family members in the pathogenesis of bladder tumors. Anticancer research 2007, 27 (5A), 3051-3058.

26. Wang, T.; Huo, X.; Chong, Z.; Khan, H.; Liu, R., A review of S100 protein family in lung cancer. Clinica Chimica Acta 2018, 476, 54-59.

27. Bresnick, A. R., S100 proteins as therapeutic targets. Biophysical reviews 2018, 10 (6), 1617-1629.

28. Hsieh, H.-L.; Schäfer, B. W.; Cox, J. A.; Heizmann, C. W., S100A13 and S100A6 exhibit distinct translocation pathways in endothelial cells. J Cell Sci 2002, 115 (15), 3149-3158.

29. Dimou, E.; Nickel, W., Unconventional mechanisms of eukaryotic protein secretion. Current Biology 2018, 28 (8), R406-R410.

30. Grieve, A. G.; Rabouille, C., Golgi bypass: skirting around the heart of classical secretion. Cold Spring Harbor perspectives in biology 2011, 3 (4), a005298.

31. Prudovsky, I.; Tarantini, F.; Landriscina, M.; Neivandt, D.; Soldi, R.; Kirov, A.; Small, D.; Kathir, K. M.; Rajalingam, D.; Kumar, T. K. S., Secretion without golgi. Journal of cellular biochemistry 2008, 103 (5), 1327-1343.

32. Voronov, E.; Shouval, D. S.; Krelin, Y.; Cagnano, E.; Benharroch, D.; Iwakura, Y.; Dinarello, C. A.; Apte, R. N., IL-1 is required for tumor invasiveness and angiogenesis. Proceedings of the National Academy of Sciences 2003, 100 (5), 2645-2650.

33. Mandinova, A.; Soldi, R.; Graziani, I.; Bagalá, C.; Bellum, S.; Landriscina, M.; Tarantini, F.; Prudovsky, I.; Maciag, T., S100A13 mediates the copper-dependent stress-induced release of IL-1α from both human U937 and murine NIH 3T3 cells. Journal of cell science 2003, 116 (13), 2687-2696.

34. Akdis, M.; Aab, A.; Altunbulakli, C.; Azkur, K.; Costa, R. A.; Crameri, R.; Duan, S.; Eiwegger, T.; Eljaszewicz, A.; Ferstl, R., Interleukins (from IL-1 to IL-38), interferons, transforming growth factor β, and TNF-α: Receptors, functions, and roles in diseases. Journal of Allergy and Clinical Immunology 2016, 138 (4), 984-1010.

35. Eigenbrod, T.; Park, J.-H.; Harder, J.; Iwakura, Y.; Núñez, G., Cutting edge: critical role for mesothelial cells in necrosis-induced inflammation through the recognition of IL-1α released from dying cells. The Journal of Immunology 2008, 181 (12), 8194-8198.

36. Sivaraja, V.; Kumar, T. K. S.; Rajalingam, D.; Graziani, I.; Prudovsky, I.; Yu, C., Copper binding affinity of S100A13, a key component of the FGF-1 nonclassical copper-dependent release complex. Biophysical journal 2006, 91 (5), 1832-1843.

37. Kathir, K. M.; Ibrahim, K.; Rajalingam, D.; Prudovsky, I.; Yu, C.; Kumar, T. K. S., S100A13–lipid interactions—role in the non-classical release of the acidic fibroblast growth factor. Biochimica et Biophysica Acta (BBA)-Biomembranes 2007, 1768 (12), 3080-3089.

38. Ridinger, K.; Schäfer, B. W.; Durussel, I.; Cox, J. A.; Heizmann, C. W., S100A13 biochemical characterization and subcellular localization in different cell lines. Journal of Biological Chemistry 2000, 275 (12), 8686-8694.

39. Kathir, K. M.; Gao, L.; Rajalingam, D.; Daily, A. E.; Brixey, S.; Liu, H.; Davis, D.; Adams, P.; Prudovsky, I.; Kumar, T. K. S., NMR characterization of copper and lipid interactions of the C2B domain of synaptotagmin I—relevance to the non-classical secretion of the human acidic fibroblast growth factor (hFGF-1). Biochimica et Biophysica Acta (BBA)-Biomembranes 2010, 1798 (2), 297-302.

40. Nickel, W., Unconventional secretory routes: direct protein export across the plasma membrane of mammalian cells. Traffic 2005, 6 (8), 607-614.

41. Makino, H.; Saijo, T.; Ashida, Y.; Kuriki, H.; Maki, Y., Mechanism of action of an antiallergic agent, Amlexanox (AA-673), in inhibiting histamine release from mast cells. International Archives of Allergy and Immunology 1987, 82 (1), 66-71.

42. Matsunaga, H.; Ueda, H., Synergistic Ca2+ and Cu2+ requirements of the FGF1–S100A13 interaction measured by quartz crystal microbalance: An initial step in amlexanox-reversible non-classical release of FGF1. Neurochemistry international 2008, 52 (6), 1076-1085.

43. Landriscina, M.; Prudovsky, I.; Carreira, C. M.; Soldi, R.; Tarantini, F.; Maciag, T., Amlexanox reversibly inhibits cell migration and proliferation and induces the Src-dependent disassembly of actin stress fibers in vitro. Journal of Biological Chemistry 2000, 275 (42), 32753-32762.

44. Carreira, C. M.; LaVallee, T. M.; Tarantini, F.; Jackson, A.; Lathrop, J. T.; Hampton, B.; Burgess, W. H.; Maciag, T., S100A13 is involved in the regulation of fibroblast growth factor-1 and p40 synaptotagmin-1 release in vitro. Journal of Biological Chemistry 1998, 273 (35), 22224-22231.

45. Bell, J., Amlexanox for the treatment of recurrent aphthous ulcers. Clinical drug investigation 2005, 25 (9), 555-566.

46. Greer Jr, R. O.; Lindenmuth, J. E.; Juarez, T.; Khandwala, A., A double-blind study of topically applied 5% amlexanox in the treatment of aphthous ulcers. Journal of oral and maxillofacial surgery 1993, 51 (3), 243-248.

47. Rani, S. G.; Mohan, S. K.; Yu, C., Molecular level interactions of S100A13 with amlexanox: inhibitor for formation of the multiprotein complex in the nonclassical pathway of acidic fibroblast growth factor. Biochemistry 2010, 49 (11), 2585-2592.

48. Ràfols, C.; Bosch, E.; Barbas, R.; Prohens, R., The Ca2+–EDTA chelation as standard reaction to validate Isothermal Titration Calorimeter measurements (ITC). Talanta 2016, 154, 354-359.

Chapter Five

Conclusions

Conclusions

Technologies that involve recombinant DNA producing recombinant proteins have drastically changed the world's pharmaceutical market. Protein drug research development has allowed for the potential treatment of other ailments such as auto-immune diseases, cancer, hypertension, mental disorders, metabolic diseases, as well as cardiovascular disease. Many therapeutic proteins have been successfully produced by recombinant DNA technology. The overproduction and purification of recombinant proteins is a multibillion-dollar business. Significant advantages of recombinant protein drug therapy make the production efforts not only worthwhile, but also extremely important. When recombinant protein expressed as inclusion bodies in *E. coli* cells, multiple steps require to obtain soluble and biologically active target protein. As multiple steps leading to lower yield of pure protein that could hindered the study of many proteins and driven up the cost of many pharmaceuticals. Therefore, there is great interest to pharmaceutical and biotechnology industries to develop an efficient strategy for purification of recombinant proteins. In this context, several affinity tags have been successfully proposed for the purification of recombinant proteins. However, the currently commercially available affinity tags have some difficulties for example requirement of exhaustive purification conditions, high costs of the solutes used for fraction elution, protein tags are prone to denature at high conditions, weak solubility enhancer, target proteins are not recovered as a fully bioactive form, and limited pharmaceutical/biotechnology applications. This study pertains to the successful development of a novel solubility affinity tag which can be used for the simple, versatile, and cost-effective purification and detection of recombinant proteins expressed as

inclusion bodies. In addition, the affinity tag has wide range applications in pharmaceutical and biotechnological field. The novel Ark-RUBY-tag facilitates rapid, reproducible and single-step purification of recombinant proteins expressed as inclusion bodies in *E. coli* cells as it is shown in purifying IL-1 alpha and D2 domain. Purification of ArK-RUBY-fused recombinant protein(s) can be obtained by using imidazole fractions. Target protein can be easily removed from the Rd-tag by enzymatic cleavage. No requirement for desalting step in order to get purified, target protein. Rd-fused recombinant proteins can be quantitatively detected using polyclonal antibodies. Rd-tag can be used to purify small peptides. By using Ark-RUBY-tag, purified recombinant protein regains fully biologically active form. Therefore, bioactive protein has wide range of application in drug-delivery.

The non-classical secretion of signal peptide-less proteins is still unclear and under research. While some proteins have displayed good binding affinities to S100A13, the protein involves in non-classical secretion, some critical steps are still ambiguous. For example, the mechanism of multi protein complex formation that involves in interleukin-1 alpha is still unwell understood. Also, there is no suitable answer for how copper chelator prevents IL-1 alpha secretion. In this study, in order to understand plausible mechanism underlying the role of copper in non-classical secretion of IL-1 alpha, an investigation was made to study the effects of copper and different metals on IL-1 alpha. Copper involves in many crucial biological reactions in the cells. Even though copper ion is toxic when it is free, the mechanism(s) underlies intracellular copper transportation is still unknown. It is known that copper involves in non-classical secretion of many signal peptide-less proteins. The IL-1α is shown to bind to Cu^{++} with apparent binding constant

value in nanomolar range. It seems that Cu^{++} induces protein conformational changes leading to protein dimerization which we believe the dimerization event play a crucial role in protein secretion by non-conventional mechanism. Also, we believe that S100A13 is Cu^{++} donor since S100A13 is copper binding protein. In this study IL-1α was also tested to interact with several metals in order to examine whether or not copper is specific for dimerization. The results are shown that cupric form of copper is the only metals that underlies protein dimerization, whereas cuprous form copper shows good binding with no conformational changes. Copper induced IL-1α dimerization was inhibited when reducing agents is added, so that an attempt is made to design mutation on Cys134 position since IL-1α has only one cysteine. The results of this study reveal that the dimerization is mediated by disulfide bridge of two cystine. Both monomer and dimer form show good binding affinity to S100A13 which suggests that S100A13 binding site to IL-1α has no conformational changes.

In previous study on FGF-1, Amelexanox (AMX), the drug that is used for reducing inflammatory reaction, was able to inhibit FGF-1 secretion. The results of this study showed that AMX binds to IL-1α in constant affinity in the micromolar range. AMX induces protein conformational changes around Cys134 because it prevents protein dimerization. Also, AMX shows a good binding to copper which we believe that AMX works as copper chelator reagent or it binds to Cys134 and prevents copper to reduce Cys134. Another event may occur in dimerization prevention mechanism which is AMX converts corpus to cupric which in return it prevents dimerization. The results of AMX are promising to design a drug that may help in inhibiting IL-1α secretion that is associated with many diseases.